

Constraints on the origin of early high-heat producing (U-Th enriched) granitic magmatism in central Australia

Thesis submitted in accordance with the requirements of the University of
Adelaide for an Honours Degree in Geology/Geophysics

Maria Then
November 2016



CONSTRAINTS ON THE ORIGIN OF EARLY HIGH-HEAT PRODUCING (U-TH ENRICHED) GRANITIC MAGMATISM IN CENTRAL AUSTRALIA

ORIGIN OF PROTEROZOIC GRANITES IN MT BOOTHBY

ABSTRACT

The southern margin of central Australia is characterised by anomalous heat production, 3–5 times higher than global averages. Paleoproterozoic voluminous granitoid complexes in the region are important in the study of this anomalous heat flow. Ca.1800 Ma high-heat producing granites in Mt Boothby have A/NCK (molecular $\text{Al}_2\text{O}_3/(\text{CaO}+\text{Na}_2\text{O}+\text{K}_2\text{O})$) ratios > 1 , indicating a predominant origin from partial melting of metasedimentary rocks. The Boothby Orthogneiss is characterised by moderately negative Eu anomalies ($\text{Eu}/\text{Eu}^*: 0.03–0.43$) and strong depletion in Ba, Rb, Nb and Sr. The enrichment of Ba and Rb relative to Sr and high K_2O contents also support a metasedimentary source. The heat production values calculated for the Boothby Orthogneiss and the surrounding Lander formation show that the region is enriched in heat producing elements. The U-Pb zircon age data of inherited zircons in these granites are similar to the detrital zircons of the widespread outcropping; Lander formation. ε_{Nd} values of -3.5 to 1.3 of the granites infer an evolved crustal source coupled with mixing of a newly mantle-derived component through lower crust assimilation. Zircon saturation temperatures calculated suggest that the Boothby intrusive complex was emplaced at 688–845 °C, with a maximum temperature of 776 °C, implying an arc environment with associated fluid-flux melting in the mantle wedge, ultimately controlled by subduction dynamics.

KEYWORDS

Heat production, geochemistry, geochronology, isotopes, Central Australia, Reynolds Range, Mt Boothby, Proterozoic

TABLE OF CONTENTS

Abstract	i
Keywords	i
List of Figures and Tables.....	3
Introduction.....	4
Geological Setting.....	6
Regional Geology of the Arunta region.....	7
Reynolds Range	11
Methods.....	12
U-Pb Zircon dating	12
Whole-rock geochemistry.....	13
Sm-Nd isotopes analysis	14
Results.....	15
Petrography	15
Geochemistry Major Elements	18
Geochemistry Trace and Rare earth elements	22
Sm-Nd Isotope systematics	24
Heat Production	26
Zircon Saturation Temperature.....	27
Geochronology.....	29
Discussion.....	33
Source Nature of Boothby Granitoids	33
Sm-Nd Isotope Systematics.....	36
Heat Production	37
Zircon Saturation Thermometry and Tectonic Implications	38
Conclusion	41
References.....	43
Acknowledgments	43
Appendix A: Geochemistry additional data for fields (Browne 2015).....	47
Appendix B: Heat Production data	49
Appendix C: U-Pb Zircon Geochronology data	53

LIST OF FIGURES AND TABLES

Figure 1: Histogram of global modern heat flow data in Australia	6
Figure 2: Location map of the Arunta Region and study area showing rocks units of the Reynolds and Anmatjira Range	8
Figure 3: Study area of Mt Boothby with corresponding sample locations	12
Figure 4: Photomicrographs of petrological analysis on selected samples.....	16
Figure 5: Total Alkali Silica diagram after Middlemost (1985)	17
Figure 6: Alumina Saturation Index diagram after Shand (1943)	17
Figure 7: Harker Plots of SiO ₂ vs major elements.....	22
Figure 8: Harker Plots of SiO ₂ vs trace elements	24
Figure 9: Spiderplots of trace and rare earth elements	25
Figure 10: Epsilon-Neodymium vs time diagram.....	26
Figure 11: Heat production graph	27
Figure 12: Zircon saturation temperature histogram	29
Figure 13: Representative CL images of zircon in samples for U-Pb ages	31
Figure 14: Comparative Probability histogram of U-Pb zircon ages	32
Table 1: Major Element geochemical data	19
Table 2: Trace Element geochemical data	20
Table 3: Trace Element geochemical data	21
Table 4: Sm-Nd isotopic data	26
Table 5: Zircon saturation thermometry data.....	29

INTRODUCTION

A significant proportion of the crustal heat production budget is contained within granites, and the transfer of these elements during granite generation, migration and emplacement results in major changes in the thermal regime of the lithosphere (McLennan & Taylor 1996; Bea 2012). Major controls on the availability of these high heat-producing elements (HPE) within a magmatic system are the composition of the source, degree of partial melting, and degree of differentiation during magma emplacement (Chappell & Hine 2006, McLaren et al., 2005). Three major source regions for granitic melts are; fractionation of mantle-derived melts, intracrustal melting and mixing of mantle-derived melts with lithospheric components (Marshall 2013). The distribution and concentration of U and Th elements in the crust gives a first order constraint on the thermal stability of the continental lithosphere, controlling its tectonic evolution (Sandiford et al., 2002).

A region of HHP Proterozoic granitoids exists in the Arunta Region. It is characterised by voluminous granitic intrusions emplaced over the 1820–1620 Ma time interval (Hand & Buick 2001; Scrimgeour 2003), and is a significant part of the North Australian Craton (NAC). Existing radiometric heat production measurements infer that many of these intrusions are characterised as HHP Proterozoic granitoids, typically containing between 3 to 5 times the global averages in U-Th concentration (Fig. 1) (Sandiford et al., 2002; McLaren & Powell 2014; McLaren et al., 2005). They are derived from the melting of existing crust and many have co-magmatic mantle-derived input into the system (Collins & Shaw 1995). This provides an ideal opportunity to compare the roles of intracrustal recycling and juvenile mantle inputs. The paucity of exposed source regions in these shallowly emplaced granites (Chappell

& Hine 2006) makes it challenging to constrain melting parameters. However, the spatial association of the HHP granites with Proterozoic basement which itself is often enriched in HPE (Wyborn et al., 1992; Neumann et al., 2000), suggests these granites are an indication of what was driving the system but also implies that the HPE enrichment was derived from an already enriched source. The Paleoproterozoic ca. 1800–1780 Ma intrusive complex at Mt Boothby in the south eastern Reynolds Range could represent one of the earliest suites of HHP granitoids and associated mafic rocks in central Australia, allowing a new model of genesis.

In this paper a variety of analyses will be used to determine compositions, geochemistry and isotopic nature of the Mt Boothby complex in the SE Reynolds Range. These units are the Boothby Orthogneiss, Mafic-Felsic gneiss and associated metasedimentary units. This study primarily aims to constrain the origin of the earliest Paleoproterozoic HHP granitic magmatism at Mt Boothby, in order to test the hypothesis that the region represented a HHP granitic suite that was associated with mantle input into the source region to produce the HPE enrichment. U-Pb inherited zircon ages in conjunction with detrital ages from previous studies will be used to assess provenance affinities with exposed metasedimentary units in the region. Major, trace and REE geochemistry as well as Sm-Nd isotopic systematics will be used to determine the degree of crustal and mantle input and if the mantle input came from an anomalously enriched source. Zircon saturation thermometry on inheritance-rich granites will be used to determine the maximum temperature constraint for that granite. The results of this study will be interpreted in the context of the broader tectonic evolution of the North Australian Craton.

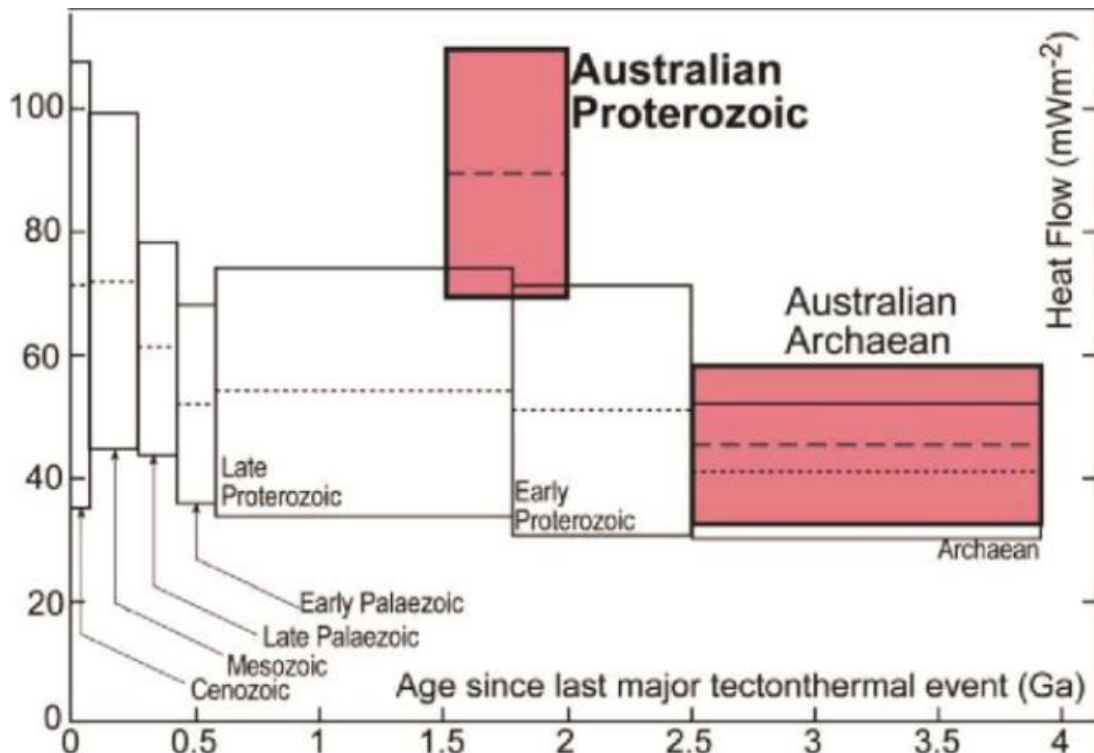


Figure 1: Histogram of global modern continental surface heat flow data (McLaren et al., 2003), where heat flow data is grouped by age (Ga) based on tectono-thermal events that have occurred. It shows that compared to global norms, Australian Proterozoic continental lithosphere is highly concentrated in U and Th (modified from McLaren et al., 2003).

GEOLOGICAL SETTING

The North Australian Craton (NAC), central Australia (Fig. 1a) consists of Paleoproterozoic cratonic blocks that preserve a complex history spanning from the late Archean to the early Mesoproterozoic. Archean basement inliers are evident in the Pine Creek and Tanami regions and are likely to be more widespread based on geophysical analysis (Cawood & Korsh 2008). The NAC underwent numerous tectonothermal events and basin phases between 1870-1570 Ma (Scrimgeour 2003). Contrasting styles of metamorphism, magmatism, deformation and sedimentation reflect varying tectonic processes. Numerous extensional and compressional intraplate events occurred at the craton margins. Evidence for these plate margin events is preserved in the Arunta on the southern margin of the NAC (Betts & Giles 2006; Scrimgeour et al., 2005).

REGIONAL GEOLOGY OF THE ARUNTA REGION

The Arunta Region of central Australia (Fig 1a) is a geologically complex and tectonically long-lived terrane, which has been subjected to several periods of magmatism. The region comprises a 200,000 km² exposure of metamorphosed and highly deformed Paleoproterozoic to Mesoproterozoic units (Clauoe-Long et al., 2008). The Arunta Region is subdivided into three distinct provinces; the Aileron, Warumpi and Irindina Province (Scrimgeour et al., 2005; Anderson et al., 2013). The largest of the three provinces is the Aileron Province, which has depositional and intrusive ages that lie between 1870–1710 Ma, similar to other proximal Paleoproterozoic basement terranes in the North Australian Craton (Clauoe-Long et al., 2008). The Warumpi Province located on the south western margin of the Arunta is considered an exotic terrane and comprises intrusive and sedimentary protolith ages between ca. 1690–1600 Ma (Scrimgeour et al., 2005; Scrimgeour 2013).

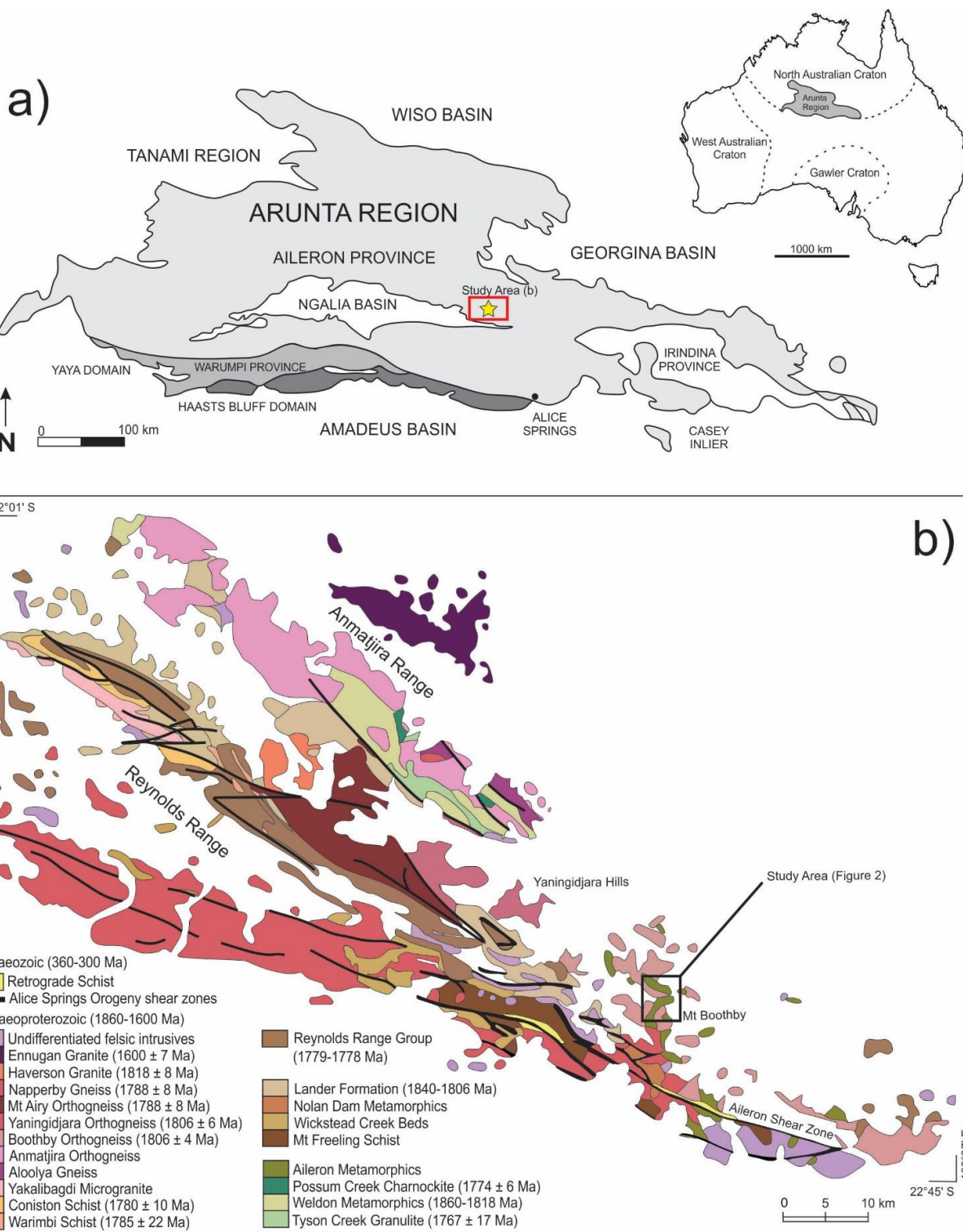


Figure 1: a) Location map of the Arunta Region illustrating the study area shown in Fig. 1b and 2 (modified from Wong et al., (2015)) b) Location map of the Reynolds and Anmatjira Range showing the distribution of major rock types with protolith ages and geometry of regional shear zones (modified from Howlett et al., (2015)).

The Irindina Province is situated on the south eastern end of the Arunta and consists of Neoproterozoic to Cambrian intrusive ages (Hand & Buick 2001; Hoatson et al., 2005). The thermal regime and tectonic evolution of the Arunta Region occurred over a prolonged period from the Stafford event (1810–1790 Ma) to the Alice Springs Orogeny (400–300 Ma) (Collins & Shaw 1995).

The oldest exposed rocks in the Arunta Region are the widespread interbedded pelitic and psammitic metasedimentary package, collectively known as the Lander Formation, comprising 60% of identified outcrop (Scrimgeour 2013). Extensive geochronological data have constrained a depositional age of the formation between 1840–1830 Ma (Claoue-Long et al., 2008). There is some ambiguity surrounding the architecture and timing of assembly of the elements within the North Australian Craton. There was a fundamental shift in the tectonic regime of the NAC at 1820 Ma, particularly in the southern margin of the Arunta region (Hand & Buick 2001). It is characterised by high-grade, medium- to high-P metamorphism with evident burial and exhumation of rocks in a plate margin setting. The northern Arunta is characterised by lower-grade phases with localised higher-grade, high-T, low-P metamorphism, reflecting intraplate responses to events occurring in the south (Rubatto et al., 2001; Morrissey et al., 2014; Collins & Vernon 1991). Previous studies have proposed an evolving north-dipping back-arc subduction system along the southern margin of the NAC (ca. 1800–1600 Ma), associated with arc magmatism, accretionary tectonism and continental collision, particularly evident in the Arunta Region (Betts & Giles 2006; Zhao 1994; Zhao & McCulloch 1995; Giles et al., 2002). Zhao (1994) proposed this evolved Proterozoic back-arc regime based on Sm-Nd and geochemical analysis on two amphibolite groups in the southern Arunta Region.

These two groups comprised affinities to island-arc basalts, with magmatic precursors being derived from partial melting of a mantle wedge, metasomatised by an enriched subduction component, reflected by the pattern of HFS and REE elements as well as isotope depleted mantle compositions (Zhao 1994). Fluid-absent melting and a high geothermal gradient is envisaged for a back-arc regime in the Southern Arunta based on earlier findings (Zhao & Cooper 1992; Zhao & Bennett 1995; Betts & Giles 2006).

The first thermal event to affect the Arunta Region was the Stafford Event (1820–1800 Ma), which produced voluminous felsic and lesser mafic magmatism. Felsic intrusive granitic bodies include the Anmatjira Orthogneiss (1795 ± 4 Ma; Scrimgeour 2013), Aloolya Gneiss (1807 ± 6 Ma; Scrimgeour 2013) and the Mt Boothby Orthogneiss (1806 ± 6 Ma; Worden et al., 2008). Lesser mafic rocks occur further south, including the Johannsen Metagabbro (1805 ± 3 Ma; Hoatson et al., 2005a). The Yambah event (1790–1770 Ma) came after and involved extensive magmatic episodes of more mafic and felsic magmatism in the south eastern Aileron Province (Hand & Buick 2001; Collins & Williams 1995; Howlett et al., 2015). These two events are associated with extensive low-pressure high-temperature greenschist to granulite grade metamorphism (Vernon et al., 1990; Morrissey et al., 2015) throughout the Reynolds and Anmatjira Range (Scrimgeour 2003). The Inkamulla igneous event is associated with 1760–1740 Ma granitoids in the south eastern Arunta region (Scrimgeour 2003; Dirks et al., 1991). The ca. 1730–1690 Ma Strangways Orogeny is associated with widespread deformation and metamorphism in the Arunta region (Teyssier et al., 1988; Vry et al., 1996; Hand & Buick 2001). The Liebig Orogeny (1640–1635 Ma) resulted in widespread granulite facies metamorphism as a

result of burial to 30km depth (Scrimgeour et al., 2005). The ca. 1590–1570 Chewings Orogeny was a prolonged event that produced low-pressure greenschist to granulite facies metamorphism throughout the terrain without obvious associated magmatism (Vry et al., 1996). During the mid-Palaeozoic Alice Springs Orogeny (400–300 Ma), the region was separated by greenschist to amphibolite facies shear zones. This resulted in the exhumation of deep crustal rocks ~40km, exposing the Arunta Region and isolating sedimentary basins Amadeus, Georgina, Wiso and Ngalia basins (Collins & Shaw 1995; Haines et al., 2001; Cartwright et al., 1999).

REYNOLDS RANGE

The Reynolds Range in the central Aileron Province was extensively intruded by voluminous granites emplaced at 1810–1770 Ma (Vry et al., 1996). These voluminous magmatic rocks intrude the oldest exposed metasedimentary rocks in the Reynolds Range; the Lander Formation. The distribution of major rock packages in the Reynolds Range and contiguous Anmatjira Range are shown in (Fig. 1b). Magmatism during the emplacement of these magmatic rocks is associated with the aforementioned Stafford and Yambah tectonothermal events (Collins & Shaw 1995; Hoatson et al., 2005). Mt Boothby is located in the south eastern margin of the Reynolds Range region and comprises the Palaeoproterozoic ca. 1800–1780 Ma Boothby intrusive complex, representative of high-heat producing suites in Australian Proterozoic terrains (Fig. 2). The intrusion comprises of two major lithologies, the Boothby Orthogneiss and composite mafic-felsic gneiss. U-Pb zircon age data has constrained the Boothby Orthogneiss to 1806 ± 4 Ma (Worden et al., 2008).

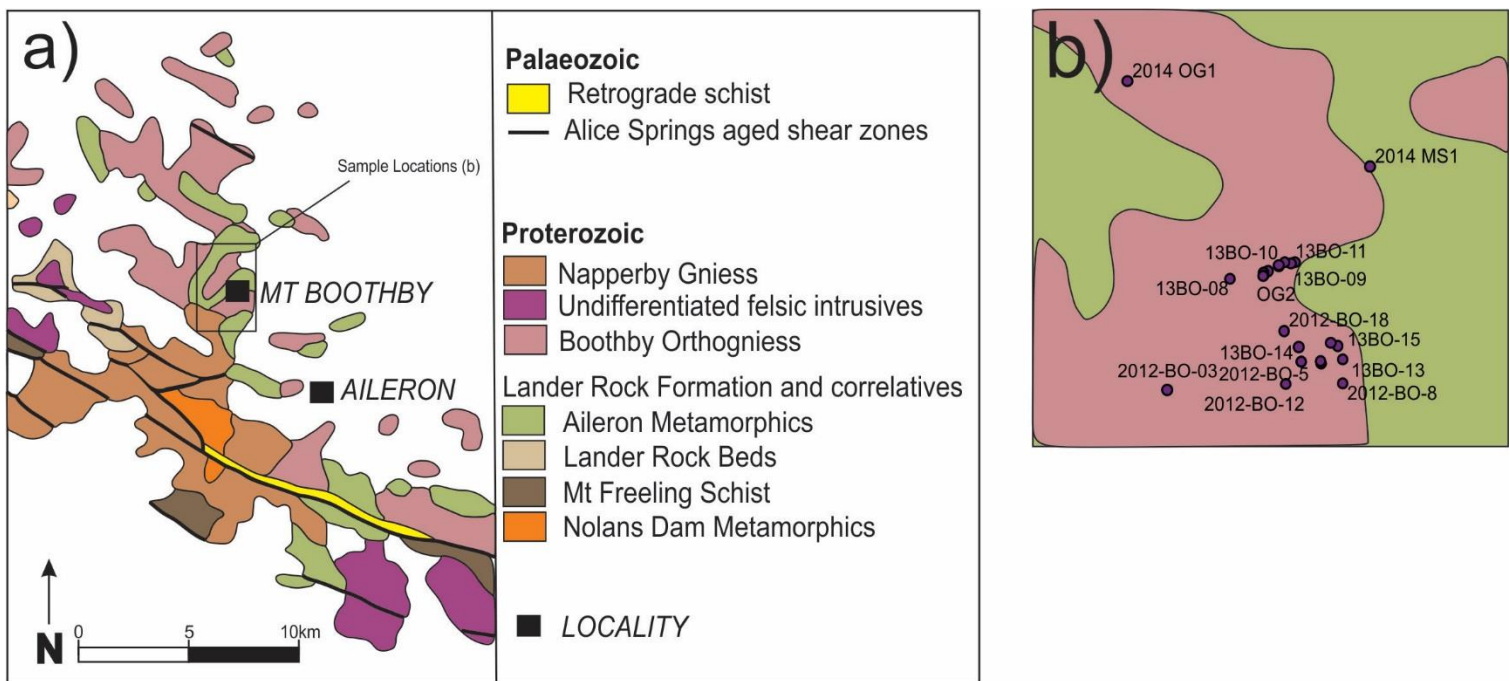


Figure 2: Field area showing rock units of Mt Boothby in the SE Reynolds Range with sample locations (modified from Morrissey et al., (2014) and Raimondo et al., (2011)).

METHODS

U-Pb Zircon Dating

Four samples selected for U-Pb zircon dating follow those of Payne et al., (2006).

Zircons obtained from samples from the Boothby Orthogneiss, mafic-felsic gneiss and metasediments in the Mt Boothby region were dated by U-Pb zircon methods. Rock samples were crushed and further sieved, collecting the 79-300 μm portion. Zircon concentrates were obtained using panning, hand-magnet separation and heavy liquid methods before zircon grains were handpicked and mounted into epoxy resin blocks. To determine microstructural location and internal composition variation within the zircon grains, they were imaged (Fig. 13) using Cathode Luminescence (CL) imaging on a FEI Quanta 600 Scanning Electron Microscope with attached Gatan Cathode Luminescence analyser. U-Pb isotopic analyses were obtained using a New Wave 213nm Nd-YAG laser with attachment on spectroscope in a He ablation atmosphere,

coupled to an Agilent 7500cx ICP-MS at Adelaide Microscopy, The University of Adelaide. The laser beam diameter at the sample surface was 30 μ m for zircon analysis. U-Pb fractionation was corrected using the GJ zircon standard (TIMS normalisation data $^{207}\text{Pb}/^{206}\text{Pb} = 608.3$ Ma, $^{206}\text{Pb}/^{238}\text{U} = 600.7$ Ma and $^{207}\text{Pb}/^{235}\text{U} = 602.2$ Ma following that of Jackson et al., 2004). U-Pb fractionation was corrected using the GJ-1 zircon standard and accuracy was checked with Plesovice zircon standard (Sláma et al., 2008). The $^{207}\text{Pb}/^{206}\text{Pb}$ zircon ages were used and zircon cores larger than 30 μ m were targeted. A number of zircon grains were omitted from analysis due to metamict cores, small size and complex recrystallized metamorphic rims. Data processing was done by using Iolite software and in data interpretation, a <10% discordancy limit was used for all grains analysed.

Whole Rock Geochemistry

Whole-rock chemical compositions for use in geochemical analysis were obtained from Australian Laboratory Services Pty. Ltd. A representative amount of all 23 samples were prepared for external geochemical analysis. Samples were cut with a diamond rock saw, crushed with a steel jaw crusher before being homogenised to a powder using a tungsten carbide mill at the University of Adelaide. Major and trace elements were analysed using inductively coupled plasma-optical emission spectroscopy (ICP-OES) and rare earth elements (REE) were analysed using ICP-MS methods at the Australian Laboratory Services Pty. Ltd.

Sm-Nd isotope analysis

Ten samples were analysed for Sm-Nd isotopes: four augen gneiss, four mafic-felsic gneiss and two metasediment samples. Analytical methods for whole rock Sm-Nd isotopic data followed that of Wade et al., (2006) using a small portion of rock powder prepared for geochemical analysis. Sm-Nd isotope analyses were conducted at the University of Adelaide. Samples were spiked with a $^{150}\text{Nd}/^{147}\text{Sm}$ solution. HF was further added to the samples in Teflon ‘bombs’ and evaporated before oven digestion. REE were separated in Biorad Polyprep columns and were further separated in columns containing HDEHP to isolate Sm and Nd contents using ion chromatography. The portions were then loaded onto filaments and ratios measured by thermal ionization mass spectrometry on a Finnigan MAT 262 and MAT261 mass spectrometer. Throughout the experimental procedure, blanks were between 104 to 240 pg Nd and the long term average for the La Jolla standard is 0.511838 ± 0.000008 (1σ , n=6). The results are listed in table 3.

RESULTS

PETROGRAPHY

Petrographic analysis was undertaken upon samples from Mt Boothby; the Boothby Orthogneiss and Mafic-Felsic Gneiss respectively.

13-BO-09: Boothby augen gneiss

The Boothby Orthogneiss comprises quartz, K-feldspar, garnet, biotite, plagioclase and minor magnetite. Garnet grains are seen as very coarse poikoblastic porphyroblasts, commonly 4mm in diameter and contain inclusions of biotite and quartz. Biotite comprises a large proportion of the sample (about 25-30%) and is seen as forming a strong foliation that wraps around garnet. Magnetite occurs along biotite grain boundaries. The matrix comprises quartz, K-feldspar and plagioclase. K-feldspar is seen as rounded coarse-grains often mantled by biotite.

12-BO-05: Boothby mafic-felsic gneiss

The sample contains quartz, K-feldspar, plagioclase, biotite with minor hornblende. Biotite defines a slight foliation throughout the sample, usually in contact with plagioclase and K-feldspar. The matrix assemblage is predominantly quartz, plagioclase and some K-feldspar, which, are coarse-grained. Plagioclase preserves multiple twinning. Hornblende shows two cleavages intersecting at $120^\circ/60^\circ$.

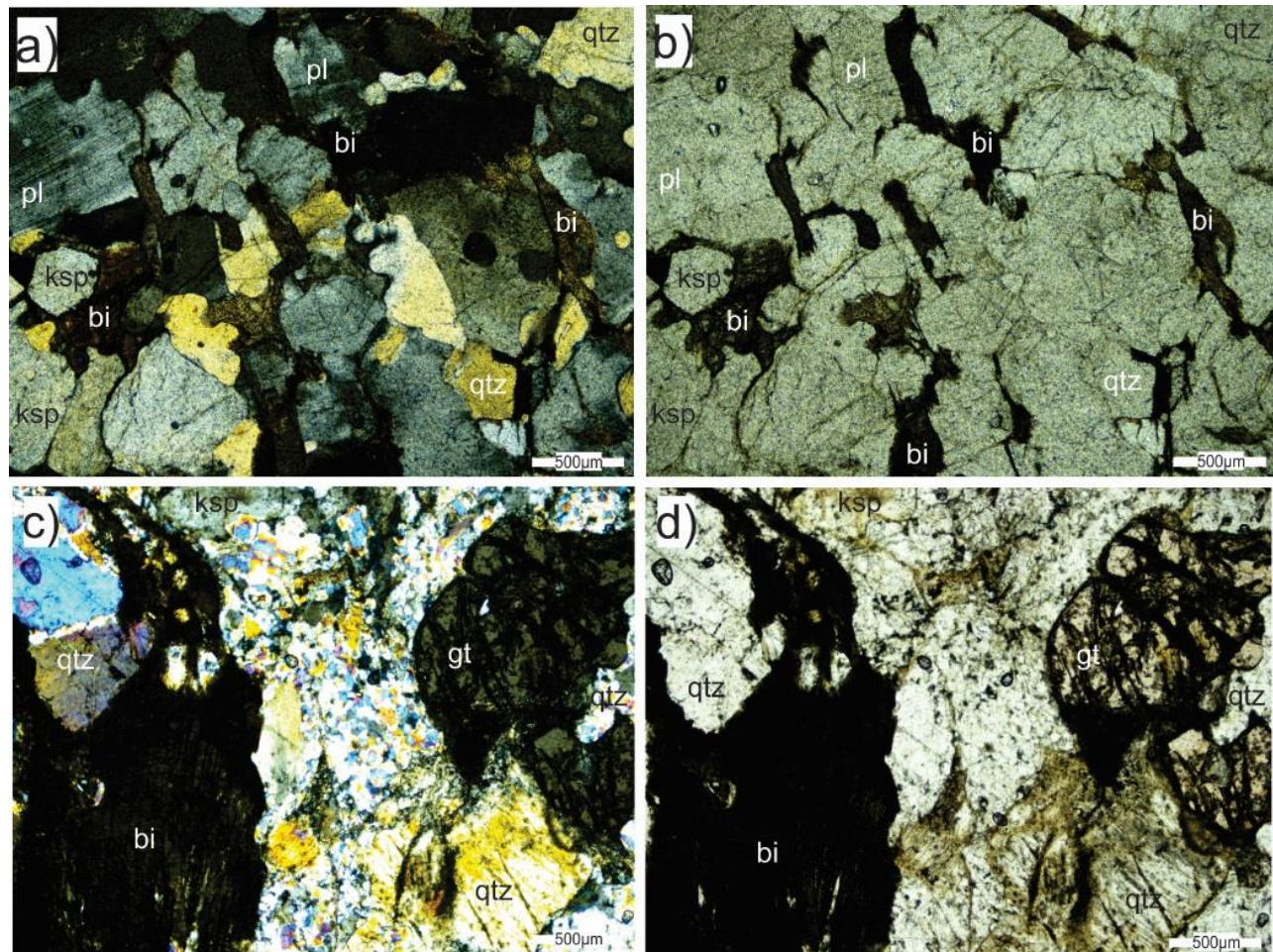


Figure 3: Photomicrographs of petrological relationships and mineral assemblages within the Boothby mafic-felsic gneiss and Boothby augen gneiss. a) XPL image of 12-BO-05 mafic-felsic gneiss showing a matrix of quartz, k-feldspar and plagioclase with biotite occurring throughout. b) PPL image of 12-BO-05 mafic-felsic gneiss. c) XLP image of the sample 13-BO-09 augen gneiss showing poikoblastic porphyroblasts of garnet containing inclusions of biotite and quartz. d) PPL image of the sample 13-BO-09 augen gneiss.

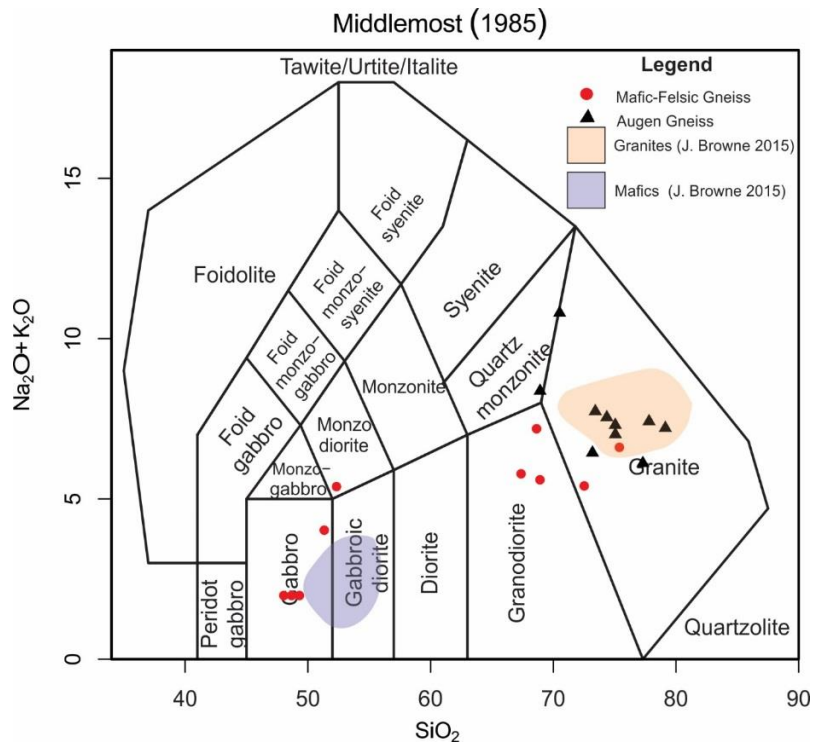


Figure 4: Total Alkali Silica diagram after Middlemost (1985) with samples plotted as per the key and fields of additional datasets showing correlations between other samples of the region

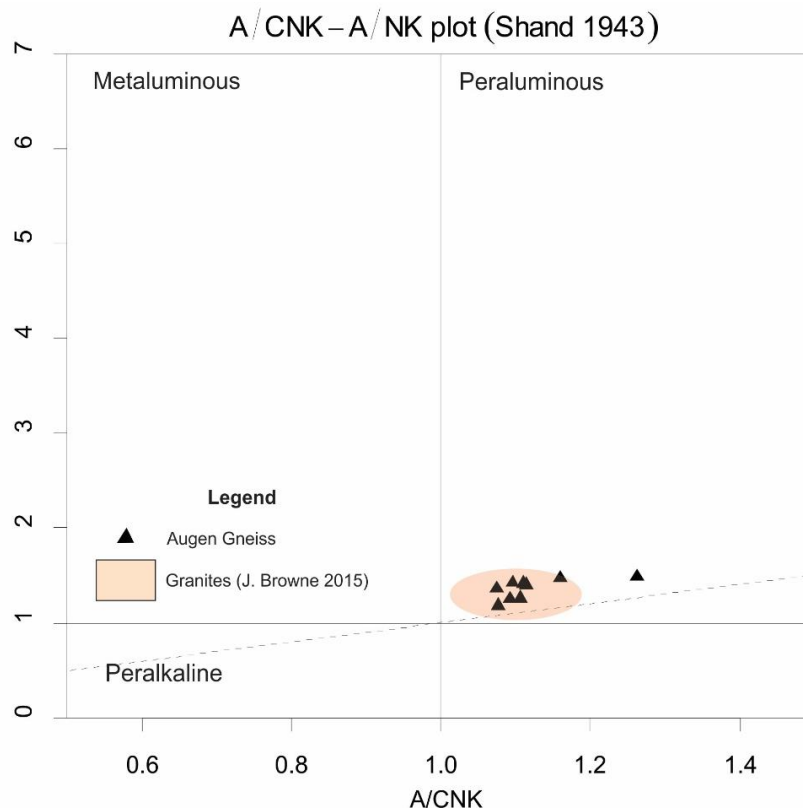


Figure 5: Alumina Saturation Index plot for the Augen Gneiss and Mafic-Felsic samples from the Reynolds Range following Shand (1943).

GEOCHEMISTRY

Major Elements

Major element geochemical results for all samples are displayed in table 1, Figure 6 and Appendix A. On the Total Alkali Silica classification diagram (Middlemost 1985) (Fig 4), the augen gneiss plots as granitic and the mafic-felsic gneiss ranges from gabbroic to granitic. Additional geochemical data from Browne (2015) of the ca.1800 Ma granitoids in the Anmatjira range are shown as fields for comparison.

Harker Plots were made of SiO_2 vs major elements analysed and are displayed in (Fig. 6) to indicate mafic and felsic trends. The SiO_2 content of the augen gneiss range from 65.4-78.9% and the mafic-felsic gneiss range from 47.8-69.06%.

The Boothby samples show considerable lithological variability, highlighted geochemical variability as SiO_2 increases. The overall trends for the full compositional range from gabbroic through to granitic (Fig 4) define a negative trend for most major elements including Al_2O_3 , MgO , CaO , TiO_2 and FeOt , where a positive trend is shown for K_2O , and $\text{K}_2\text{O}/\text{Na}_2\text{O}$ as SiO_2 content increases. High K_2O contents for the augen gneiss are 4.27-8.72 wt%, reflected by the predominance of the orthomagmatic phase K-feldspar. $\text{K}_2\text{O}/\text{Na}_2\text{O}$ ratios for the mafic phases are 0.11-2.60 and are particular high for the felsic portions of (1.98-3.96). Na_2O scatters progressively with a small inflection at ~68 wt% as SiO_2 increases, also showing a slight positive trend. P_2O_5 scatters progressively with a general increase then decrease as SiO_2 increases.

On the Alumina Saturation Index plot (Fig 5), the augen gneiss samples have high ASI values (>1) on the Alumina Saturation Index. This indicates a peraluminous feature and in the case of these samples, a general enrichment in K.

Table 1: Major element geochemical data presented with rock description and classification

Sample	Rock Unit	Classification	SiO ₂	TiO ₂	Al ₂ O ₃	Fe ₂ O ₃	FeO	MnO	MgO	CaO	Na ₂ O	K ₂ O	P ₂ O ₅	LoI	Total
13BO-06	Augen Gneiss	Granite	72.2	0.4	13.96	0.27	1.53	0.03	3.55	0.25	1.39	4.96	0.09	1.43	100
13BO-08	Augen Gneiss	Granite	77.6	0.21	11.51	0.79	1.19	0.02	0.21	0.73	2.12	5.28	0.07	0.4	100
13BO-09	Augen Gneiss	Granite	76.8	0.07	11.25	0.74	3.28	0.13	0.19	0.73	1.8	4.27	0.08	0.52	99
13BO-09a	Augen Gneiss	Granite	78.9	0.21	11.16	0.19	1.08	0.01	0.22	0.67	1.94	5.25	0.07	0.42	100
12BO-18	Augen Gneiss	Quartz Monzonite	65.4	0.56	14.5	4.05		0.04	0.89	1.44	2.3	5.64	0.07		
12BO-17	Augen Gneiss	Quartz Monzonite	71.3	0.25	15.45	1.63		0.01	0.63	0.71	2.2	8.72	0.21		
2014 OG1	Augen Gneiss	Granite	75.1	0.38	12.45	2.88		0.02	0.48	1.33	2.22	5.09	0.12		
13BO-02	Augen Gneiss	Granite	73	0.37	13.53	0.56	2.14	0.05	0.55	1.44	2.22	5.47	0.1	1.14	100
13BO-03	Augen Gneiss	Granite	74.5	0.46	12.58	0.54	1.93	0.02	0.71	1.45	2.33	4.63	0.1	0.94	100
13BO-04	Augen Gneiss	Granite	73.6	0.36	12.98	0.75	1.84	0.04	0.55	1.3	2.12	5.35	0.09	1.08	100
13BO-14	Mafic-Felsic Gneiss	Gabbro	48.8	0.43	17.06	3.01	7.95	0.21	8.13	11.3	1.69	0.19	0.04	0.98	99
13BO-13	Mafic-Felsic Gneiss	Gabbro	49.2	0.52	15.95	2.26	9.41	0.22	8.29	10.8	1.76	0.25	0.06	1.02	99
13BO-12	Mafic-Felsic Gneiss	Granodiorite	69.1	0.75	12.85	3.31	3.03	0.09	0.62	2.66	2.22	4.94	0.19	0.68	100
13BO-15	Mafic-Felsic Gneiss	Granodiorite	68.9	0.45	15.22	0.67	2.87	0.05	1.27	4.28	3.33	2.27	0.1	0.61	99
12BO-7	Mafic-Felsic Gneiss	Gabbro	47.8	0.4	16.4	12.45		0.2	8.78	10.4	1.61	0.32	0.04		
12BO-8	Mafic-Felsic Gneiss	Granite	72	0.28	14.5	2.38		0.01	0.83	3.24	3.2	2.24	0.01		
12BO-5	Mafic-Felsic Gneiss	Granodiorite	66.1	0.34	15.1	4.18		0.07	1.93	4.35	3.22	2.48	0.11		
12BO-6	Mafic-Felsic Gneiss	Gabbro	52.6	0.85	15.4	11.55		0.17	7.07	9.79	2.42	1.7	0.11		
12BO-03	Mafic-Felsic Gneiss	Granite	76.8	0.51	12.35	2.86		0.01	0.68	1.44	2.26	4.42	0.11		
12BO-05	Mafic-Felsic Gneiss	Monzo-diorite	50.3	0.64	30.7	2.29		0.05	5.4	0.25	1.41	3.68	0.18		
12BO-12	Metasediment	Diorite	61.8	0.93	17.3	7.4		0.03	3.53	0.09	0.56	3.79	0.1		
2014 MS1	Metasediment	Granodiorite	65.2	0.63	17.75	4.41		0.01	3.74	0.08	0.79	4.69	0.05		
13BO-07	Metasediment	Granodiorite	62.1	0.45	19.51	0.43	3.56	0.04	8	0.11	0.74	3.72	0.08	1.1	99

Table 2: Trace element geochemical data for samples of this work

Sample	13BO-06	13BO-08	13BO-09	13BO-09a	12-BO-18	12-BO-17	2014 OG1	13BO-02	13BO-03	13BO-04	13BO-14	13BO-13	13BO-12
Ga	20.18	18.11	17.35	15.92	19.9	16	18.2	17.71	18.83	18.12	13.51	13.94	18.27
Rb	408.19	574.07	388.82	541.88	468	521	422	402.23	378.63	427.78	3.90	3.12	191.52
Sr	9.19	18.68	22.20	26.03	65.5	126	60.4	53.58	43.09	38.96	46.62	46.85	93.12
Y	37.55	61.22	281.45	25.12	65.3	54.8	29.9	45.12	38.90	30.47	15.58	19.04	53.33
Zr	215.42	123.55	147.64	109.16	269	97	198	213.34	230.64	137.06	20.54	31.45	438.04
Nb	12.15	12.63	5.23	11.12	15.8	14.2	12.5	10.92	14.14	12.81	1.01	1.54	15.22
Ba	200.73	96.79	82.24	86.16	436	789	323	335.80	282.11	287.96	23.35	33.91	458.03
La	41.37	44.65	77.10	39.07	71.1	31.9	39.2	46.75	57.69	37.41	1.64	2.60	40.65
Ce	86.47	101.74	188.63	86.83	151	65.6	99.3	94.92	119.56	82.47	3.69	5.88	90.03
Pr	9.83	11.84	23.42	9.99	17.05	7.56	9.31	10.75	13.54	9.45	0.52	0.79	10.96
Nd	33.93	40.18	81.67	34.00	58.6	25.8	31.7	36.96	46.21	33.15	2.46	3.59	41.46
Sm	7.13	9.46	19.84	7.71	12.4	6.14	6.32	7.62	9.34	7.15	0.96	1.38	9.28
Eu	0.80	0.30	0.26	0.28	0.97	0.96	0.63	0.82	0.71	0.59	0.42	0.49	1.44
Gd	7.18	9.67	22.77	7.46	11.25	7.45	5.91	7.67	9.07	6.92	1.95	2.49	10.23
Tb	1.17	1.74	5.06	1.15	1.8	1.36	0.98	1.28	1.40	1.15	0.41	0.51	1.64
Dy	6.99	10.91	41.43	5.86	10.6	8.63	5.66	8.08	7.72	6.76	2.94	3.77	10.15
Ho	1.40	2.21	10.39	0.96	2.23	1.91	1.07	1.73	1.48	1.27	0.67	0.87	2.08
Er	3.99	6.53	35.25	2.32	6.46	5.19	2.7	5.23	3.97	3.52	2.10	2.67	5.95
Tm	0.55	0.90	5.47	0.28				0.76	0.53	0.46	0.31	0.38	0.79
Yb	3.37	5.43	34.99	1.53	6.38	3.35	1.92	4.72	3.11	2.76	1.98	2.50	4.83
Lu	0.49	0.75	4.78	0.21	0.9	0.4	0.23	0.67	0.44	0.38	0.31	0.39	0.69
Hf	6.76	4.02	5.05	3.79	8.1	2.7	6.1	6.65	7.27	4.34	0.64	0.96	11.71
Pb	16.38	44.38	46.83	39.65				38.87	31.01	37.10	1.27	1.41	12.14
Th	40.28	55.20	118.49	49.25	78.1	25.3	49.1	38.79	49.58	35.70	0.22	0.52	5.00
U	5.50	19.44	17.97	9.10	10.9	2.19	4.62	7.67	7.58	9.63	0.10	0.21	1.47

Table 3: Trace element geochemical data for samples of this work

Sample	13BO-15	12BO-7	12BO-8	12BO-5	12BO-6	12BO-03	12BO-05	12BO-02	13BO-10	13BO-11	12BO-12	2014 MS1	13BO-07
Ga	18.48	14.8	19	18.6	18.3	17.4	40.3	16.5	28.10	27.52	29.1	31.2	31.01
Rb	128.96	12.1	155.5	110	142	394	296	441	165.63	252.40	287	240	459.59
Sr	147.24	50.3	322	254	78	48.4	9.6	52.8	41.42	67.03	21.6	30.1	8.45
Y	13.09	21.3	4.4	25.2	31.7	55.4	134.5	47.1	67.92	24.72	41.6	23.7	44.72
Zr	163.73	19	373	115	87	238	512	142	277.33	213.21	341	211	257.72
Nb	7.95	1.2	8.2	7.6	4.9	13.6	31.3	10.7	71.52	21.26	18.3	16	14.53
Ba	294.28	32.6	396	489	203	287	241	345	235.99	700.72	519	688	185.81
La	19.53	2.4	15.6	22.2	13.5	60.7	31.7	38.6	70.94	68.97	75.6	61.1	70.29
Ce	36.31	5	20.1	44.1	29.5	128.5	70.1	77.4	140.10	133.14	138	117.5	145.90
Pr	3.97	0.63	1.83	4.9	3.71	14.25	8.29	8.41	16.02	15.25	14.4	13.1	16.60
Nd	14.00	3	5.3	18.2	15.1	48	28.6	28.6	55.95	53.32	50	47.6	56.66
Sm	2.75	1.14	0.67	3.52	3.7	10.05	7.17	6.39	10.91	9.64	8.62	8.2	11.54
Eu	0.95	0.45	0.54	0.81	1.02	0.72	0.56	0.8	1.24	1.98	1.39	1.57	0.78
Gd	2.78	2.4	0.68	3.91	4.73	9.49	11.35	6	10.57	8.07	7.54	6.27	10.52
Tb	0.43	0.47	0.1	0.65	0.82	1.61	2.43	1.15	1.76	1.08	1.17	0.89	1.57
Dy	2.49	3.47	0.65	4.04	5.35	9.09	17.55	7.26	11.17	5.55	7.08	4.66	8.77
Ho	0.51	0.78	0.14	0.86	1.17	1.9	4.39	1.57	2.41	0.96	1.44	0.87	1.65
Er	1.46	2.34	0.43	2.54	3.46	5.01	13.75	4.69	7.53	2.51	4.17	2.28	4.52
Tm	0.20								1.08	0.33			0.60
Yb	1.32	2.42	0.49	2.43	3.19	4.01	13.7	4.04	6.71	1.93	3.99	2.05	3.56
Lu	0.20	0.36	0.07	0.36	0.5	0.58	2.01	0.61	0.97	0.28	0.57	0.28	0.51
Hf	4.48	0.7	10.1	3.2	2.5	6.8	15.2	4.3	8.00	5.85	9.2	5.7	8.15
Pb	7.11								15.78	16.04			13.88
Th	1.74	1.04	0.85	11.45	3.17	63.2	107	34.3	36.33	26.72	28.1	23.4	56.84
U	0.62	0.27	2.07	0.87	1.32	9.54	17.5	6.56	5.77	4.39	3.6	3.69	6.65

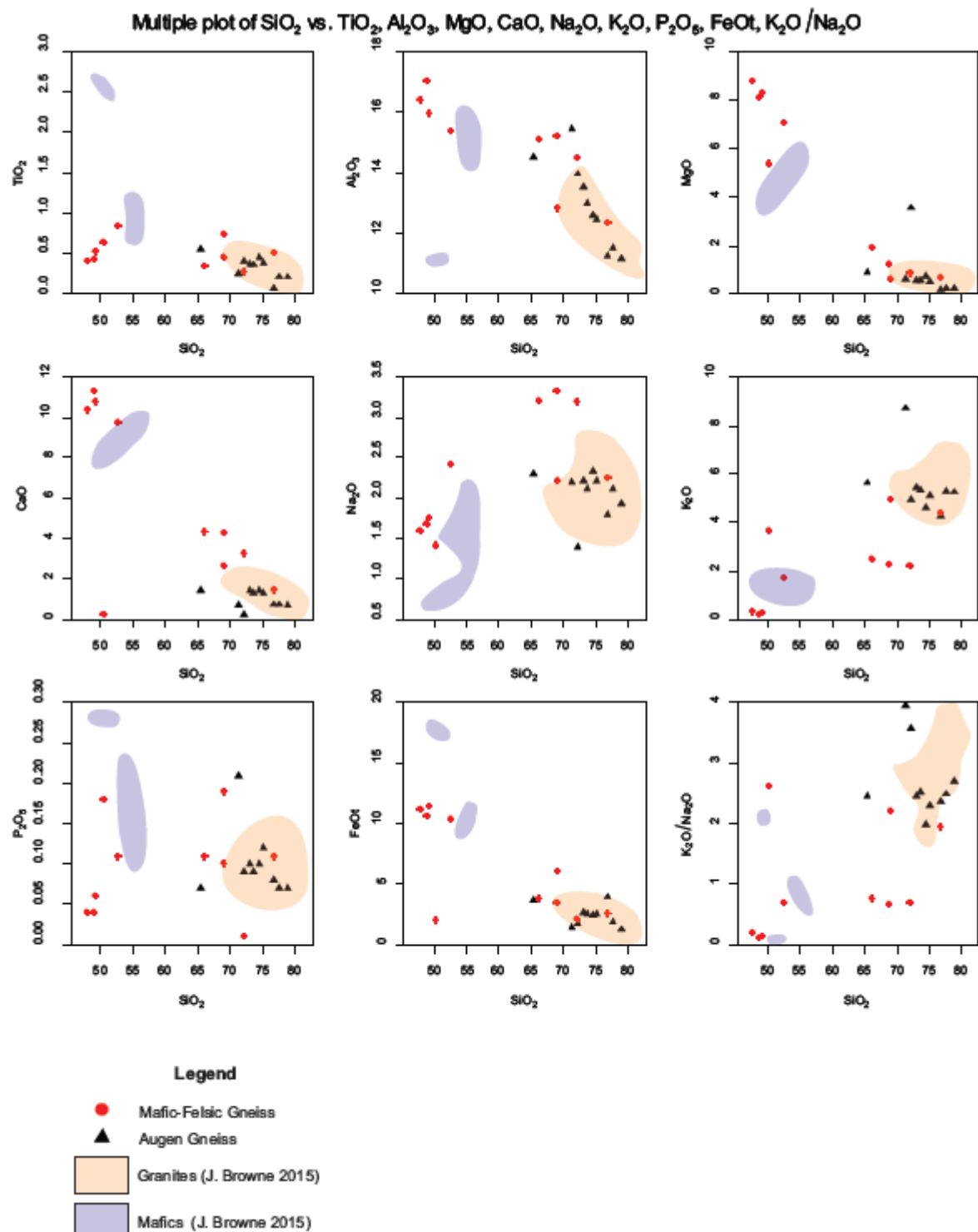


Figure 6: Harker variation diagrams illustrating major element characteristics of the Arunta Region. Major elements vs SiO_2 are analysed with samples plotted as per legend and fields showing similarities of each of granitic and mafic rocks from the Anmatjira Range (Browne 2015).

Trace and Rare Earth Elements

Trace element geochemical results can be seen in table 2 and figure 7.

Trace elements U, Th, Rb, Zr all define positive correlations for the full compositional range from gabbroic to granitic.

Trace and REE multi-element spiderplots normalised to primitive mantle and chondrite following McDonough & Sun (1995) and Boynton (1984) respectively, are presented in (Fig. 8). Trace element spiderplots show the trace elements are all enriched compared to primitive mantle. The augen gneiss samples display coherent REE patterns characterised by relative enrichment of ($\text{sumREE} = 130.8\text{--}370.8$). The mafic-felsic samples have less enrichment of REE ($\text{sumREE} = 12.8\text{--}251.4$). The elements Cs, Rb and Ba yield a negative anomaly, and the HFSE elements Nb, Sr and Ti show large negative anomalies, particularly for the high-K granitoids. In comparison, Pb, U and Th show high values compared to primitive mantle.

REE multi-element diagrams normalised to chondrite following Boynton (1984) are presented in (Fig. 8). It can be observed that the granites display strongly fractionated REE compositions with a steep REE pattern compared with chondrite. All samples show enrichments and moderately steep REE patterns where they are relatively enriched in light REE, with noticeable negative Eu anomalies ($\text{Eu/Eu}^* = 0.03 = 0.92$).

Two samples of the composite mafic-felsic gneiss, however differentiate from this pattern. Their REE signatures are the least fractionated and are relatively depleted in REE in comparison to the other samples, having an overall flatter REE pattern and positive European anomalies ($\text{Eu/Eu}^* = 1.04$ and 2.42).

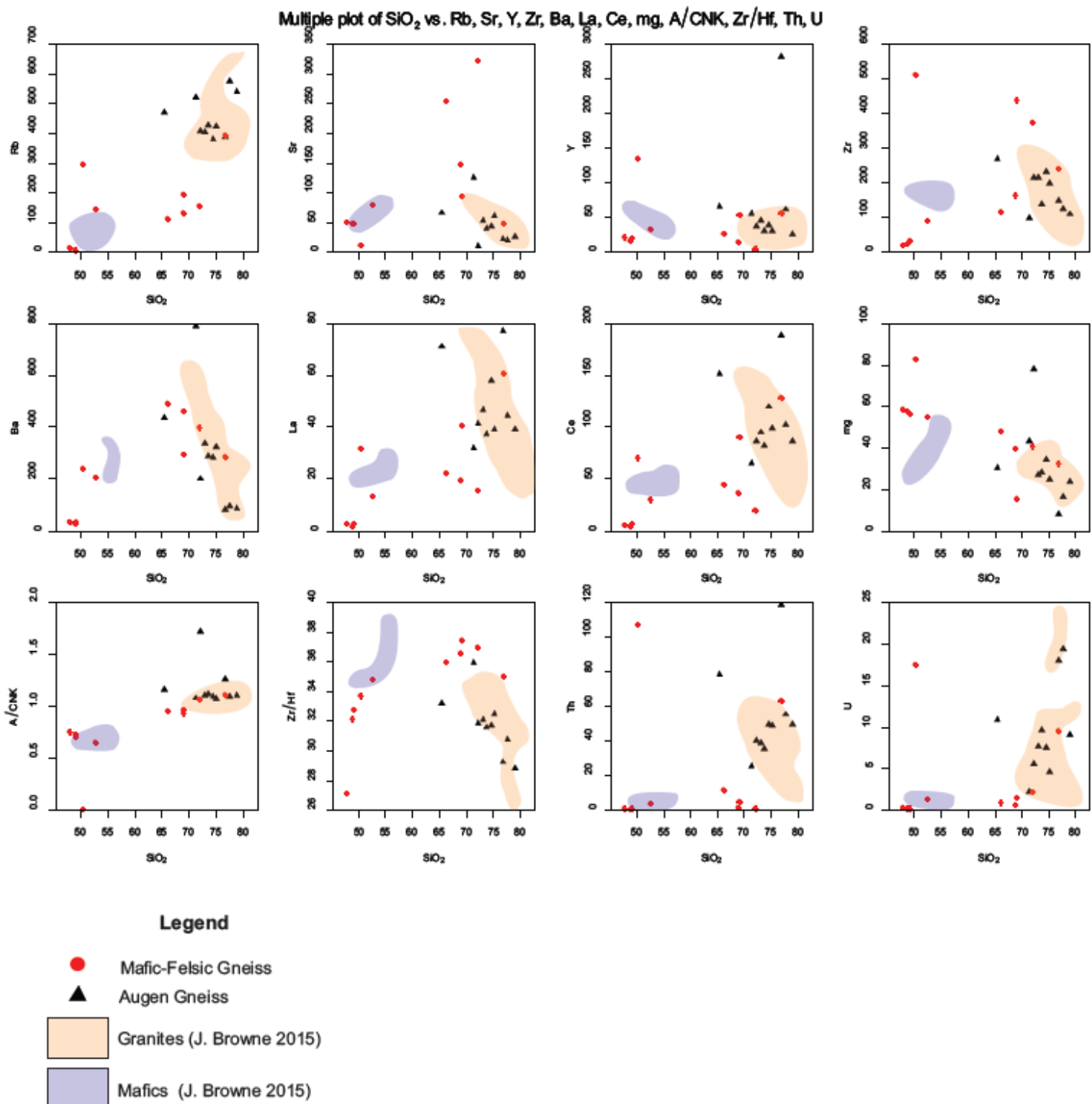


Figure 7: Harker variation diagrams illustrating selected trace element variations in the Arunta Region. Samples are plotted vs SiO_2 as per legend and fields showing similarities of each of granitic and mafic rocks from the Anmatjira Range (Browne 2015).

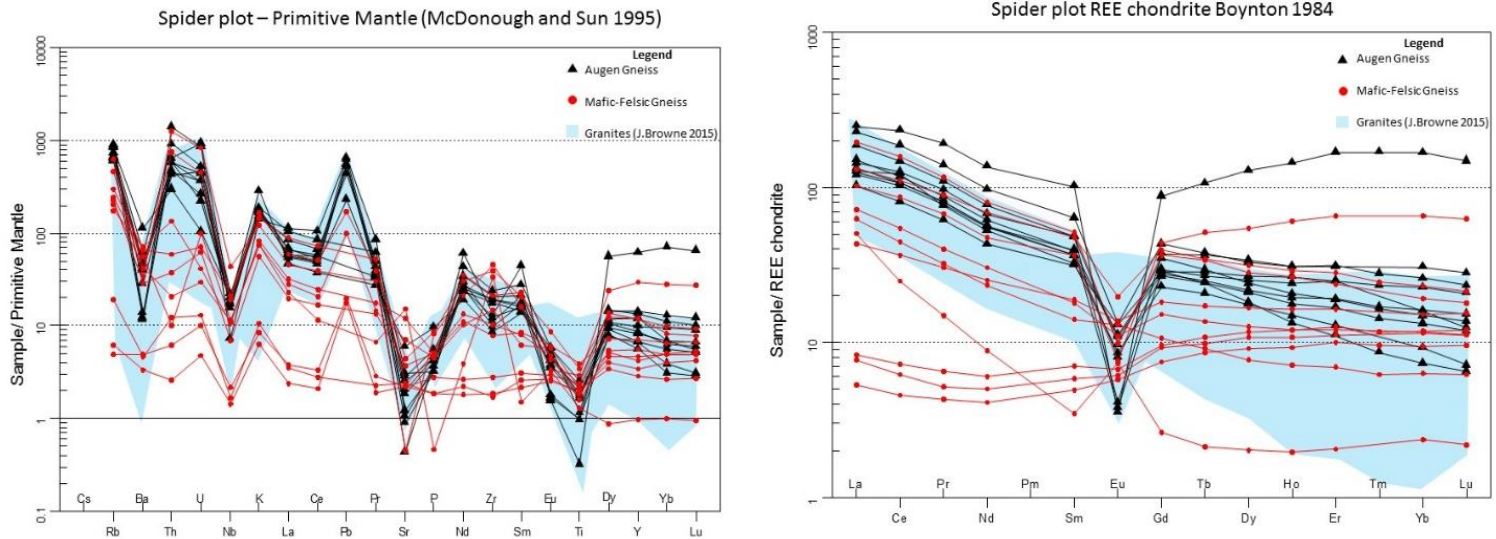


Figure 8: Spiderplots of trace and rare earth elements normalised to Primitive Mantle (McDonough and Sun 1995) and Chondrite (Boynton 1984) respectively. Nineteen elements are arranged in order of increasing compatibility with respect to a small percentage melt of the mantle and are plotted on a logarithmic scale.

SM-ND ISOTOPE SYSTEMATICS

Sm-Nd isotope results for 10 of the Boothby samples are presented in Table 3 and Fig 9. Initial ϵ_{Nd} values are calculated at the estimated magmatic age of 1806 Ma (Worden et al., 2008). Nd isotope data expressed as ϵ_{Nd} are plotted against age for the 10 data points in (Fig. 9), along with additional ϵ_{Nd} datasets for granitoids from the Anmatjira Region (Browne 2015). Average crustal evolution lines for proximal basement terrains are indicated, including the isotopic evolution of the ca. 2510 Ma Tanami region Billabong complex, ca. 1837 Ma Lander Formation and Stafford beds as well as depleted mantle and CHUR evolution lines. The ϵ_{Nd} values range from 1.37 to -26.45, with $^{143}\text{Nd}/^{144}\text{Nd}$ ratios 0.50999–0.1131 for all samples plotted (Fig. 9).

Table 4. Sm-Nd isotopic data for selected Mt Boothby samples

Sample	Input Age (Ma)	Rock Description	Nd (ppm)	Sm (ppm)	$^{147}\text{Sm}/^{144}\text{Nd}^a$	$\varepsilon\text{Nd}_{(T=0)}$	$^{143}\text{Nd}/^{144}\text{Nd}^a$	$2s^a(x1E-6)$	$\varepsilon\text{Nd}_{(T)}$	T_{DM} (Ma) ^b
13BO-6	1806	Augen Gneiss	33.9	7.1	0.1233	-20.18	0.510138	8	-3.2	2572
13BO-8	1806	Augen Gneiss	40.1	9.4	0.1391	-16.69	0.510128	9	-3.4	2752
13BO-2	1806	Augen Gneiss	36.9	7.6	0.1212	-20.96	0.510122	7	-3.5	2581
13BO-3	1806	Augen Gneiss	46.2	9.3	0.1190	-21.11	0.510140	9	-3.1	2533
13BO-14	1806	Mafic-Felsic	2.4	0.9	0.2282	8.70	0.510372	10	1.3	-732
13BO-13	1806	Mafic-Felsic	3.5	1.3	0.2173	4.40	0.510280	10	-0.4	-16016
13BO-12	1806	Mafic-Felsic	41.4	9.2	0.1328	-16.25	0.510226	9	-1.4	2499
13BO-15	1806	Mafic-Felsic	14.0	2.7	0.1150	-19.47	0.510271	11	-0.5	2305
2014 MS1	1806	Metasediment	47.6	8.2	0.1054	-26.45	0.511281	1	-5.3	2598
12BO-12	1806	Metasediment	50	8.6	0.1032	-25.80	0.511314	2	-4.1	2501

^a Isotope error measurements are 2 SE. $^{143}\text{Nd}/^{144}\text{Nd}_{\text{CHUR}}(0) = 0.512638$, $^{147}\text{Sm}/^{144}\text{Nd}_{\text{CHUR}}(0) = 0.1967$. CHUR= chondritic uniform reservoir

^b Depleted mantle model ages as per (Goldstein et al., 1984): $^{143}\text{Nd}/^{144}\text{Nd} = 0.51315$, $^{147}\text{Sm}/^{144}\text{Nd} = 0.2145$.

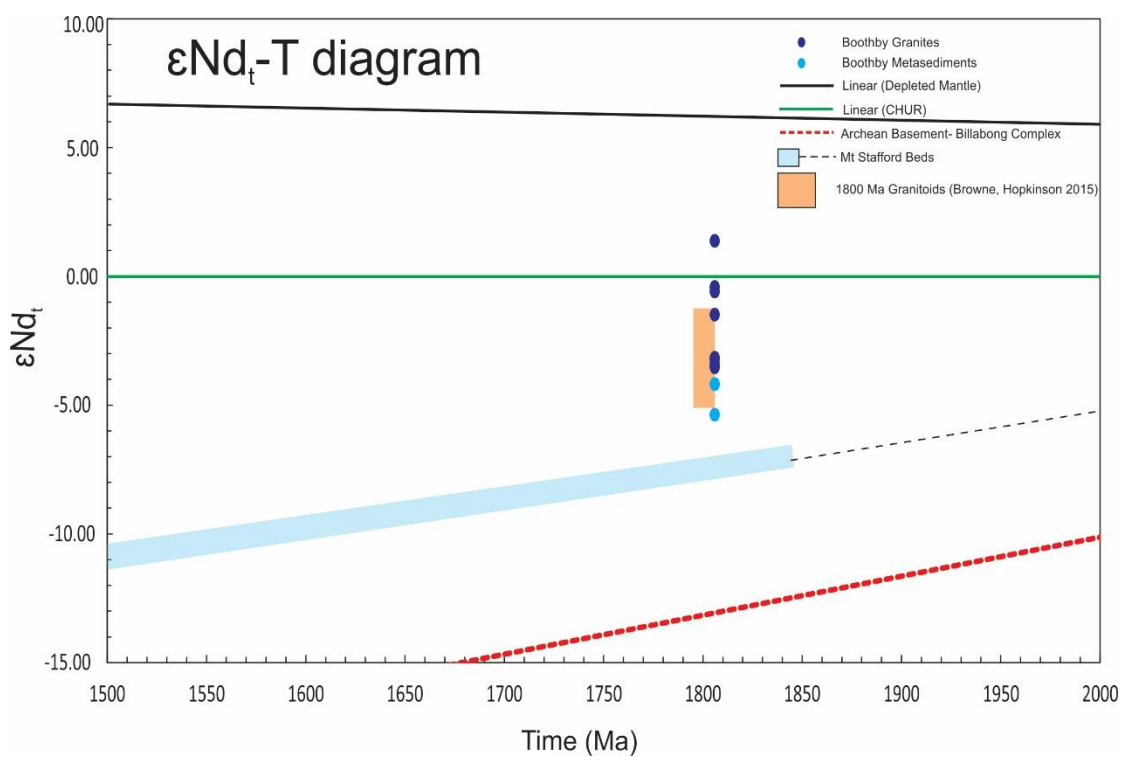


Figure 9: ε_{Nd} vs time evolution diagram comparing samples from this work. A field of granite samples from the Anmatjira Range (Browne, Hopkinson 2015) are shown for comparison. The general trend of ε_{Nd} with time for these granites. The Archean crust evolution is shown including Depleted Mantle, Chur and a general trend for the underlying Mt Stafford beds.

Heat Production

Heat production values using K%, U (ppm) and Th (ppm) calculated at crystallisation age are displayed in Appendix B. Fig 10 shows all geochemical data points from this work and additional data obtained from Geoscience Australia's online OZChem database of Archean basement rocks of the Arunta region as well as granitoids from the Anmatjira Range from Browne (2015). Lower, upper and whole crustal averages of 0.85, 1.68 and 1.27 μWm^{-3} (Wedepohl 1995) and a Post Archean Average Shale composite value of 2.15 μWm^{-3} (Taylor & McLennan 1985) are also included in the calculations.

Heat production values calculated for the Boothby Orthogneiss and the surrounding Lander Formation show that the region is enriched in heat producing elements. The Lander Formation samples have heat production around 3.8 μWm^{-3} , nearly twice the value of the post-Archean average shale (PAAS). The Boothby augen gneiss on average is around 6.84 μWm^{-3} , but ranges up to 14. It is similar in HPE enrichment to the Anmatjira and Aloolya Gneiss. Datasets analysed can be found in Appendix B.

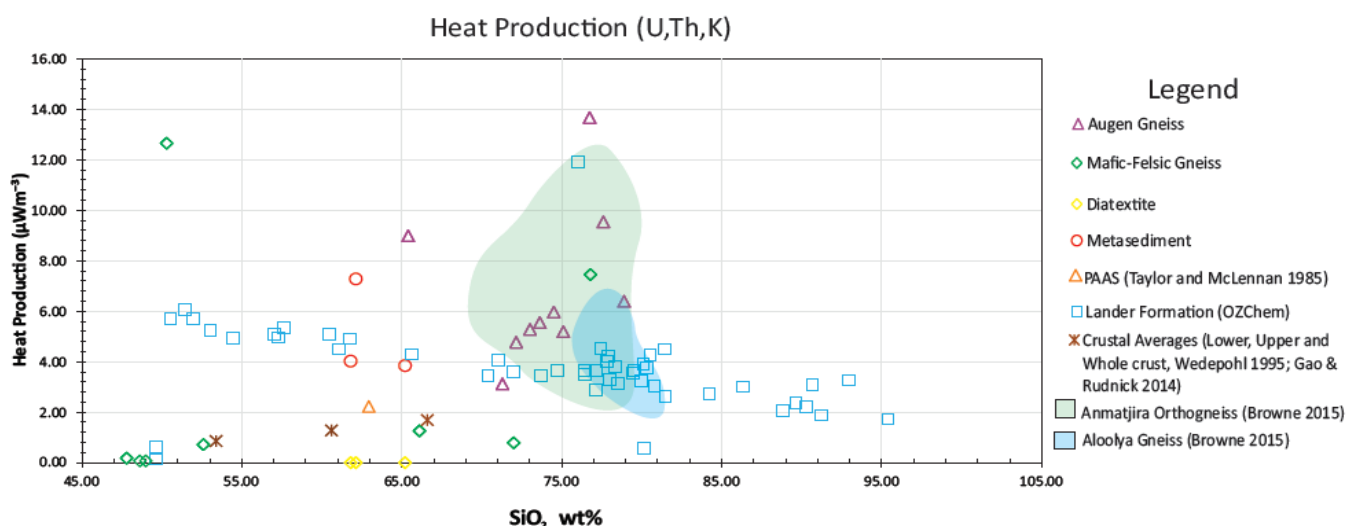


Figure 10: Heat production graph showing all data points from this study and geochemical data from the Geoscience Australian Ozchem database, global crustal averages (Wedepohl 1995; Gao & Rudnick 2014) and PAAS (Taylor & McLennan 1985) are shown as data points. Granitoids from the Anmatjira range are shown as fields (Browne 2015).

Zircon Saturation Temperature

Zircon inheritance in granites makes an assumption that the ability of granitic melts to access zircons in the source region allowed a zirconium saturation criterion to develop (Miller et al., 2003). Provided the granite genesis was not able to dissolve all the zircon, an assumption can be made where a temperature can be calculated from various calibrations that look at the relationship between granitic chemistry and zirconium content of the granites. Following previous calibrations (Watson & Harrison 1983), the updated zircon solubility calibration of (Boehnke et al., 2013) was used to calculate zircon saturation temperatures (T_{zr}) for both the augen gneiss and mafic-felsic samples.

$$(\text{Eqn 1}): \ln D_{\text{Zr}} = (10108 \pm 32)/T(\text{K}) - (1.16 \pm 0.15)(M-1) - (1.48 \pm 0.09) \quad (\text{Boehnke et al., 2013})$$

Where D_{Zr} is the concentration ratio of Zr in zircon to Zr in the melt, M is the cation ratio $(\text{Na} + \text{K} + 2.\text{Ca})/(\text{Al}.\text{Si})$, and T is the temperature. M values must be from 1-2 for an appropriate application of this equation. The Zr-saturation temperature ranges from 456–845.3°C for the granitic melt. The average Zr-saturation temperature yields a maximum temperature for the granite of 776°C for the augen gneiss samples and 644°C mafic-felsic samples (Fig. 11).

Table 5. Zircon saturation temperatures for selected samples of the Boothby granitoids

Sample	Rock Unit	Zr (ppm)	TZr (°C)	M value
13BO-06	Augen Gneiss	215	845	0.83
13BO-08	Augen Gneiss	123	733	1.22
13BO-09	Augen Gneiss	147	774	1.03
13Bo-09a	Augen Gneiss	109	724	1.19
2012-BO-18	Augen Gneiss	269	813	1.25
2012-BO-17	Augen Gneiss	97	687	1.43
2014 OG1	Augen Gneiss	198	773	1.30
13BO-02	Augen Gneiss	213	784	1.27
13BO-03	Augen Gneiss	230	797	1.24
13BO-04	Augen Gneiss	137	735	1.30
13BO-14	Mafic-Felsic Gneiss	20.5	459	2.92
13BO-13	Mafic-Felsic Gneiss	31.4	489	2.81
13BO-12	Mafic-Felsic Gneiss	438	826	1.58
13BO-15	Mafic-Felsic Gneiss	164	723	1.55
12BO-07	Mafic-Felsic Gneiss	19	456	2.91
12BO-08	Mafic-Felsic Gneiss	373	837	1.36
12BO-05	Mafic-Felsic Gneiss	115	679	1.66
12BO-06	Mafic-Felsic Gneiss	87	527	3.15
12BO-03	Mafic-Felsic Gneiss	238	800	1.25

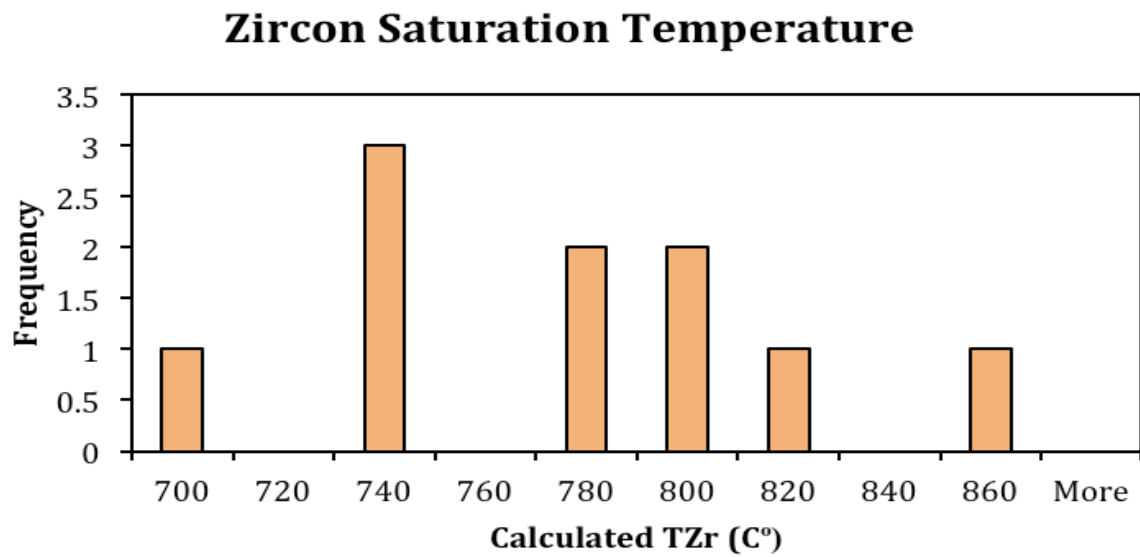


Figure 11: Zircon Saturation Temperature graph based on statistical analyses from (Boehnke et al., 2013) on geochemical data from the Boothby granitoids.

GEOCHRONOLOGY

In situ U-Pb zircon geochronology data was undertaken on samples 13-BO-12, MB08-18, 12-BO-12 and OSM from the Mafic-Felsic Gneiss, Boothby Orthogneiss, and two Metasedimentary units, respectively. Individual analyses for each sample are provided in Appendix C. Fig. 13 presents comparative probability density histograms for samples from this work and compiled published data. Zircon morphologies are shown as Cathodoluminescence (CL) images in Fig. 12. Based on CL images, inherited ages are interpreted as cores surrounded by oscillatory zoning and metamorphic rims (Corfu et al., 2003). Only concordant ages <10% are plotted, >10% discordant spots were removed due to data having low Th/U and high common lead (>0.001 $^{204}\text{Pb}/^{206}\text{Pb}$).

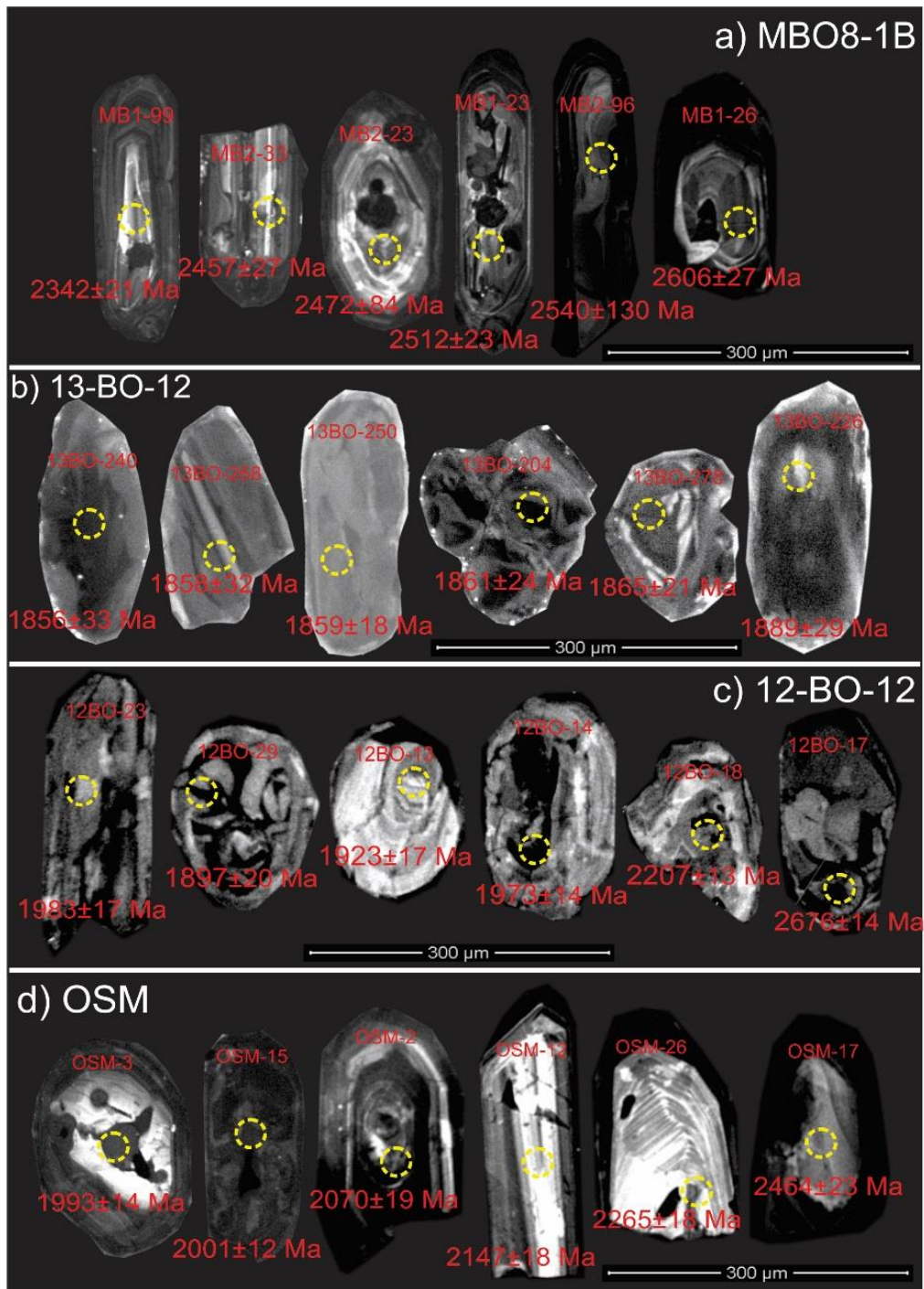


Figure 12: Selected CL images of variable zircon morphologies with corresponding inherited ages yielded and sample number.

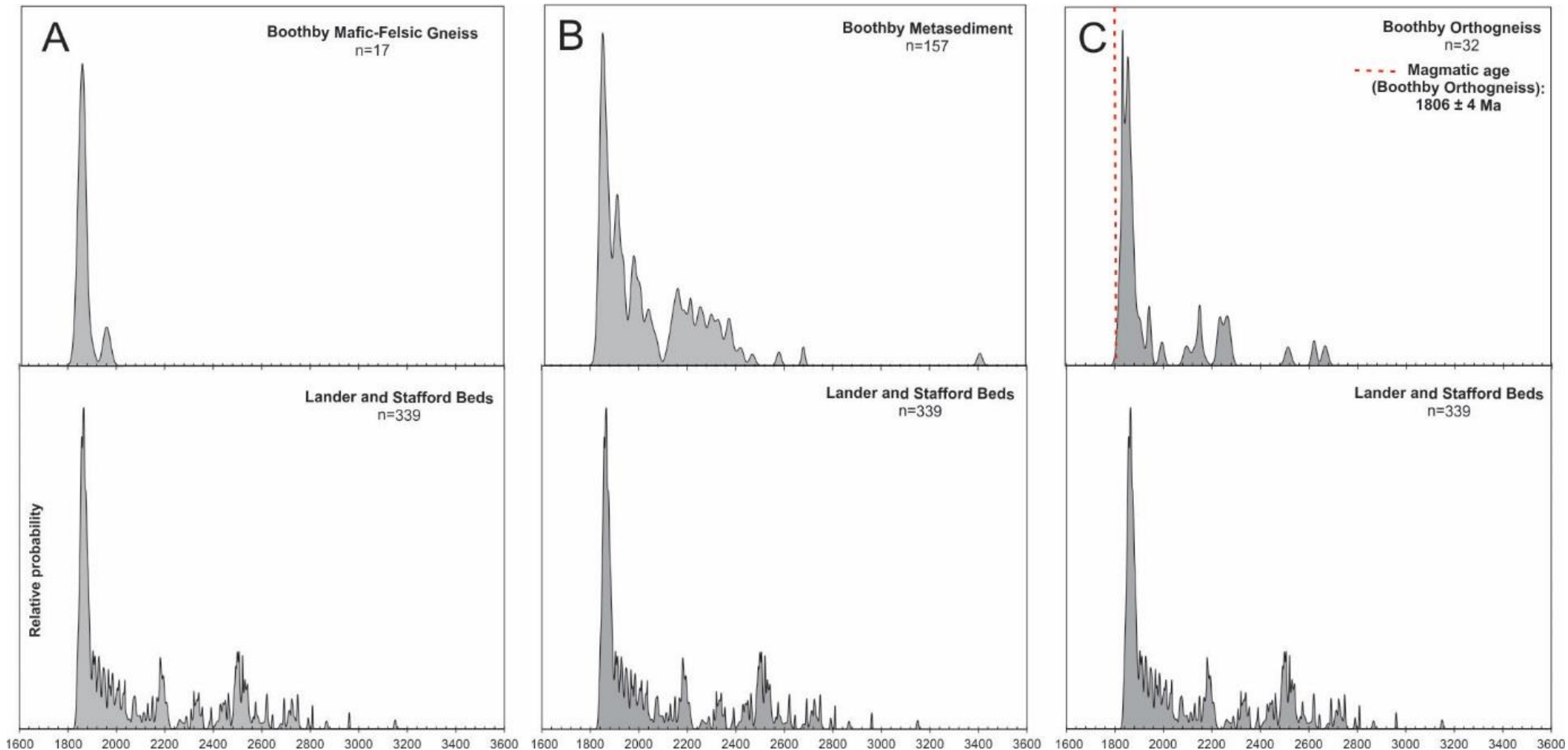


Figure 13: Comparative Probability Histograms comparing $^{207}\text{Pb}/^{206}\text{Pb}$ ages for the Lander formation and Stafford beds (Claoue-Long et al., 2008; Claoue-Long 2008; Claoue-Long & Edgoose 2008) with zircon ages from samples of this work compiled with published ages (Worden et al., 2008; Howlett et al., 2015).

Zircons from sample 13-BO-12 are 80–200 µm in size, dominated by euhedral-subhedral and some sub-rounded grains. Complex internal zoning patterns are revealed by catholuminescence imaging where core-rim relationships are rare. The internal structure of these igneous grains show mainly dark and metamict/recrystallization textures, with minimal grains indicating clear preserved internal zoning. However, there are some grains with subtle oscillatory zoning. Zircon is abundant within the matrix of this sample with a Zr content of 438 ppm (Table 2) and 805 grains picked, though often difficult to target inherited cores for geochronological analysis due to the metamict nature of the grains. 798 analyses were done, where a clear population of 11 zircons was interpreted to be xenocrystic based on their ages and appearance in CL.

Zircons from sample MB08-18 are 80–150 µm in size and have typically subhedral-anhedral grains. Dark-medium response oscillatory zoned and metamict zircons are in abundance under CL, where precursor cores are present but are often mantled by oscillatory-zoning, typical of magmatic growth (Corfu et al., 2003). 188 analyses were done, where the population of xenocrystic zircons were found to be discordant >10%. As such, an inherited age has not been calculated for the grains in this sample, rather this sample is solely to demonstrate the presence of similarly aged grains to the compiled data (Howlett et al., 2015) and (Worden et al., 2008).

Two samples of the Boothby Metasedimentary Gneiss were selected for U-Pb dating; 12-BO-12 and OSM respectively. Zircon morphology for sample 12-BO-12 is euhedral-subhedral, with dominant oscillatory zonation which range from pristine zoning to disrupted and convoluted patterns. Only 26 zircon grains were found to be

within 10% concordancy. Detrital ages occur at 1828 and 1761 Ma, with minor peaks at 2768, 2208, 2158, 2030 and 1978 Ma. The 23 youngest detrital zircon grains provide a mean weighted average maximum depositional age of 1830 ± 44 Ma (MSWD = 36). Maximum depositional ages of the metasediments were determined to constrain the deposition of the sedimentary protolith. The Boothby OSM sample shows similar zircon morphology to 12-BO-12, with more sub-rounded grains and oscillatory zone banding slightly thicker and darker. 53 zircon grains were analysed, and 49 were less than 10% discordant. Prominent Archean activity peaks of variable duration are evident. Dominant age peaks occur at 1993, 1904 and 1836 Ma with minor peaks at 2462, 2268, 2145 and 2069 Ma. The 32 youngest detrital zircon grains give a mean weighted age 1835 ± 22 Ma (MSWD= 11.9), which can be considered the maximum depositional age. The metasediment and granite samples were plotted against the Lander Formation to see if they share provenance affinities, along with compiled data from (Howlett et al., 2015) and (Worden et al., 2008).

DISCUSSION

Source nature of Boothby Granitoids

The Boothby augen gneiss samples are geochemically characterized by a high Alumina Saturation Index ($A/CNK > 1$), which indicates the strong peraluminous nature of the granitoids. This gives a first order constraint their magma sources were dominated by metasedimentary rocks (Miller 1985). The enrichment of Ba and Rb relative to Sr, and high K_2O values also support that a metasedimentary source was important in the generation of the Boothby Orthogneiss (Clemens & Wall 1981). The Boothby augen gneiss samples have low CaO/Na_2O (0.17–0.64), high Rb/Sr (4.13–

44.43), high $\text{Al}_2\text{O}_3/\text{TiO}_2$ (25.89–160.71) and $\text{K}_2\text{O}/\text{Na}_2\text{O}$ values > 1 . Such characteristics indicate that they were derived from a plagioclase-poor and clay-rich pelitic source, whereas the mafic-felsic samples are likely derived from a plagioclase-rich and clay-poor psammitic source (Chappell 1999; Sylvester 1998). Fractional crystallization processes were important in both the Boothby augen gneiss and mafic-felsic gneiss. This is suggested by decreasing concentrations of CaO , FeOt , MgO , TiO_2 , Al_2O_3 , Zr , Sr , and Ba with increasing SiO_2 inferring fractional crystallization of biotite, K-feldspar, plagioclase and zircon. The mafic-felsic gneiss had two samples with positive Eu anomalies (Eu/Eu^* : 1.04 and 2.42) and also contained relatively low REE content compared to the other samples, inferring a slightly more mafic source region and less significant intracrustal fractionation. The augen gneiss samples contain large negative Eu anomalies (Eu/Eu^* : 0.03–0.43) and higher LREE abundances (La_N/Yb_N 1.48–17.21) consistent with rocks that have undergone a high degree of intracrustal melting and fractional crystallization (Taylor & McLennan 1985), particularly of LREE-enriched accessory phases. Differences in trace element ratios (Rb/Sr , Sr/Ba) and REE abundances between the two granitoid types from the Boothby region are likely related to differences in source and/or depth of melting, and different proportions of plagioclase, garnet and biotite in the source (Jung at al., 1998). Granites in the Arunta region have been subdivided into three main groups based on their geochemistry; the Calcalkaline-trondhjemite Group (CAT), High heat-production Group (HHP) and the Main Group (Zhao & McCulloch 1995, Giles et al., 2002). The Boothby granitoids have similar geochemical signatures to the ca. 1800 Ma granitoids of the Anmatjira Range (Browne 2015), both geochemically analogous to the volumetrically significant Main Group, which occurs throughout the Arunta region. The characteristic high-Y and Sr-depleted geochemical compositions of most

of the U-Th rich granites in the NAC is seen in the Boothby granitoid samples, suggesting these granites were derived from relatively shallow sources (Wyborn et al., 1992).

U-Pb zircon analysis suggest that the potential source of the Boothby Orthogneiss is similar in composition to the exposed metasedimentary Lander Bed Formation based on the overlap of detrital patterns in the Lander Formation with the inherited zircon patterns in the Boothby granitoids. This infers a reasonably strong argument that metasedimentary units underlying the Lander Formation was derived from a source quite similar to the Lander Formation source, is likely to be what sourced the Boothby intrusive complex. The Lander Formation and its equivalents at depth were sourced from earlier Proterozoic and Archean crustal components and were derived from older continental crust, reflected isotopically as evolved felsic crust. There is a lack of knowledge on the metasedimentary components in the mid-lower crust due to the absence of exposure of units below the Lander Formation (Scrimgeour 2013). The dominant detrital zircon population for the Lander Formation occurs over a relatively small Paleoproterozoic (1880–1840) Ma age range, comprising 40% of detrital ages. Other subordinate detrital populations are 2175–2205 Ma, 2305–2355 Ma and 2490–2550 Ma. The U-Pb inherited zircon ages of all the samples analysed overlap this prominent detrital age peak (1880–1840 Ma). The Boothby Orthogneiss shows a distinct overlap of the Lander Formation and Stafford beds in the main peak at 1880–1840 Ma with older subordinate Archean populations.

Sm-Nd Isotope systematics

Sm-Nd isotopes can be used to determine the source region and the contribution of crustal and mantle material in magma generation. The Boothby granitoids indicate progressive crustal input with magmatic evolution, as a result of increasingly negative $\epsilon_{\text{Nd}}(t)$ values with increasing SiO_2 , particularly for the Boothby augen gneiss samples with the highest SiO_2 content ~73 wt.%. This suggests fractional crystallization and assimilation of the wall rock during magma evolution. One sample of the boothby mafic-felsic gneiss has a more juvenile ϵ_{Nd} value than the other granitoids, suggesting some mantle input from a mafic source component. Fields of the Proterozoic Stafford beds and the Archean Billabong complex have been plotted as likely source regions. These possible source regions are significantly more evolved than all the Boothby samples analysed, therefore it is unlikely that these granitoids represent direct in-situ partial melting of lower to mid-crust. Therefore, two or more end member source regions are required to produce the range in isotopic compositions. The initial ϵ_{Nd} isotopic values for the Boothby granitoids are heterogeneous, with a range in values of -3.5 to 1.4 at 1806 Ma. This suggests mixing between a Palaeoproterozoic mantle component and older crustal sources containing a heterogeneous geochemical signature, together with large amounts of fractional crystallization, required to produce the trace element and isotopic characteristics of the Proterozoic granites within this terrain. The similar ϵ_{Nd} values for other Proterozoic granitoids in the Anmatjira Range (Browne 2015) suggests that these lithologies contain similar proportions of crust and mantle source material. Mantle input into the source region of these earliest high heat-producing granites of central

Australia was clearly part of their generation, providing high thermal energy required for large proportions of crustal melting in the Boothby region.

Heat Production

Heat flow data provides an insight into the geochemistry of the crust as they constrain the abundance of the heat producing elements U, Th and K in the lithosphere (Taylor & McLennan 1985; McLennan & Taylor 1996). Heat production values calculated for the Boothby Orthogneiss and the surrounding Lander Formation show that the region is enriched in heat producing elements. In order to evaluate the cause of these elevated heat production values, the relative contribution of mantle heat flow and crustal heat production are constrained using geochemical datasets.

The Boothby augen gneiss on average is around $6.84 \mu\text{Wm}^{-3}$, but ranges up to 14. It is similar in HPE enrichment to the Anmatjira and Aloolya Gneiss. The HPE enrichment evident in the Boothby granitoids suggests progressive extraction of the heat-producing elements from a mid-lower crustal source, which was an already pre-enriched source. Heat production values generally increase with increasing silica content in magmatic rocks, with averages of 0.1 for basalts and 2.5 for granites (Fowler 1990), which suggests that the metasedimentary source of the Boothby complex is relatively hotter than normal post-Archean sediment. This is supported by the Lander formation heat production values of around $3.8 \mu\text{Wm}^{-3}$, nearly twice the value of the Post-Archean Average Shale (PAAS). This trend is also seen in the augen gneiss samples, which show a significant increase with increasing SiO_2 content.

Zircon Saturation Thermometry and Tectonic Implications

There is wide debate on the tectonic framework of the North Australian Craton (NAC). Current insights from previous workers suggest an accretionary-collisional or extensional-divergent system, (Betts & Giles 2006; Etheridge et al., 1987; Wyborn et al., 1992). Previous studies done across the Arunta Region have suggested based on geochemical and isotopic findings, accreted fragments along convergent plate margins (Cawood & Tyler 2004; Zhao & McCulloch 1995; Zhao 1994). Further work suggested the evolution of Proterozoic Australia involved significant accretionary and collisional events (Myers et al., 1996; Giles et al., 2002; 2004; Tyler 2005).

Paleoproterozoic arc-related magma emplacement following the Yambah event (ca. 1770–1750 Ma) has been recognised in the southern margin of the Arunta Region suggesting a subduction setting with extensional continental formation behind the arc, where melting was generated by thermal perturbations (Zhao 1994; Zhao & McCulloch 1995; Giles et al., 2002). Zhao (1994) further proposed formation of the Arunta granites in an island-arc/back-arc setting via extension, in agreement with other geochemical and isotopic studies on felsic and mafic rocks in the Arunta region (Zhao & McCulloch 1995; Sivell & Foden 1988). The precursor magmas were suggested to have been derived from fluid-absent melting in the subducting slab and melting of enriched mantle metasomatised by sediment subduction via lithospheric extension during the early history of the Arunta (ca. 1780–1800 Ma).

Based on calculated zircon saturation temperatures for the Boothby granitoids, they contradict a back-arc setting model previously proposed along the southern margin of the Arunta region. The Arunta terrain comprises 50% granites, which appears to require a water-rich source to produce such voluminous melt. The zircon saturation

temperatures of the Boothby augen gneiss suggest that it was emplaced at 688–845 C° (T_{Zr}), yielding a maximum temperature of 776 C° (T_{Zr}) (Fig. 11) and are saturated with zircon between 65 and 78 wt.% SiO₂. The peak at 776 C° suggests that the melting temperatures in the deep crust were attributed to infiltration of the source region by a water-rich fluid phase as likely the cause of large-scale melting at T < 800 C°. This suggests that the Boothby granitoids are ‘cold inheritance-rich granites’ with T_{Zr} < 800 C°. They yield lower temperatures than expected by dehydration melting of mafic crust T_{Zr} > 900 C° (Miller et al., 2003). This fluid could come from the ascent of water into a melting zone due to dehydration melting of underlying metasedimentary rocks or hydrous mafic silicates in ultramafic-mafic rocks (Weinberg & Hasalova 2011). The calculated zircon saturation temperatures of the Boothby mafic-felsic gneiss are 459–837 C°, yielding a minimum temperature of 644 C° for the felsic portions as the mafic phases contain minimal inherited zircons. This could be an underestimation of T_{Zr}; where a clear Zr inflection is seen at <65 wt.% SiO₂ content (Fig. 7); suggesting fractional crystallization from hotter magmas is likely the cause of this underestimation and T_{Zr} cannot be correctly applied (Collins et al., 2016).

Collins et al., (2016) recognised that fluid flux melting is important in the genesis of Cordilleran batholiths. The results from this study suggested that basalts derived from melting of the wedge under plating and crystallized, which in turn fluxed a thermally anomalous overlying crust with fluid. This mechanism could be what has produced the Boothby intrusive complex and large granitic provinces in the Arunta Region. A model for the genesis of the Boothby granitoids is presented, suggesting the

voluminous granitic magmas form in magmatic arcs where hydrous basaltic magmas crystallize in the arc root, producing mafic-under plates that release fluids, that fluxed the crust and stimulated very large amounts of melting at low temperatures to produce the Boothby complex at a maximum temperature of about 776 C° (Weinberg & Hasalova 2016; Collins et al., 2016; Grove et al., 2006; 2012).

The Boothby granitoids are situated further north (present-day) compared to the 1780 Ma arc magmatism in the Arunta that Zhao (1994) proposed. It could be that the 1780–1760 Ma granitic magmatism in the southern Arunta could also represent fluid-flux melting in an arc-like setting and could be a timing continuum with the 1810–1790 Ma magmatism seen further north. The patterns of evolving magmatism in the Southern part of the NAC could represent the granitic provinces being stimulated by a large and spatially evolving source of fluid. The addition of water-rich fluid phases produces a more fertile lower crust where granitic melt increments are constrained by the volume of water in the source region, usually producing melts at temperatures < 800 C° (Holtz et al., 2001). These granitic melt fractions in the Boothby region could be a result of the amount of underplating events, where incremental assembly can occur for millions of years (Coleman et al., 2004). The control of subduction processes on water content and magmatic temperatures in granitic magma systems is evident in the Boothby complex. The Proterozoic history of the Boothby region is suggested to be characterised by crustal addition in an island-arc setting involving subduction related processes and a mantle origin for the water-rich fluids.

CONCLUSIONS

Based on correlation of zircon U-Pb xenocrystic granite ages and Lander Formation detrital zircon ages, together with the peraluminous nature of Mt Boothby, it is evident that these rocks originated dominantly from partial melting of metasedimentary successions older than the Lander Formation but with a very similar provenance. Geochemical variation of the Boothby granitoids reflects source heterogeneity and significant intracrustal melting and fractional crystallization processes, due to differences in depth of melting and different proportions of biotite, garnet and plagioclase in the source. The presence of mafic rocks and the Nd isotopic data seem to require input of a more juvenile source component, as the Boothby orthogneiss is not as evolved as surrounding exposed crustal rocks. The HPE enrichment evident in the Boothby granitoids suggests progressive extraction of the heat-producing elements from a mid-lower crustal source, which was an already pre-enriched source, as evidenced by the Lander Formation being much hotter than normal post-Archean sediment. Zircon saturation temperatures of these peraluminous granites seem to require a large and spatially evolving source of fluid, analogous to Cordilleran batholiths. This fluid is coming from the crystallization of wet arc-related basalts, which transfer to the crust and promote water-fluxed partial melting at an average Zr saturation temperature of 776 °C. This study suggests an arc-like setting, with subsequent fluid-flux melting in the mantle wedge, associated with oceanic crust subduction processes for the Boothby region, indicating an active margin between the North Australian Craton and the South Australian Craton.

ACKNOWLEDGMENTS

Most importantly, I would like to thank Professor Karin Barovich for her supervision, encouragement, guidance and expertise all throughout the year. Professor Martin Hand is also thanked for his invaluable expertise, support and assistance. Thanks go to Aoife McFadden and Ben Wade at Adelaide Microscopy for their excellent assistance and knowledge with SEM imaging and LA-ICP-MS. David Bruce is thanked for his help with collecting and analysing isotopic datasets. The New Zealand field trip was an extremely successful and amazing trip thanks to Professor Alan Collins and Professor John Foden. Katie Howard is thanked for her invaluable help all throughout the year, particularly with lab work and her patience for going through lab training and constant questions. Last but not least, I would like to give my upmost gratitude to the 2016 Honours cohort, who kept me on my feet and always provided positivity when needed, especially Adrienne Brotodewo for studying with me through many late nights in the office.

REFERENCES

- ANDERSON J. R., KELSEY D. E., HAND M. & COLLINS W. J. 2013. Conductively driven, high-thermal, gradient metamorphism in the Anmatjira Range, Arunta region, central Australia. *Journal of Metamorphic Geology*, 31, 1003-1026.
- BEA F. 2012. The sources of energy for crustal melting and the geochemistry of heat-producing elements. *Lithos*, 153, 278-291.
- BETTS P. G. & GILES D. 2006. The 1800–1100Ma tectonic evolution of Australia. *Precambrian Research* 144, 92-125.
- BOEHNKE P., WATSON EB, TRAIL D, HARRISON TM, SCHMITT AK (2013) Zircon saturation re-revisited. *Chem Geol* 351:324–334
- BOYNTON W. V. 1984. Geochemistry of the rare earth elements: Meteorite studies. In: Henderson P. ed. Rare earth element geochemistry, pp. 63–114. Elsevier.
- BROWNE J. 2015. Geochemical and isotopic investigation into the source of U and Th enrichment in the Proterozoic, high heat producing granites of the Anmatjira Range. School of Earth and Environmental Science. University of Adelaide: Honours Thesis
- CARTWRIGHT I., BUICK I. S., FOSTER D. A. & LAMBERT D. D. 1999. Alice Springs age shear zones from the southeastern Reynolds Range, central Australia. *Australian Journal of Earth Science* 46, 355-363.
- CAWOOD P. A. & KORSCH R. J. 2008. Assembling Australia: Proterozoic building of a continent. *Precambrian Research*, 166, 1-35.
- CAWOOD P. A., AND TYLER I. M. 2004. Assembling and reactivating the Proterozoic Capricorn Orogen: litho- tectonic elements, orogenies, and significance. *Precambrian Res.* 128:201–218.
- CHAPPELL B. W. & HINE R. 2006. The Cornubian batholith: an example of magmatic fractionation on a crustal scale. *Resource Geology* 56, 203-244.
- CHAPPELL B. W., 1999. Aluminium saturation in I- and S- type granites and the characterization of fractionated haplogranites. *Lithos* 46, 535-551.
- CLAOUÉ-LONG J. C. & HOATSON D. M. 2005. Proterozoic mafic–ultramafic intrusions in the Arunta Region, central Australia: Part 2: Event chronology and regional correlations. *Precambrian Research* 142, 134-158.
- CLAOUÉ -LONG J., EDGOOSE C. J. & WORDEN K. 2008. A correlation of Aileron Province stratigraphy in central Australia. *Precambrian Research* 166, 230-245.
- CLEMENS J. D., & WALL, V. J., 1981. Origin and crystallization of some peraluminous (S-type) granitic magmas. *Can. Miner.* 19, 111-31.

- COLEMAN D. S., GRAY W. & GLAZNER A. F. 2004. Rethinking the emplacement and evolution of zoned plutons: Geochronologic evidence for incremental assembly of the Tuolumne Intrusive Suite, California: *Geology*, v. 32, p. 433-436.
- COLLINS W. J. & VERNON R. H. 1991. Orogeny associated with anticlock-wise P-T-t paths: Evidence from low-P, high- T metamorphic terranes in the Arunta Inlier, central Australia. *Geology* **19**, 835-838.
- COLLINS W. J., HUANG Q. H. & JIANG X. 2016. Water-fluxed crustal melting produces Cordilleran batholiths. *Lithos*, v. 44(2), p. 143(4).
- COLLINS W. J. & SHAW R. D. 1995. Geochronological constraints on orogenic events in the Arunta Inlier: a review. *Precambrian Research* **71**, 315-346.
- COLLINS W. J. & WILLIAMS I. S. 1995. SHRIMP ionprobe dating of short-lived Proterozoic tectonic cycles in the northern Arunta Inlier, central Australia. *Precambrian Research* **71**, 69-89.
- CORFU F., HANCHAR, J. M., HOSKING, P. W. W. & KINNY, P. D. 2003. Atlas of zircon texture. *Reviews in Mineralogy and Geochemistry* **53**, 469-500.
- DIRKS P. H. G. M. & WILSON C. J. L. 1990. The geological evolution of the Reynolds Range, Central Australia: Evidence for three distinct structural/metamorphic cycles. *Journal of Structural Geology* **12**, 651-665.
- ETHERIDGE M.A., RUTLAND R.W.R. AND WYBORN L.A.I., 1987. Orogenesis and tectonic process in the early to middle Proterozoic of Northern Australia. In: A. Kröner (Edi- tor), *Proterozoic Lithospheric Evolution*. Am. Geophys. Union, Geodyn. Ser., **17**: 131-147.
- FOWLER C. M. R., 1990. *The Solid Earth: An introduction to global geophysics*. Cambridge University, Cambridge, 472p.
- GILES D., BETTS P. G. & LISTER G. 2002. Far-field continental backarc setting for the 1.80-1.67 Ga basins of northeastern Australia. *Geological Society of America* **30**, 823-826.
- GILES D., BETTS P., AND LISTER G. 2004. 1.8-1.5-Ga links between the North and South Australian Cratons and the Early-Middle Proterozoic configuration of Australia. *Tectonophysics* **380**:27-41.
- GOLDSTEIN S.L., O'NIONS R.K., HAMILTON, P.J., 1984. A Sm-Nd isotopic study of atmospheric dusts and particulates from major river systems. *Earth Planet. Sci. Lett.* **70**, 221-236.
- GROVE T. L., TILL C. B. & KRAWCZYNSKI M. J. 2012. The role of H_2O in subduction zone magmatism: Annual Review of Earth and Planetary Sciences, v. 40, p. 413-439
- HAINES P. W., HAND M. & SANDIFORD M. 2001. Palaeozoic synorogenic sedimentation in central and northern Australia: a review of distribution and timing with implications for the evolution of intra-continental orogens. *Australian Journal of Earth Science* **48**, 911-928.
- HAND M. & BUICK I. 2001. Tectonic evolution of the Reynolds-Anmatjira Ranges: a case study in terrain reworking from the Arunta Inlier, central Australia. *Geological Society, London, Special*
- HOATSON D.M., SUN, S., CLAQUE-LONG J.C. 2005. Proterozoic mafic-ultramafic intrusions in the Arunta Region, central Australia Part 1: Geological setting and mineral potential. *Precambrian Research* **142**, 93-133.
- HOLTZ F., JOHANNES W., TAMIC N. & BEHRENS H. 2001. Maximum and minimum water contents of granitic melts generated in the crust: A reevaluation and implications: *Lithos*, v. 56, p. 1-14.
- HOWLETT D., RAIMONDO T., HAND M. 2015. Evidence for 1808-1770 Ma bimodal magmatism, sedimentation, high-temperature deformation and metamorphism in the Aileron Province, central Australia. *Australian Journal of Earth Sciences*, **62**:7, 831-852.
- JACKSON S.E., PEARSON N.J., GRIFFIN W.L., BELOUSOVA E.A., 2004. The application of laser ablation-inductively coupled plasma-mass spectrometry to in-situ U/Pb zircon geochronology. *Chemical Geology* **211**, 47e69.
- JUNG S., MEZGER, K., MASBERG P., HOFFER E., HOERNES S., 1998. Petrology of an intrusion-related high-grade migmatite: implications for partial melting of metasedimentary rocks and leucosome-forming processes. *Journal of Metamorphic Geology* **16**, 425-445.
- MARSHALL V. 2013. Petrological, geochemical and geochronological characterisation of heat-producing granites. School of Earth Sciences. Queensland: The University of Queensland.
- MCDONOUGH W. F. & SUN S.-S. 1995. The composition of the Earth. *Chemical Geology* **120**, 223-253.

- MCLAREN S., SANDIFORD M., HAND, M., NEUMANN N., WYBOR, L., BASTRAKOVA I., 2003. The hot southern continent: heat flow and heat production in Australian Proterozoic terranes. *Spec. Pap., Geol. Soc. Am.* 372, 157–167.
- MCLAREN S., SANDIFORD M. & POWELL R. 2005. Contrasting styles of Proterozoic crustal evolution: a hot-plate tectonic model for Australian terranes. *Geology* 33, 673–676.
- MCLENNAN S. M. & TAYLOR S. R., 1996. Heat flow and the chemical composition of continental crust. *Journal of Geology*, 104, 369–377
- MCLAREN S. & POWELL R. 2014. Magmatism, orogeny and the origin of high-heat-producing granites in Australian Proterozoic terranes. *J. Geol. Soc.*, 171, 149–152.
- MIDDLEMOST E. A. K. (1985). Naming materials in the magma/igneous rock system. *Earth-Sciences Reviews* 37, 215–224
- MILLER C. F., MCDOWELL S. M., & MAPES R. W. 2003. Hot and cold granites? Implications of zircon saturation temperatures and preservation of inheritance: *Geology*, v. 31, pp. 529–532.
- MILLER C. F., 1985, Are strongly peraluminous magmas derived from pelitic sedimentary sources?: *The Journal of Geology*, v. 93, no. 6, p. 673–689.
- MORRISSEY L. J., HAND M., RAIMONDO T. & KELSEY D. E. 2014. Long-lived high-temperature, low-pressure granulite facies metamorphism in the Arunta Region, central Australia. *Journal of Metamorphic Geology* 32, 25–47.
- MYERS J. S.; SHAW R. D.; AND TYLER I. M. 1996. Tectonic evolution of Proterozoic Australia. *Tectonics* 15: 1431–1446.
- NEUMANN N., SANDIFORD M., AND FODEN J., 2000, Regional geochemistry and continental heat flow: implications for the origin of the South Australian heat anomaly: *Earth and Planetary Science Letters*, v. 183, p. 107–120.
- PAYNE J. L., BAROVICH K. M. & HAND M. 2006. Provenance of metasedimentary rocks in the northern Gawler Craton, Australia: implications for Palaeoproterozoic reconstructions. *Precambrian Research* 148, 275–291.
- RUBATTO D., WILLIAMS I. S. & BUCK I. S. 2001. Zircon and monazite response to prograde metamorphism in the Reynolds Range, central Australia. *Contributions to Mineralogy and Petrology* 140, 458–468.
- SANDIFORD M., MCLAREN S., & NEUMANN N. 2002. Long-term thermal consequences of the redistribution of heat-producing elements associated with large-scale granitic complexes. *Journal of Metamorphic Geology*, 20, 87–98.
- SCRIMGEOUR IR, 2013. Chapter 12: Aileron Province: in Ahmad M and Munson TJ (compilers). ‘Geology and mineral resource of the Northern Territory’. Northern Territory Geological Survey, Special Publication 5.
- SCRIMGEOUR I. R., KINNY P. D., CLOSE D. F. & EDGOOSE C. J. 2005. High-T granulites and polymetamorphism in the southern Arunta Region, central Australia: Evidence for a 1.64 Ga accretional event. *Precambrian Research* 142, 1–27.
- SCRIMGEOUR I. 2003. Developing a revised framework for the Arunta Region. *Northern Territory Geological Survey Record* 1, 1–3.
- SHAND S. J. (1943). Eruptive Rocks. Their Genesis, Composition, Classification, and Their Relation to Ore-Deposits with a Chapter on Meteorite. New York: John Wiley & Sons
- SIVELL W. J. & FODEN J. D. 1988. Amphibolites from the Entia Gneiss Complex, eastern Arunta Inlier: geochemical evidence for a Proterozoic transition from extensional to compressional tectonics. *Precambrian Res.*, 38: pp. 235–255.
- SLÁMA J., KOŠLER J., CONDON D. J., CROWLEY J. L., GERDES A., HANCHAR J. M., HORSTWOOD M. S., MORRIS G. A., NASDALA L. & NORBERG N. 2008. Plešovice zircon—a new natural reference material for U–Pb and Hf isotopic microanalysis. *Chemical Geology* 249, 1–35.
- SYLVESTER P. J., 1998. Postcollisional strongly peraluminous granites. *Lithos* 45, 29–44.
- TAYLOR S. R. & MCLENNAN S. M. 1985. The continental crust: Its composition and evolution. Blackwell, Oxford.
- VERNON R. H., CLARKE G. L. & COLLINS W. J. 1990. Mid-crustal granulite facies metamorphism: low-pressure metamorphism and melting, Mount Stafford, central Australia. In: Ashworth J. R. & Brown M. eds. *High temperature metamorphism and crustal anatexis*, pp. 272–319. Special Publication of the Mineralogical Society 2. London UK.

- VRY J., COMPSTON W. & CARWRIGHT I. 1996. SHRIMP II dating of zircons and monazites: reassessing the timing of high-grade metamorphism and fluid flow in the Reynolds Range, north- ern Arunta Block, Australia. *Journal of Metamorphic Geology* 14, 335–350.
- WADE B., BAROVICH K., HAND M., SCRIMGEOUR I. & CLOSE D. 2006. Evidence for early Mesoproterozoic arc magmatism in the Musgrave Block, central Australia: implications for Proterozoic crustal growth and tectonic reconstructions of Australia. *The Journal of geology* 114, 43–63.
- WATSON E.B., HARRISON T.M., 1983. Zircon saturation revisited: temperature and composition effects in a variety of crustal magma types. *Earth and Planetary Science Letters* 64, 295–304.
- WEINBERG R. F. & HASALOVA P. 2015. Water-fluxed melting of the continental crust: A review: *Lithos*, v. 212-215, p. 158-188.
- WORDEN K. E., CARSON C. J., CLOSE D. F., DONNELLAN N. & SCRIMGEOUR I. R. 2008. Summary of results. Joint NTGS-GA geochronology project: Tanami Region, Arunta Region, Pine Creek Orogen and Halls Creek Orogen correlatives, January 2005 March 2007. Northern Territory Geological Survey, record 2008-003.
- WYBORN L. A. I., WYBORN D., WARREN D. G. & DRUMMOND B. J., 1992. Proterozoic granite types in Australia: implications for lower crust composition, structure and evolution. *Trans. R. Soc. Edinburgh, Earth Sci.*, 83: 201-209.
- WEDEPOHL K. H. 1995. The composition of the continental crust. *Geochimica et cosmochimica Acta* 59, 1217- 1232.
- ZHAO J. & COOPER J. A. 1992. The Atnarpa Igneous Complex, southeast Arunta Inlier, central Australia: implications for subduction at an Early Mid Proterozoic continental margin. *Precambrian Research* 56, 227-253.
- ZHAO J. & BENNETT V. C. 1995. SHRIMP U Pb zircon geochronology of granites in the Arunta Inlier, central Australia: implications for Proterozoic crustal evolution. *Precambrian Research* 71, 17-43.
- ZHAO J. & MCCULLOCH T. 1995. Geochemical and Nd isotopic systematics of granites from the Arunta Inlier, central Australia: implications for Proterozoic crustal evolution. *Precambrian Research* 71, 265-299.
- ZHAO J. X. 1994. Geochemical and Sm-Nd isotopic study of amphibolites in the southern Arunta Inlier, central Australia: evidence for subduction at a Proterozoic continental margin. *Precambrian research* 65, 71-94

APPENDIX A: GEOCHEMISTRY OF ADDITIONAL DATA USED
Major and Trace element geochemical data sets from Browne (2015) from the
Anmatjira Range

Sample ID	Suite Name	SiO ₂	TiO ₂	Al ₂ O ₃	Fe ₂ O ₃	Mn O	Mg O	Ca O	Na ₂ O	K ₂ O	P ₂ O ₅	LOI	Tot al
AMJ - GP - 01a	Anmatjira Orthogneiss	73.7	0.4	13.9	2.91	0.03	0.64	1.85	2.65	4.8	0.1	101.55	0.49
AMJ - GP - 01b	Anmatjira Orthogneiss	51.4	2.4	11.1	19.4	0.11	5.32	6.73	1.52	0.12	0.28	99.68	1.14
AMJ - GP - 02	Anmatjira Orthogneiss	78.2	0.1	12.3	1.71	0.04	0.14	0.57	2.07	6.18	0.08	101.64	0.18
AMJ - GP - 03	Anmatjira Orthogneiss	73.2	0.3	12.5	3.02	0.03	0.58	1.43	2.05	5.37	0.11	98.97	0.25
AMJ - GP - 04	Aloolya Gneiss	78.5	0.1	11.7	0.57	0.01	0.13	0.47	1.74	6.96	0.05	100.54	0.21
AMJ - GP - 05	Aloolya Gneiss	76.6	0.1	12.5	1.17	0.01	0.29	0.95	1.85	6.73	0.07	100.66	0.22
AMJ - GP - 06	Aloolya Gneiss	54.5	0.7	15.9	10.5	0.16	5.87	9.86	1.02	1.03	0.12	99.91	0.08
AMJ - GP - 07	Aloolya Gneiss	55.4	0.9	15.2	11.5	0.16	5.91	9.94	1.18	0.96	0.11	101.39	0.01
AMJ - GP - 08	Anmatjira Orthogneiss	75.2	0.4	12.0	2.61	0.01	0.57	1.33	2.57	4.37	0.1	99.84	0.59
AMJ - GP - 09	Anmatjira Orthogneiss	74	0.3	13	2.74	0.03	0.51	1.11	2.07	6.04	0.09	100.65	0.66
AMJ - GP - 10	Anmatjira Orthogneiss	73.2	0.4	13.1	3.19	0.02	0.68	1.24	2.34	5.53	0.11	100.44	0.54
AMJ - GP - 12	Aloolya Gneiss	79.5	0.1	11.2	1.48	0.02	0.29	0.76	1.93	5.23	0.08	100.95	0.31
AMJ - GP - 13	Aloolya Gneiss	80.4	0.0	10.7	0.48	<0.01	0.09	0.43	1.72	5.92	0.03	100.23	0.35
AMJ - GP - 14	Aloolya Gneiss	55.2	1.1	14.4	12.2	0.17	5.43	9.19	2.12	1.45	0.16	101.49	-0.11
AMJ - GP - 15	Aloolya Gneiss	49.4	2.6	11.1	20	0.28	3.64	7.74	0.77	1.47	0.28	98.03	0.69
AMJ - GP - 16	Aloolya Gneiss	78.1	0.3	11.5	2.12	0.01	0.41	0.92	1.76	5.97	0.07	101.57	0.28
AMJ - GP - 17	Anmatjira Orthogneiss	70.1	0.5	13.4	3.89	0.04	0.88	1.78	2.03	5.71	0.09	98.81	0.18
AMJ - GP - 19	Aloolya Gneiss	78.1	0.0	11.5	0.24	<0.01	0.04	0.49	1.76	6.76	0.11	99.34	0.24
AMJ - GP - 21	Anmatjira Orthogneiss	72.5	0.3	13	2.83	0.03	0.58	1.59	2.17	5.68	0.08	99.16	0.25
AMJ - GP - 22	Anmatjira Orthogneiss	72.1	0.4	12.9	3.58	0.03	0.75	1.62	2.01	5.65	0.12	99.65	0.33
AMJ - GP - 23	Anmatjira Orthogneiss	74.2	0.5	11.7	4.19	0.06	0.83	1.34	1.59	4.99	0.11	100.28	0.67
AMJ - GP - 24	Anmatjira Orthogneiss	75.7	0.3	12.2	2.24	0.02	0.42	1.29	2.12	5.26	0.05	100.25	0.52
AMJ - GP - 25	Anmatjira Orthogneiss	76.7	0.3	12.2	2.54	0.03	0.47	1.44	1.94	5.21	0.18	101.38	0.34
AMJ - GP - 27	Anmatjira Orthogneiss	78.8	0.1	11.4	1.9	0.02	0.21	0.42	1.92	5.42	0.11	100.92	0.53
AMJ - GP - 29	Anmatjira Orthogneiss	77.2	0.1	12	1.22	0.01	0.18	0.56	2.34	6.02	0.15	100.57	0.7
AMJ - GP - 30	Anmatjira Orthogneiss	75.3	0.4	11.9	2.61	0.03	0.88	1.18	2.37	4.47	0.18	100.08	0.75
AMJ - GP - 31	Anmatjira Orthogneiss	74.8	0.4	12.3	3.05	0.03	0.65	1.58	2.24	4.64	0.12	100.52	0.64
AMJ - GP - 32	Anmatjira Orthogneiss	75.3	0.4	12.5	2.93	0.05	0.56	1.46	1.86	5.13	0.17	101.07	0.73
AMJ - GP - 33	Anmatjira Orthogneiss	75.5	0.4	12.3	3.53	0.04	0.63	1.53	2	5.07	0.11	101.81	0.55

Maria Then
Origin of Proterozoic granites in Mt Boothby

Sample ID	Suite Name	Sr	Cs	Rb	Ba	Th	U	Nb	Zr	Hf	Y	Co	Cr	Ni	V	Zn	Sc	La	Ce	Pr	Nd	Sm	Eu
AMJ - GP - 01a	Anmatjira Orthogneiss	67.5	12.2	357	357	47.5	11.35	11.7	224	6.7	33.1	35	20	5	47	26	7	49.5	102.5	10.25	34.8	7.34	0.82
AMJ - GP - 01b	Anmatjira Orthogneiss	76.7	0.12	3.9	6.7	3.78	1.15	6.8	171	4.9	53.1	37	40	4	492	48	6	21.6	46.7	5.59	24.4	6.79	2.83
AMJ - GP - 02	Anmatjira Orthogneiss	16.6	3.79	419	64.6	12.8	1.8	4.2	84	3	52.1	66	10	2	11	8	1	17.6	37.1	3.86	12.4	2.94	0.24
AMJ - GP - 03	Anmatjira Orthogneiss	45.3	7.65	326	354	29.3	2.98	8.3	167	5.2	32.5	60	20	3	45	20	2	45.7	89.7	9.85	33.7	6.72	0.79
AMJ - GP - 04	Aloolya Gneiss	47.7	3.75	354	282	14.05	1.16	2.3	24	0.8	4.4	70	10	106	18	92	30	18	29.9	3.01	10	1.96	0.71
AMJ - GP - 05	Aloolya Gneiss	44.9	4.07	342	325	31.8	3.14	4.1	144	4.3	20.2	66	10	102	14	95	34	46	91.7	9.59	33	7.05	0.63
AMJ - GP - 06	Aloolya Gneiss	80.6	6.5	115.5	211	4	0.96	5.7	142	4	27.3	73	200	5	220	11	6	22.2	42.3	4.82	18.6	3.9	1.16
AMJ - GP - 07	Aloolya Gneiss	84.9	3.38	71.5	241	4.44	0.91	6.4	146	3.8	30.3	45	140	5	232	29	6	22.6	45	5.27	20.3	4.7	1.22
AMJ - GP - 08	Anmatjira Orthogneiss	52.9	13.35	351	312	56.2	17.35	13.2	226	7.1	47.9	50	20	6	35	15	7	53.3	119.5	11.7	38.9	8.08	0.75
AMJ - GP - 09	Anmatjira Orthogneiss	53.1	15.2	477	391	43.6	7.85	11.8	193	5.7	43	41	10	2	39	19	2	62.3	115	11.7	38.4	7.8	0.75
AMJ - GP - 10	Anmatjira Orthogneiss	58.1	31.2	516	426	45.1	7.48	11.5	205	6.2	38.5	70	20	1	46	17	1	42.4	89.7	8.96	30.1	6.34	0.62
AMJ - GP - 12	Aloolya Gneiss	46.2	6.86	365	173.5	15.05	3.54	5.7	139	4.5	30.5	68	10	68	23	106	34	21.8	41.2	4.28	14.1	3.42	0.47
AMJ - GP - 13	Aloolya Gneiss	35.3	3.63	423	237	11	1.25	1.9	43	1.4	14.9	78	10	29	18	149	45	17.1	33.1	3.27	11	2.42	0.45
AMJ - GP - 14	Aloolya Gneiss	83.6	1.32	64.4	328	2.09	0.38	8.9	183	4.9	37.7	62	130	6	265	33	4	28.2	56.9	6.05	24	5.85	1.26
AMJ - GP - 15	Aloolya Gneiss	37.8	3	87.6	616	3.18	1.2	7.3	180	5.2	60.6	54	20	10	464	48	9	19.8	43.5	5.23	22.6	6.8	2.04
AMJ - GP - 16	Aloolya Gneiss	37.1	8.01	400	239	48.6	5.3	11.1	209	6.4	28.2	57	10	4	35	59	25	52.2	105.5	10.95	36.5	7.62	0.6
AMJ - GP - 17	Anmatjira Orthogneiss	88.7	8.6	360	631	55.8	4.22	13.8	296	8.6	32.8	36	20	1	61	6	<1	76.1	149	15.25	52.5	9.97	1.22
AMJ - GP - 19	Aloolya Gneiss	24.9	4.06	472	90.3	19.85	2.87	1.5	79	2.9	31.2	53	<10	6	7	38	6	18.1	35.2	3.49	12	3.16	0.39
AMJ - GP - 21	Anmatjira Orthogneiss	64.5	9.45	425	451	60.3	5.61	11.6	159	4.9	20.2	70	20	8	41	47	10	70.2	141.5	14.1	48.1	9.31	0.88
AMJ - GP - 22	Anmatjira Orthogneiss	63.2	6.2	402	413	37.1	4.44	14.1	193	5.8	13.1	56	20	5	45	24	4	59.8	119.5	12	39	6.82	0.87
AMJ - GP - 23	Anmatjira Orthogneiss	59.9	13.55	378	417	38.5	3.75	12.3	199	5.7	53	53	20	4	53	23	4	49.1	97.1	10.25	35.7	7.54	0.87
AMJ - GP - 24	Anmatjira Orthogneiss	50.2	6.38	396	345	34.1	4.09	9.9	140	4.4	26.9	73	10	2	37	10	4	49.3	96.8	10.35	36.7	8.04	0.76
AMJ - GP - 25	Anmatjira Orthogneiss	59.5	7.07	431	353	48.8	4.4	10.8	227	6.8	26.3	76	10	2	35	6	3	39	112	8.77	29.3	6.57	0.7
AMJ - GP - 27	Anmatjira Orthogneiss	23.7	28.5	654	103.5	38.3	11.95	12.4	113	4.3	59.3	61	10	6	18	29	6	29.3	63.1	6.7	22.3	6.15	0.26
AMJ - GP - 29	Anmatjira Orthogneiss	31.7	10.8	630	154	34.9	23.7	12	102	3.6	55.7	59	10	7	16	34	7	23.1	53.2	5.33	18.2	5.2	0.31
AMJ - GP - 30	Anmatjira Orthogneiss	62.3	12.55	365	249	46.7	6.12	11.8	194	5.9	51.9	69	20	3	41	34	6	52.8	114	10.9	37.4	7.98	0.69
AMJ - GP - 31	Anmatjira Orthogneiss	57.2	12.3	378	305	43.2	6.6	12.3	202	6.1	48.3	68	20	6	40	41	7	55.3	111.5	11.25	38.7	8.55	0.83
AMJ - GP - 32	Anmatjira Orthogneiss	58.7	4.48	326	418	41.3	7.61	10.7	206	6.1	37.1	88	10	11	42	67	13	25.6	99.4	5.49	19.2	4.48	0.5
AMJ - GP - 33	Anmatjira Orthogneiss	63.2	20.9	427	366	48.5	10.75	13	231	7.1	37.7	69	10	11	38	43	9	40.9	106	9.35	30.6	6.92	0.69

APPENDIX B: HEAT PRODUCTION DATA

Data compiled to calculate heat production values for rocks of the Arunta Region presented in Results section.

Rock Unit	K wt %	Th ppm	U ppm	Time (Ma)	Heat from U	Heat from Th	Heat from K	Total Heat Production
Augen Gneiss	4.1175 936	40.2797 9217	5.50083 8427	1806	1.88742 6347	3.11251 4765	0.81288 9231	5.812830343
Augen Gneiss	4.3832 448	55.1999 9286	19.4398 4356	1806	6.67012 3727	4.26543 3945	0.86533 3698	11.80089137
Augen Gneiss	3.5447 832	118.494 8647	17.9724 6415	1806	6.16664 2195	9.15637 8326	0.69980 585	16.02282637
Augen Gneiss	4.3583 4	49.2490 6778	9.10379 8523	1806	3.12366 0041	3.80559 1896	0.86041 7029	7.789668966
augen gneiss	4.6821 024	78.1	10.9	1806	3.73996 5726	6.03497 1634	0.92433 3723	10.69927108
augen gneiss	7.2389 952	25.3	2.19	1806	0.75142 4306	1.95499 0811	1.42911 1713	4.13552683
augen gneiss	4.2255 144	49.1	4.62	1806	1.58519 6482	3.79407 3076	0.83419 4796	6.213464354
augen gneiss	4.5409 752	38.7934 4138	7.67126 8702	1806	2.63213 5965	2.99766 0926	0.89647 26	6.526269491
augen gneiss	3.8436 408	49.5819 1067	7.58052 4244	1806	2.60100 0078	3.83131 1453	0.75880 5875	7.191117406
augen gneiss	4.4413 56	35.7009 3499	9.62615 4131	1806	3.30288 8672	2.75869 5646	0.87680 5925	6.938390243
mafic	0.1577 304	0.22079 7848	0.10219 7008	1806	0.03506 5441	0.01706 1572	0.03113 8902	0.083265915
mafic	0.2075 4	0.52011 9255	0.21383 7994	1806	0.07337 1263	0.04019 0844	0.04097 2239	0.154534347
maficfelsic	4.1009 904	5.00278 8029	1.46910 3591	1806	0.50407 3126	0.38657 7258	0.80961 1452	1.700261836
maficfelsic	1.8844 632	1.74369 2547	0.61565 0017	1806	0.21123 9446	0.13473 9245	0.37202 7934	0.718006626
mafic-felsic gneiss	0.2656 512	1.04	0.27	1806	0.09264 1353	0.08036 3259	0.05244 4467	0.225449078
mafic-felsic gneiss	1.8595 584	0.85	2.07	1806	0.71025 0372	0.06568 1509	0.36711 1266	1.143043147
mafic-felsic gneiss	2.0587 968	11.45	0.87	1806	0.29851 1026	0.88476 8569	0.40644 4616	1.58972421
mafic-felsic gneiss	1.4112 72	3.17	1.32	1806	0.45291 3281	0.24495 3394	0.27861 1228	0.976477903
mafic-felsic gneiss	3.6693 072	63.2	9.54	1806	3.27332 78	4.88361 3409	0.72438 9194	8.881330404
mafic-felsic gneiss	3.0549 888	107	17.5	1806	6.00453 2128	8.26814 2956	0.60311 1365	14.87578645
diatektite	4.2836 256	34.3	6.56	1806	2.25084 1758	2.65044 2088	0.84566 7023	5.746950868
Diatektite	1.6520 184	36.3286 0605	5.76596 7528	1806	1.97839 6416	2.80719 7273	0.32613 9026	5.111732715
Diatektite	4.0843 872	26.7161 8505	4.38778 1789	1806	1.50551 867	2.06442 2778	0.80633 3673	4.376275121
Metasediment	3.1463 064	28.1	3.6	1806	1.23521 8038	2.17135 343	0.62113 915	4.027710619
Metasediment	3.8934 504	23.4	3.69	1806	1.26609 8489	1.80817 3319	0.76863 9213	3.842911021
Metasediment	3.0881 952	56.8367 7359	6.65282 4019	1806	2.28269 1175	4.39191 1862	0.60966 6923	7.28426996
Lander Rock beds	0.5894 136	24.4	3.64	1837	1.25563 4307	1.88745 195	0.11775 8251	3.260844508
Lander Rock beds	0.2764 4328	2	1.2	1837	0.41394 5376	0.15470 9176	0.05523 0278	0.62388483
Lander Rock beds	1.7574 4872	18	2.6	1837	0.89688 1648	1.39238 2586	0.35111 8616	2.64038285
Lander Rock beds	0.8907 6168	15	3	1837	1.03486 344	1.16031 8821	0.17796 423	2.373146492

Maria Then
Origin of Proterozoic granites in Mt Boothby

Lander Rock beds	0.8160 4728	17	4.7	1837	1.62128 6056	1.31502 7998	0.16303 7128	3.099351181
Lander Rock beds	1.4785 1496	15	2.2	1837	0.75889 9856	1.16031 8821	0.29539 0768	2.214609445
Lander Rock beds	0.0390 1752	11	5.9	1837	2.03523 1432	0.85090 0469	0.00779 5265	2.893927165
Lander Rock beds	2.3784 084	16	2.9	1837	1.00036 7992	1.23767 341	0.47517 9422	2.713220823
Lander Rock beds	0.3685 9104	13	2.9	1837	1.00036 7992	1.00560 9645	0.07364 0371	2.079618008
Lander Rock beds	0.3760 6248	5	4.1	1837	1.41431 3368	0.38677 294	0.07513 3081	1.87621939
Lander Rock beds	2.0870 2224	27.7	5.64	1837	1.94554 3267	2.14272 209	0.41696 3723	4.50522908
Lander Rock beds	2.8640 52	22.1	4.74	1837	1.63508 4235	1.70953 6397	0.57220 5586	3.916826218
Lander Rock beds	3.0300 84	23.7	5.16	1837	1.77996 5117	1.83330 3738	0.60537 6925	4.218645779
Lander Rock beds	6.9567 408	26.1	7.73	1837	2.66649 813	2.01895 4749	1.38987 9077	6.075331956
Lander Rock beds	2.2248 288	17.5	3.61	1837	1.24528 5673	1.35370 5292	0.44449 5934	3.043486898
Lander Rock beds	1.0792 08	19	3.84	1837	1.32462 5203	1.46973 7174	0.21561 3699	3.009976076
Lander Rock beds	2.5651 944	19.1	4.85	1837	1.67302 9228	1.47747 2633	0.51249 7177	3.662999038
Lander Rock beds	5.2715 16	21.9	6.26	1837	2.15941 5045	1.69406 5479	1.05318 9992	4.906670516
Lander Rock beds	4.9062 456	23.6	6.59	1837	2.27325 0023	1.82556 8279	0.98021 3048	5.07903135
Lander Rock beds	1.7599 392	19.1	4.29	1837	1.47985 4719	1.47747 2633	0.35161 6186	3.308943538
Lander Rock beds	2.2082 256	19.6	4.48	1837	1.54539 607	1.51614 9927	0.44117 88	3.502724797
Lander Rock beds	2.6565 12	81	14.87	1837	5.12947 3117	6.26572 1636	0.53074 1413	11.92593617
Lander Rock beds	2.0421 936	22.4	4.09	1837	1.41086 3823	1.73274 2773	0.40800 7462	3.551614058
Lander Rock beds	2.3576 544	21.6	4.68	1837	1.61438 6966	1.67085 9103	0.47103 3004	3.756279074
Lander Rock beds	2.9138 616	20.6	4.26	1837	1.46950 6085	1.59350 4515	0.58215 6988	3.645167587
Lander Rock beds	5.8858 344	24.7	5.86	1837	2.02143 3253	1.91065 8326	1.17592 3944	5.108015523
Lander Rock beds	4.2587 208	17.8	5.99	1837	2.06627 7335	1.37691 1668	0.85084 4828	4.294033831
Lander Rock beds	5.0224 68	21.6	5.29	1837	1.82480 9199	1.67085 9103	1.00343 2985	4.499101287
Lander Rock beds	5.7281 04	22.5	7.09	1837	2.44572 7263	1.74047 8232	1.14441 1173	5.330616668
Lander Rock beds	6.8820 264	26.7	6.61	1837	2.28014 9113	2.06536 7502	1.37495 1974	5.720468589
Lander Rock beds	3.2376 24	16.2	4.95	1837	1.70752 4676	1.25314 4327	0.64684 1098	3.607510101
Lander Rock beds	5.4707 544	22.6	6.15	1837	2.12147 0052	1.74821 3691	1.09299 5598	4.962679341
Lander Rock beds	6.4835 496	26.2	6.88	1837	2.37328 6822	2.02669 0208	1.29534 0762	5.695317792
Lander Rock beds	2.4738 768	17	3.8	1837	1.31082 7024	1.31502 7998	0.49425 2941	3.120107963
Lander Rock beds	6.3590 256	25.9	5.7	1837	1.96624 0536	2.00348 3832	1.27046 2258	5.240186626
Lander Rock beds	3.2542 272	20.4	5.33	1837	1.83860 7378	1.57803 3597	0.65015 8231	4.066799207
Lander Rock beds	6.1763 904	23.1	5.59	1837	1.92829 5543	1.78689 0985	1.23397 3786	4.949160314

Maria Then
Origin of Proterozoic granites in Mt Boothby

Lander Rock beds	2.1003 048	20.3	4.77	1837	1.64543 2869	1.57029 8138	0.41961 743	3.635348438
Lander Rock beds	1.7433 36	27.3	5.21	1837	1.79721 2841	2.11178 0255	0.34829 9053	4.257292148
Lander Rock beds	1.4029 704	27.2	6.14	1837	2.11802 0507	2.10404 4796	0.28029 7809	4.502363112
Lander Rock beds	1.9508 76	21.8	3.36	1837	1.15904 7053	1.68633 002	0.38976 3226	3.235140299
Lander Rock beds	2.3493 528	20.8	4.57	1837	1.57644 1973	1.60897 5432	0.46937 4438	3.654791843
Lander Rock beds	0.5329 6272	8	2.9	1837	1.00036 7992	0.61883 6705	0.10647 9996	1.725684693
Lander Rock beds	2.1252 096	19	4.48	1837	1.54539 607	1.46973 7174	0.42459 3131	3.439726375
Lander Rock beds	2.5568 928	21.1	4.86	1837	1.67647 8773	1.63218 1809	0.51083 861	3.819499192
Lander Rock beds	0.2282 94	0.7	0.1	1837	0.03449 5448	0.05414 8212	0.04561 059	0.13425425
Lander Rock beds	2.7934 884			1837	0	0	0.55810 7768	0.558107768
Lander Rock beds	3.5630 4672	18	3.9	1837	1.34532 2472	1.39238 2586	0.71185 6921	3.449561978
Lander Rock beds	0.1743 336	24	13	1837	4.48440 8239	1.85651 0114	0.03482 9905	6.375748259
Lander Rock beds	3.0217 824	13	7	1837	2.41468 136	1.00560 9645	0.60371 8358	4.024009363
Global AVG UPPER continental crust	2.865	10.3	2.5	0	0.65551 1333	0.74808 9	0.28219 104	1.685791373
Global Avg Lower continental crust	1.314	6.6	0.93	0	0.24385 0216	0.47935 8	0.12942 3744	0.85263196
Whole crust avg	2.14	8.5	1.7	0	0.44574 7706	0.61735 5	0.21078 144	1.273884146

APPENDIX C: U-PB ZIRCON GEOCHRONOLOGY DATA

My samples: Boothby Orthogneiss (MB08-18), Mafic-Felsic Gneiss (13-BO-12), Metasediment (12-BO-12, OSM)

Compiled data: Howlett et al., (2015): Boothby Orthogneiss (OG1, OG2, OG3), Mafic-Felsic Gneiss (MF1, MF2), Metasediment (MS1, MS2)

Source file 13-BO-12	Final207_235	Final206_238	FinalAge206_238	FinalAge207_206	Concordance
13BO-1.D	4.913	0.3363	1867	580	321.8965517
13BO-10.D	4.499	0.3113	1748	596	293.2885906
13BO-100.D	4.895	0.3164	1771	606	292.2442244
13BO-101.D	4.39	0.2968	1673	614	272.47557
13BO-102.D	4.649	0.3055	1717	1468	116.9618529
13BO-103.D	4.738	0.3098	1738	1469	118.3117767
13BO-104.D	4.79	0.3227	1803	1471	122.5696805
13BO-105.D	4.612	0.3183	1780	1474	120.7598372
13BO-106.D	3.677	0.2482	1427	1490	95.77181208
13BO-107.D	4.434	0.3003	1693	1509	112.1935056
13BO-108.D	4.75	0.3119	1746	1527	114.3418468
13BO-109.D	4.198	0.2907	1643	1530	107.3856209
13BO-111.D	4.557	0.3124	1754	1533	114.4161774
13BO-110.D	4.61	0.3107	1743	1550	112.4516129
13BO-111.D	4.469	0.3023	1706	1551	109.9935525
13BO-112.D	4.418	0.293	1657	1565	105.8785942
13BO-113.D	4.559	0.3061	1720	1575	109.2063492
13BO-114.D	4.466	0.3014	1699	1578	107.6679341
13BO-115.D	4.401	0.294	1664	1591	104.5883092
13BO-116.D	4.462	0.2942	1661	1602	103.6828964
13BO-117.D	4.572	0.3009	1695	1602	105.8052434
13BO-118.D	3.7	0.2507	1439	1603	89.76918278
13BO-119.D	4.446	0.2939	1660	1606	103.362391
13BO-12.D	4.526	0.3071	1725	1615	106.8111455
13BO-120.D	4.699	0.302	1702	1617	105.2566481
13BO-121.D	4.499	0.2958	1671	1619	103.2118592
13BO-122.D	4.264	0.2859	1622	1625	99.81538462
13BO-123.D	4.89	0.3147	1763	1625	108.4923077
13BO-124.D	4.326	0.2869	1628	1627	100.0614628
13BO-125.D	4.608	0.2996	1690	1627	103.8721573
13BO-126.D	4.735	0.3065	1722	1628	105.7739558
13BO-127.D	4.656	0.2963	1671	1629	102.5782689
13BO-128.D	4.835	0.3063	1721	1630	105.5828221
13BO-129.D	4.101	0.287	1627	1634	99.57160343
13BO-13.D	4.63	0.3182	1780	1634	108.9351285
13BO-130.D	4.765	0.3196	1787	1635	109.2966361
13BO-131.D	3.723	0.2778	1579	1641	96.22181597
13BO-132.D	4.899	0.3301	1838	1644	111.8004866
13BO-133.D	3.531	0.2583	1480	1644	90.0243309
13BO-134.D	4.609	0.3067	1727	1645	104.9848024
13BO-135.D	4.373	0.2989	1685	1645	102.4316109
13BO-136.D	4.516	0.3031	1705	1646	103.5844471
13BO-137.D	4.587	0.3046	1713	1648	103.9441748
13BO-138.D	4.722	0.3112	1746	1648	105.9466019

Maria Then
Origin of Proterozoic granites in Mt Boothby

13BO-139.D	4.805	0.3143	1762	1649	106.852638
13BO-14.D	4.498	0.3134	1756	1653	106.231095
13BO-140.D	4.364	0.3002	1693	1654	102.3579202
13BO-141.D	4.381	0.2979	1682	1655	101.6314199
13BO-142.D	4.585	0.3043	1712	1657	103.3192517
13BO-143.D	4.592	0.3021	1701	1658	102.5934861
13BO-144.D	4.349	0.2911	1647	1662	99.09747292
13BO-145.D	4.772	0.3165	1771	1663	106.4942874
13BO-146.D	5.017	0.3342	1857	1664	111.5985577
13BO-147.D	4.457	0.3029	1706	1664	102.5240385
13BO-148.D	4.663	0.3175	1776	1664	106.7307692
13BO-149.D	4.363	0.2894	1637	1666	98.25930372
13BO-15.D	4.57	0.3111	1745	1667	104.6790642
13BO-150.D	4.78	0.3195	1791	1668	107.3741007
13BO-151.D	4.476	0.3084	1737	1669	104.074296
13BO-152.D	4.261	0.2856	1618	1670	96.88622754
13BO-153.D	4.594	0.309	1734	1670	103.8323353
13BO-154.D	4.972	0.3352	1862	1670	111.497006
13BO-155.D	3.768	0.289	1639	1671	98.08497905
13BO-156.D	4.906	0.3329	1850	1673	110.5797968
13BO-157.D	4.346	0.2927	1656	1673	98.98386133
13BO-158.D	4.516	0.3018	1701	1673	101.6736402
13BO-159.D	5.03	0.336	1865	1674	111.4097969
13BO-16.D	4.231	0.2849	1615	1674	96.47550777
13BO-160.D	4.235	0.298	1682	1675	100.4179104
13BO-161.D	3.441	0.2337	1355	1675	80.89552239
13BO-162.D	4.745	0.3141	1761	1676	105.071599
13BO-163.D	4.533	0.3011	1695	1676	101.1336516
13BO-164.D	4.674	0.3057	1719	1676	102.5656325
13BO-165.D	4.654	0.3054	1716	1676	102.3866348
13BO-166.D	4.775	0.3167	1774	1677	105.7841383
13BO-167.D	4.731	0.3082	1730	1678	103.0989273
13BO-168.D	4.01	0.2697	1538	1679	91.60214413
13BO-169.D	4.468	0.2936	1658	1679	98.74925551
13BO-17.D	3.574	0.2541	1459	1680	86.8452381
13BO-170.D	4.653	0.3048	1713	1683	101.7825312
13BO-171.D	4.678	0.2995	1690	1683	100.4159239
13BO-172.D	4.116	0.2825	1604	1683	95.30600119
13BO-173.D	4.805	0.3027	1708	1683	101.4854427
13BO-174.D	4.777	0.3027	1705	1683	101.3071895
13BO-175.D	4.874	0.3039	1711	1684	101.6033254
13BO-176.D	4.327	0.2715	1549	1684	91.98337292
13BO-177.D	4.812	0.2953	1667	1685	98.93175074
13BO-178.D	4.426	0.287	1625	1685	96.43916914
13BO-179.D	5	0.3354	1863	1685	110.5637982
13BO-18.D	4.488	0.3072	1725	1686	102.3131673

Maria Then
Origin of Proterozoic granites in Mt Boothby

13BO-180.D	4.546	0.3124	1751	1686	103.8552788
13BO-181.D	5.096	0.3318	1846	1686	109.489917
13BO-182.D	4.784	0.3192	1785	1686	105.8718861
13BO-183.D	4.747	0.3101	1742	1687	103.2602253
13BO-184.D	4.663	0.3138	1758	1687	104.2086544
13BO-185.D	3.873	0.2621	1500	1688	88.86255924
13BO-186.D	4.615	0.3076	1729	1688	102.42891
13BO-187.D	4.8	0.3113	1748	1688	103.5545024
13BO-188.D	4.588	0.3009	1694	1688	100.3554502
13BO-189.D	4.528	0.2884	1638	1688	97.03791469
13BO-19.D	3.842	0.2617	1502	1689	88.92835998
13BO-190.D	4.484	0.2903	1643	1689	97.27649497
13BO-191.D	4.307	0.2907	1646	1689	97.45411486
13BO-192.D	4.815	0.3074	1727	1690	102.1893491
13BO-193.D	4.2	0.2728	1559	1690	92.24852071
13BO-194.D	4.92	0.3144	1761	1690	104.2011834
13BO-195.D	5.023	0.3163	1771	1690	104.7928994
13BO-196.D	5.124	0.3241	1808	1690	106.9822485
13BO-2.D	4.571	0.3165	1772	1690	104.852071
13BO-20.D	3.564	0.2512	1444	1690	85.44378698
13BO-21.D	4.443	0.2941	1663	1692	98.28605201
13BO-22.D	4.57	0.3064	1721	1693	101.6538689
13BO-23.D	4.628	0.3081	1734	1693	102.4217366
13BO-24.D	3.968	0.2853	1624	1693	95.92439457
13BO-25.D	4.012	0.2678	1528	1694	90.20070838
13BO-26.D	4.176	0.308	1729	1694	102.0661157
13BO-27.D	4.625	0.3192	1784	1694	105.3128689
13BO-28.D	4.639	0.323	1805	1694	106.5525384
13BO-29.D	4.025	0.3086	1732	1694	102.2432113
13BO-3.D	3.979	0.2758	1571	1695	92.68436578
13BO-30.D	4.768	0.3209	1792	1695	105.7227139
13BO-31.D	4.833	0.3233	1809	1695	106.7256637
13BO-32.D	4.086	0.2972	1679	1695	99.0560472
13BO-33.D	4.26	0.2818	1599	1696	94.28066038
13BO-34.D	4.31	0.2893	1636	1697	96.40542133
13BO-35.D	4.586	0.3107	1747	1697	102.946376
13BO-36.D	4.676	0.3135	1756	1697	103.4767236
13BO-37.D	4.352	0.2985	1685	1698	99.2343934
13BO-38.D	4.661	0.3095	1737	1698	102.2968198
13BO-39.D	3.372	0.2298	1335	1699	78.57563273
13BO-4.D	4.522	0.3116	1749	1699	102.9429076
13BO-40.D	4.439	0.3021	1700	1699	100.0588582
13BO-41.D	4.257	0.287	1625	1700	95.58823529
13BO-42.D	4.629	0.3065	1722	1701	101.2345679
13BO-43.D	4.742	0.3113	1746	1701	102.6455026
13BO-44.D	4.435	0.298	1684	1701	99.00058789

Maria Then
Origin of Proterozoic granites in Mt Boothby

13BO-45.D	4.436	0.2921	1653	1702	97.12103408
13BO-46.D	4.1	0.2785	1582	1702	92.94947121
13BO-47.D	4.552	0.2974	1677	1702	98.53113984
13BO-48.D	4.432	0.2947	1663	1703	97.65120376
13BO-49.D	4.519	0.2978	1685	1703	98.94304169
13BO-5.D	4.309	0.2952	1666	1704	97.76995305
13BO-50.D	4.416	0.2871	1626	1704	95.42253521
13BO-51.D	3.938	0.2904	1642	1704	96.36150235
13BO-52.D	4.289	0.3082	1733	1704	101.7018779
13BO-53.D	4.525	0.3174	1776	1705	104.1642229
13BO-54.D	2.982	0.2384	1377	1705	80.76246334
13BO-55.D	4.441	0.3129	1754	1705	102.8739003
13BO-56.D	4.581	0.3258	1819	1705	106.686217
13BO-57.D	4.656	0.329	1832	1705	107.4486804
13BO-58.D	4.084	0.295	1665	1706	97.59671747
13BO-59.D	4.016	0.2912	1647	1706	96.54161782
13BO-6.D	4.643	0.3188	1784	1706	104.5720985
13BO-60.D	4.509	0.3244	1813	1706	106.2719812
13BO-61.D	4.453	0.3119	1749	1706	102.5205158
13BO-62.D	3.895	0.2775	1577	1707	92.38429994
13BO-63.D	4.16	0.3058	1719	1707	100.7029877
13BO-64.D	3.407	0.2406	1389	1707	81.37082601
13BO-65.D	4.457	0.3127	1758	1707	102.9876977
13BO-66.D	4.3	0.3026	1703	1707	99.76567077
13BO-67.D	4.594	0.3222	1799	1708	105.3278689
13BO-68.D	3.7	0.252	1410	1709	82.50438853
13BO-69.D	4.472	0.3144	1761	1709	103.042715
13BO-7.D	4.489	0.3091	1737	1709	101.638385
13BO-70.D	4.678	0.3192	1787	1710	104.502924
13BO-71.D	4.204	0.2897	1639	1710	95.84795322
13BO-72.D	4.512	0.3096	1740	1711	101.6949153
13BO-73.D	4.714	0.3181	1779	1711	103.974284
13BO-74.D	4.49	0.3064	1725	1711	100.818235
13BO-75.D	4.609	0.3135	1759	1712	102.7453271
13BO-76.D	3.721	0.278	1580	1712	92.28971963
13BO-77.D	5.287	0.3328	1852	1712	108.1775701
13BO-78.D	5.079	0.3238	1809	1712	105.6658879
13BO-79.D	4.785	0.3064	1726	1712	100.817757
13BO-8.D	4.013	0.2753	1566	1713	91.41856392
13BO-80.D	4.728	0.3097	1742	1713	101.6929364
13BO-81.D	4.758	0.3065	1724	1713	100.6421483
13BO-82.D	5.025	0.3147	1762	1713	102.8604787
13BO-83.D	4.71	0.3064	1725	1713	100.7005254
13BO-84.D	4.954	0.3168	1776	1713	103.6777583
13BO-85.D	4.357	0.2875	1628	1714	94.98249708
13BO-86.D	4.809	0.3099	1741	1714	101.5752625

Maria Then
Origin of Proterozoic granites in Mt Boothby

13BO-87.D	4.901	0.3133	1755	1714	102.3920653
13BO-88.D	4.953	0.3138	1760	1714	102.6837806
13BO-89.D	3.752	0.2615	1497	1714	87.33955659
13BO-9.D	4.298	0.3007	1694	1714	98.83313886
13BO-90.D	4.728	0.3082	1730	1714	100.9334889
13BO-91.D	4.932	0.316	1769	1714	103.2088681
13BO-92.D	5.032	0.3172	1775	1715	103.4985423
13BO-93.D	4.804	0.3071	1727	1715	100.6997085
13BO-94.D	4.497	0.2961	1670	1715	97.37609329
13BO-95.D	4.981	0.3178	1780	1715	103.7900875
13BO-96.D	4.671	0.3047	1713	1716	99.82517483
13BO-97.D	4.739	0.3104	1747	1716	101.8065268
13BO-98.D	4.071	0.2732	1559	1716	90.85081585
13BO-99.D	4.267	0.281	1596	1716	93.00699301
13BO-197.D	4.65	0.3034	1707	1716	99.47552448
13BO-198.D	2.312	0.1512	909	1716	52.97202797
13BO-199.D	4.755	0.3028	1704	1716	99.3006993
13BO-200.D	4.68	0.2983	1682	1716	98.01864802
13BO-201.D	4.816	0.3032	1706	1717	99.3593477
13BO-202.D	3.848	0.2512	1446	1717	84.21665696
13BO-203.D	4.365	0.2754	1571	1718	91.443539
13BO-204.D	4.757	0.2998	1689	1718	98.31199069
13BO-206.D	4.646	0.2949	1665	1718	96.91501746
13BO-207.D	4.99	0.3093	1738	1718	101.1641444
13BO-208.D	3.511	0.2515	1445	1718	84.10942957
13BO-209.D	4.747	0.3029	1704	1718	99.18509895
13BO-210.D	4.075	0.2653	1520	1718	88.4749709
13BO-211.D	4.356	0.2846	1613	1719	93.8336242
13BO-212.D	4.607	0.3	1690	1719	98.31297266
13BO-213.D	4.616	0.3025	1705	1719	99.18557301
13BO-214.D	4.702	0.3048	1714	1719	99.70913322
13BO-215.D	4.732	0.3044	1712	1719	99.5927865
13BO-216.D	4.829	0.3074	1731	1720	100.6395349
13BO-217.D	4.644	0.2987	1683	1720	97.84883721
13BO-218.D	4.282	0.2775	1582	1720	91.97674419
13BO-219.D	4.87	0.3161	1772	1720	103.0232558
13BO-220.D	4.168	0.2753	1565	1720	90.98837209
13BO-221.D	4.854	0.3171	1773	1721	103.0214991
13BO-222.D	4.27	0.2891	1635	1721	95.00290529
13BO-223.D	4.302	0.2793	1586	1721	92.15572342
13BO-224.D	3.699	0.2541	1458	1721	84.7181871
13BO-225.D	4.829	0.3009	1694	1722	98.37398374
13BO-226.D	4.624	0.2839	1612	1722	93.61207898
13BO-227.D	4.666	0.2889	1637	1722	95.06387921
13BO-228.D	4.88	0.3007	1692	1722	98.25783972
13BO-229.D	4.41	0.2793	1588	1723	92.16482879

Maria Then
Origin of Proterozoic granites in Mt Boothby

13BO-230.D	4.988	0.3063	1723	1723	100
13BO-231.D	4.87	0.2936	1657	1723	96.16947185
13BO-232.D	4.71	0.2907	1645	1724	95.41763341
13BO-233.D	4.97	0.2969	1674	1724	97.09976798
13BO-234.D	4.54	0.2758	1576	1724	91.41531323
13BO-235.D	4.596	0.2879	1632	1724	94.66357309
13BO-236.D	5.036	0.3031	1710	1725	99.13043478
13BO-237.D	4.886	0.2986	1682	1725	97.50724638
13BO-238.D	5.08	0.3066	1722	1725	99.82608696
13BO-239.D	5.05	0.3076	1733	1725	100.4637681
13BO-240.D	5.042	0.3064	1721	1725	99.76811594
13BO-241.D	5.048	0.315	1764	1726	102.2016222
13BO-242.D	3.38	0.208	1211	1726	70.1622248
13BO-243.D	5.002	0.3105	1744	1726	101.0428737
13BO-244.D	4.595	0.2905	1644	1726	95.24913094
13BO-245.D	4.695	0.3003	1691	1726	97.97219003
13BO-246.D	5.053	0.3168	1773	1726	102.7230591
13BO-247.D	4.57	0.3006	1696	1726	98.26187717
13BO-248.D	4.828	0.3171	1774	1726	102.7809965
13BO-249.D	4.911	0.323	1803	1727	104.4006948
13BO-250.D	4.401	0.298	1679	1727	97.22061378
13BO-251.D	4.607	0.3014	1699	1727	98.37869137
13BO-252.D	4.48	0.3008	1693	1727	98.03126809
13BO-253.D	4.964	0.3216	1798	1727	104.1111754
13BO-254.D	4.72	0.3121	1751	1727	101.3896931
13BO-255.D	4.811	0.3114	1750	1727	101.3317892
13BO-256.D	4.55	0.2964	1671	1727	96.75738274
13BO-257.D	4.918	0.3089	1736	1728	100.462963
13BO-258.D	4.429	0.2894	1639	1728	94.84953704
13BO-259.D	4.798	0.3073	1725	1728	99.82638889
13BO-260.D	4.755	0.311	1744	1729	100.8675535
13BO-261.D	4.91	0.3159	1768	1729	102.2556391
13BO-262.D	4.542	0.2996	1687	1729	97.5708502
13BO-263.D	5.086	0.3295	1835	1729	106.1307114
13BO-264.D	4.72	0.3041	1710	1729	98.9010989
13BO-265.D	4.723	0.3081	1731	1729	100.1156738
13BO-266.D	4.772	0.3103	1743	1729	100.8097166
13BO-267.D	4.825	0.3107	1742	1729	100.7518797
13BO-268.D	4.69	0.3036	1709	1729	98.843262
13BO-269.D	4.71	0.3022	1700	1730	98.26589595
13BO-270.D	4.999	0.3299	1839	1730	106.300578
13BO-271.D	4.039	0.2741	1562	1730	90.28901734
13BO-273.D	3.947	0.2633	1508	1730	87.16763006
13BO-274.D	4.99	0.3265	1820	1730	105.2023121
13BO-275.D	4.98	0.3321	1847	1730	106.7630058
13BO-276.D	3.25	0.2304	1338	1730	77.34104046

Maria Then
Origin of Proterozoic granites in Mt Boothby

13BO-277.D	4.67	0.312	1751	1730	101.2138728
13BO-278.D	4.765	0.3196	1786	1730	103.2369942
13BO-279.D	4.895	0.3294	1837	1731	106.123628
13BO-280.D	3.978	0.2664	1522	1731	87.9260543
13BO-281.D	3.607	0.2435	1403	1731	81.05141537
13BO-282.D	4.32	0.2976	1680	1731	97.05372617
13BO-283.D	4.98	0.3358	1863	1732	107.5635104
13BO-284.D	4.49	0.3065	1721	1732	99.36489607
13BO-285.D	3.231	0.222	1292	1732	74.59584296
13BO-286.D	2.885	0.205	1201	1732	69.34180139
13BO-287.D	4.464	0.304	1709	1732	98.67205543
13BO-288.D	4.93	0.331	1841	1733	106.2319677
13BO-289.D	4.707	0.3144	1763	1733	101.7311021
13BO-290.D	4.204	0.2884	1631	1733	94.11425274
13BO-291.D	2.68	0.1893	1116	1733	64.39699942
13BO-292.D	4.7	0.3125	1753	1734	101.0957324
13BO-293.D	4.55	0.3044	1710	1734	98.61591696
13BO-294.D	4.387	0.302	1705	1734	98.32756632
13BO-295.D	4.61	0.3046	1711	1734	98.67358708
13BO-296.D	4.761	0.3171	1774	1734	102.3068051
13BO-297.D	4.95	0.3375	1872	1735	107.8962536
13BO-298.D	4.849	0.3234	1804	1735	103.9769452
13BO-299.D	5.126	0.3364	1867	1735	107.6080692
13BO-300.D	4.95	0.3343	1860	1735	107.204611
13BO-301.D	4.135	0.2757	1571	1735	90.54755043
13BO-302.D	4.412	0.3027	1703	1735	98.1556196
13BO-303.D	4.816	0.322	1800	1736	103.6866359
13BO-304.D	4.7	0.3215	1795	1736	103.3986175
13BO-305.D	5.09	0.3349	1860	1736	107.1428571
13BO-306.D	5.18	0.3367	1869	1736	107.6612903
13BO-307.D	4.97	0.3331	1852	1736	106.6820276
13BO-308.D	5.192	0.3306	1843	1736	106.1635945
13BO-309.D	5.062	0.3316	1844	1736	106.2211982
13BO-310.D	4.16	0.266	1519	1736	87.5
13BO-311.D	5.137	0.335	1861	1737	107.138745
13BO-312.D	5.22	0.3348	1860	1737	107.0811744
13BO-313.D	5.107	0.3251	1813	1737	104.3753598
13BO-314.D	4.957	0.3246	1810	1737	104.2026482
13BO-315.D	5.018	0.3275	1828	1737	105.2389177
13BO-316.D	4.3	0.2775	1577	1737	90.78871618
13BO-317.D	4.444	0.2873	1626	1737	93.60967185
13BO-318.D	4.508	0.304	1712	1738	98.50402762
13BO-319.D	4.57	0.295	1665	1738	95.79976985
13BO-320.D	4.417	0.2932	1656	1738	95.28193326
13BO-321.D	4.53	0.3005	1691	1738	97.29574223
13BO-322.D	5.11	0.3315	1844	1738	106.0989643

Maria Then
Origin of Proterozoic granites in Mt Boothby

13BO-323.D	4.74	0.3138	1758	1738	101.150748
13BO-324.D	4.954	0.3221	1802	1738	103.6823936
13BO-325.D	5.02	0.3238	1807	1738	103.9700806
13BO-326.D	4.65	0.3063	1721	1739	98.96492237
13BO-327.D	4.178	0.2845	1615	1739	92.86946521
13BO-328.D	4.238	0.2927	1654	1739	95.11213341
13BO-329.D	3.51	0.24	1385	1739	79.64347326
13BO-330.D	3.308	0.2294	1331	1740	76.49425287
13BO-331.D	4.312	0.2961	1672	1740	96.09195402
13BO-332.D	4.64	0.318	1778	1740	102.183908
13BO-333.D	4.215	0.294	1660	1740	95.40229885
13BO-334.D	4.883	0.3304	1846	1740	106.091954
13BO-335.D	4.507	0.3124	1751	1740	100.6321839
13BO-336.D	4.503	0.3146	1761	1740	101.2068966
13BO-337.D	4.49	0.3056	1722	1740	98.96551724
13BO-338.D	4.35	0.3032	1708	1740	98.16091954
13BO-339.D	4.773	0.3313	1843	1741	105.8587019
13BO-340.D	4.33	0.3051	1714	1741	98.44916715
13BO-341.D	4.255	0.3033	1706	1741	97.98966111
13BO-342.D	4.71	0.3205	1793	1741	102.9867892
13BO-343.D	4.162	0.2879	1632	1741	93.73923033
13BO-344.D	4.353	0.2932	1656	1742	95.06314581
13BO-345.D	4.324	0.2937	1660	1742	95.29276693
13BO-346.D	4.808	0.3234	1808	1742	103.7887486
13BO-347.D	4.1	0.2905	1643	1742	94.31687715
13BO-348.D	4.676	0.3159	1773	1742	101.7795637
13BO-349.D	4.613	0.3058	1718	1742	98.62227325
13BO-350.D	4.574	0.3119	1749	1742	100.401837
13BO-351.D	4.65	0.3149	1763	1742	101.2055109
13BO-352.D	4.573	0.3127	1755	1743	100.6884682
13BO-353.D	5.02	0.3203	1792	1743	102.811245
13BO-354.D	4.4	0.2905	1643	1743	94.26276535
13BO-355.D	4.976	0.3201	1789	1743	102.6391279
13BO-356.D	5.319	0.3345	1861	1743	106.7699369
13BO-357.D	4.933	0.3162	1772	1743	101.663798
13BO-358.D	5.421	0.3362	1867	1743	107.114171
13BO-359.D	4.7	0.3044	1711	1743	98.16408491
13BO-360.D	4.84	0.299	1679	1743	96.32816982
13BO-361.D	5.185	0.3235	1806	1743	103.6144578
13BO-362.D	5.3	0.3342	1857	1744	106.4793578
13BO-363.D	5.086	0.3145	1761	1744	100.9747706
13BO-364.D	4.46	0.2941	1663	1744	95.35550459
13BO-365.D	5.09	0.3234	1804	1744	103.440367
13BO-366.D	5.111	0.32	1791	1744	102.6949541
13BO-367.D	5.174	0.3123	1750	1744	100.3440367
13BO-368.D	4.98	0.3102	1745	1745	100

Maria Then
Origin of Proterozoic granites in Mt Boothby

13BO-369.D	3.99	0.2464	1419	1745	81.31805158
13BO-370.D	5.34	0.3377	1873	1745	107.3352436
13BO-371.D	4.62	0.3081	1729	1745	99.08309456
13BO-372.D	5.074	0.3219	1799	1745	103.0945559
13BO-373.D	5.37	0.334	1855	1745	106.3037249
13BO-374.D	5.385	0.3395	1881	1746	107.7319588
13BO-375.D	5.15	0.323	1805	1746	103.3791523
13BO-376.D	5.06	0.3255	1814	1746	103.8946163
13BO-377.D	5.16	0.3299	1835	1746	105.0973654
13BO-378.D	4.69	0.3089	1733	1746	99.25544101
13BO-379.D	4.86	0.3138	1756	1746	100.5727377
13BO-380.D	4.575	0.3094	1736	1746	99.42726231
13BO-381.D	5.15	0.3327	1856	1746	106.3001145
13BO-382.D	3.76	0.2439	1405	1746	80.4696449
13BO-383.D	5.02	0.337	1873	1746	107.2737686
13BO-384.D	5.193	0.3419	1893	1747	108.3571837
13BO-385.D	5.19	0.3336	1854	1747	106.1247853
13BO-386.D	5.12	0.338	1882	1747	107.7275329
13BO-387.D	4.129	0.2839	1610	1747	92.15798512
13BO-388.D	4.763	0.3194	1785	1747	102.1751574
13BO-389.D	5.257	0.3366	1869	1748	106.9221968
13BO-390.D	5.05	0.3354	1863	1748	106.5789474
13BO-391.D	4.807	0.3237	1806	1748	103.3180778
13BO-392.D	4.987	0.3266	1824	1748	104.3478261
13BO-393.D	4.523	0.3068	1724	1748	98.62700229
13BO-394.D	4.399	0.3056	1722	1748	98.51258581
13BO-395.D	4.74	0.3123	1751	1748	100.1716247
13BO-396.D	4.784	0.3217	1797	1748	102.8032037
13BO-397.D	4.636	0.3002	1693	1748	96.85354691
13BO-398.D	4.666	0.3067	1723	1748	98.56979405
13BO-399.D	4.527	0.2985	1684	1749	96.28359062
13BO-400.D	4.499	0.2978	1681	1749	96.11206404
13BO-401.D	4.478	0.2972	1678	1749	95.94053745
13BO-402.D	4.599	0.3009	1695	1749	96.91252144
13BO-403.D	4.535	0.2969	1674	1749	95.71183533
13BO-404.D	4.647	0.3029	1708	1749	97.65580332
13BO-405.D	3.109	0.0717	446	1749	25.50028588
13BO-406.D	4.808	0.3112	1745	1749	99.77129788
13BO-407.D	4.772	0.3195	1785	1749	102.058319
13BO-408.D	4.525	0.2953	1668	1749	95.36878216
13BO-409.D	4.308	0.2858	1619	1749	92.56718125
13BO-410.D	4.38	0.286	1629	1749	93.13893654
13BO-411.D	4.683	0.3141	1760	1750	100.5714286
13BO-412.D	4.118	0.281	1597	1750	91.25714286
13BO-413.D	4.325	0.2923	1654	1750	94.51428571
13BO-414.D	3.677	0.2487	1431	1750	81.77142857

Maria Then
Origin of Proterozoic granites in Mt Boothby

13BO-415.D	4.56	0.2991	1688	1750	96.45714286
13BO-416.D	4.812	0.3169	1774	1751	101.3135351
13BO-417.D	4.603	0.3039	1716	1751	98.0011422
13BO-418.D	4.752	0.318	1779	1751	101.5990862
13BO-419.D	4.005	0.2962	1671	1751	95.43118218
13BO-420.D	3.835	0.2938	1661	1752	94.80593607
13BO-421.D	3.848	0.2941	1665	1752	95.03424658
13BO-422.D	4.147	0.3041	1712	1752	97.71689498
13BO-423.D	4.012	0.3033	1706	1752	97.37442922
13BO-424.D	3.705	0.2881	1631	1752	93.09360731
13BO-425.D	3.899	0.2864	1625	1752	92.75114155
13BO-426.D	4.05	0.2931	1658	1752	94.6347032
13BO-427.D	3.703	0.2826	1603	1752	91.49543379
13BO-428.D	3.999	0.2898	1639	1752	93.55022831
13BO-429.D	4.295	0.3093	1740	1753	99.25841415
13BO-430.D	4.295	0.2991	1685	1753	96.12093554
13BO-431.D	4.253	0.2939	1660	1753	94.6948089
13BO-432.D	3.48	0.2509	1444	1753	82.37307473
13BO-433.D	3.951	0.275	1570	1753	89.56075299
13BO-434.D	4.263	0.2929	1655	1753	94.40958357
13BO-435.D	3.508	0.2676	1529	1753	87.22190531
13BO-436.D	3.906	0.2659	1518	1753	86.59440958
13BO-437.D	4.253	0.2893	1639	1753	93.49686252
13BO-438.D	4.269	0.2871	1626	1753	92.75527667
13BO-439.D	3.73	0.258	1463	1753	83.45693098
13BO-440.D	4.547	0.301	1695	1754	96.63625998
13BO-441.D	4.368	0.2916	1648	1754	93.95667047
13BO-442.D	4.129	0.2726	1555	1754	88.65450399
13BO-443.D	4.895	0.3292	1833	1754	104.5039909
13BO-444.D	4.768	0.3146	1767	1754	100.7411631
13BO-445.D	4.234	0.2952	1668	1754	95.09692132
13BO-446.D	4.338	0.2992	1688	1754	96.23717218
13BO-447.D	4.604	0.3122	1756	1755	100.0569801
13BO-449.D	4.399	0.2947	1664	1755	94.81481481
13BO-450.D	4.182	0.2895	1639	1755	93.39031339
13BO-451.D	4.174	0.2862	1621	1755	92.36467236
13BO-452.D	4.476	0.3043	1713	1755	97.60683761
13BO-453.D	4.573	0.3094	1739	1755	99.08831909
13BO-454.D	4.558	0.3135	1756	1755	100.0569801
13BO-455.D	4.437	0.3027	1706	1755	97.20797721
13BO-456.D	4.393	0.3005	1696	1756	96.58314351
13BO-457.D	4.329	0.2942	1661	1756	94.58997722
13BO-458.D	4.387	0.3031	1710	1756	97.38041002
13BO-459.D	4.216	0.2926	1656	1756	94.30523918
13BO-460.D	4.331	0.3083	1733	1756	98.69020501
13BO-461.D	4.171	0.3	1690	1756	96.24145786

Maria Then
Origin of Proterozoic granites in Mt Boothby

13BO-462.D	4.221	0.2957	1668	1756	94.98861048
13BO-463.D	3.454	0.273	1557	1756	88.66742597
13BO-464.D	3.963	0.2851	1615	1756	91.97038724
13BO-465.D	4.019	0.291	1647	1756	93.79271071
13BO-466.D	4.503	0.3134	1758	1756	100.1138952
13BO-467.D	4.612	0.3103	1743	1756	99.25968109
13BO-468.D	4.827	0.3148	1763	1757	100.3414912
13BO-469.D	4.753	0.3093	1738	1757	98.91861127
13BO-470.D	4.719	0.3124	1753	1757	99.77233921
13BO-471.D	4.53	0.2978	1679	1757	95.56061468
13BO-472.D	5.076	0.3281	1828	1757	104.0409789
13BO-473.D	4.906	0.327	1822	1757	103.6994878
13BO-474.D	4.774	0.3159	1769	1757	100.6829824
13BO-475.D	4.775	0.3142	1760	1757	100.1707456
13BO-476.D	4.551	0.3005	1693	1757	96.35742743
13BO-477.D	4.806	0.3132	1760	1757	100.1707456
13BO-478.D	4.758	0.3144	1761	1757	100.2276608
13BO-479.D	4.489	0.2997	1688	1758	96.0182025
13BO-480.D	4.618	0.3067	1723	1758	98.00910125
13BO-481.D	4.259	0.2927	1653	1758	94.02730375
13BO-482.D	4.26	0.2827	1604	1758	91.24004551
13BO-483.D	4.028	0.2832	1606	1758	91.35381115
13BO-484.D	4.578	0.308	1730	1758	98.407281
13BO-485.D	4.771	0.3237	1809	1758	102.9010239
13bo235.D	0.84	0.1023	627.7	1758	35.70534699
13bo235.D	0.833	0.0929	572.3	1758	32.55403868
13bo254.D	0.802	0.0968	595.1	1758	33.85096701
13bo254.D	0.9	0.1078	659	1759	37.46446845
13bo158.D	2.106	0.1696	1009	1759	57.36213758
13bo158.D	2.032	0.158	946.4	1759	53.80329733
13bo24.D	3.677	0.2781	1581	1759	89.88061399
13bo230.D	10.72	0.777	3712	1759	211.0289937
13bo230.D	3.2	0.2345	1359	1759	77.25980671
13bo188.D	2.989	0.2112	1234	1759	70.1534963
13bo202.D	4.137	0.2395	1383	1759	78.62421831
13bo35.D	4.187	0.3033	1709	1759	97.15747584
13bo188.D	2.568	0.1867	1103	1759	62.706083
13bo202.D	3.758	0.2733	1556	1760	88.40909091
13bo164.D	3.471	0.2433	1405	1760	79.82954545
13bo164.D	3.148	0.2271	1320	1760	75
13bo246.D	3.784	0.2708	1545	1760	87.78409091
13bo231.D	7.313	0.4431	2365	1760	134.375
13bo247.D	21.94	-0.717	-8440	1760	-479.5454545
13bo231.D	3.939	0.2791	1588	1760	90.22727273
13bo247.D	4.27	0.3051	1721	1760	97.78409091
13bo170.D	4.419	0.2903	1642	1760	93.29545455

Maria Then
Origin of Proterozoic granites in Mt Boothby

13bo170.D	3.851	0.2705	1544	1761	87.67745599
13bo30.D	4.077	0.2857	1622	1761	92.10675752
13bo215.D	4.466	0.3146	1762	1761	100.0567859
13bo19.D	3.693	0.2602	1490	1761	84.61101647
13bo168.D	4.527	0.296	1671	1761	94.88926746
13bo163.D	3.857	0.2677	1529	1761	86.82566723
13bo29.D	4.151	0.2903	1642	1761	93.24247587
13bo168.D	3.932	0.274	1561	1761	88.64281658
13bo163.D	3.772	0.2632	1507	1761	85.57637706
13bo241.D	4.192	0.2949	1665	1761	94.54855196
13bo310.D	2.535	0.233	1349	1762	76.56072645
13bo261.D	3.527	0.2585	1481	1762	84.05221339
13bo21.D	4.055	0.2806	1595	1762	90.52213394
13bo175.D	4.079	0.2649	1514	1762	85.92508513
13bo20.D	3.766	0.2618	1498	1762	85.01702611
13bo175.D	3.663	0.2517	1447	1762	82.12258797
13bo197.D	4.584	0.3235	1806	1762	102.4971623
13bo197.D	4.195	0.2902	1643	1762	93.24631101
13bo176.D	3.229	0.2104	1230	1762	69.80703746
13bo271.D	3.817	0.2687	1535	1763	87.06749858
13bo182.D	4.721	0.3083	1731	1763	98.18491208
13bo26.D	4.499	0.3089	1735	1763	98.41179807
13bo176.D	2.934	0.2004	1177	1763	66.7612025
13bo191.D	4.751	0.3225	1803	1763	102.2688599
13bo182.D	4.109	0.2817	1599	1763	90.69767442
13bo221.D	4.414	0.305	1716	1763	97.33408962
13bo191.D	4.132	0.282	1602	1763	90.86783891
13bo180.D	4.634	0.3048	1715	1763	97.27736812
13bo287.D	4.358	0.3082	1730	1764	98.07256236
13bo303.D	4.431	0.3007	1697	1764	96.20181406
13bo276.D	4.736	0.3097	1740	1764	98.63945578
13bo213.D	4.9	0.2397	1384	1764	78.45804989
13bo198.D	4.579	0.3174	1778	1764	100.7936508
13bo180.D	4.117	0.2804	1593	1764	90.30612245
13bo296.D	4.145	0.2885	1635	1764	92.68707483
13bo286.D	4.595	0.3236	1806	1764	102.3809524
13bo213.D	4.393	0.3001	1691	1764	95.861678
13bo144.D	4.113	0.281	1596	1764	90.47619048
13bo198.D	4.259	0.2912	1648	1764	93.42403628
13bo219.D	4.277	0.2929	1655	1764	93.82086168
13bo153.D	3.716	0.2623	1502	1764	85.14739229
13bo162.D	4.174	0.2843	1612	1764	91.38321995
13bo199.D	4.527	0.3098	1739	1764	98.58276644
13bo313.D	1.341	0.1712	1019.4	1765	57.75637394
13bo155.D	4.781	0.3356	1865	1765	105.6657224
13bo199.D	4.246	0.2881	1631	1765	92.40793201

Maria Then
Origin of Proterozoic granites in Mt Boothby

13bo144.D	4.266	0.2888	1635	1765	92.63456091
13bo7.D	4.52	0.3053	1717	1765	97.28045326
13bo153.D	3.582	0.2425	1400	1765	79.32011331
13bo162.D	4.071	0.2768	1575	1765	89.23512748
13bo156.D	4.436	0.3113	1748	1765	99.0368272
13bo242.D	4.477	0.3086	1733	1765	98.18696884
13bo155.D	4.604	0.3098	1739	1765	98.52691218
13bo206.D	5.396	0.2305	1336	1765	75.69405099
13bo282.D	0.233	0.01582	101.2	1765	5.733711048
13bo309.D	0.2843	0.02395	152.5	1765	8.640226629
13bo25.D	4.123	0.2802	1592	1765	90.19830028
13bo156.D	4.265	0.2884	1633	1766	92.46885617
13bo206.D	4.4	0.2979	1680	1766	95.13023783
13bo249.D	3.29	0.223	1278	1766	72.36693092
13bo22.D	4.498	0.3054	1718	1766	97.2819932
13bo166.D	5.237	0.3342	1858	1766	105.209513
13bo181.D	5.101	0.3291	1833	1766	103.7938845
13bo301.D	3.08	0.205	1174	1766	66.47791619
13bo232.D	4.67	0.2671	1525	1766	86.35334088
13bo284.D	0.3884	0.02612	166.2	1766	9.411098528
13bo232.D	3.027	0.2055	1202	1766	68.06342016
13bo298.D	4.378	0.2981	1683	1766	95.30011325
13bo166.D	4.611	0.309	1735	1766	98.24462061
13bo37.D	4.612	0.3122	1751	1767	99.09451047
13bo258.D	3.63	0.27	1568	1767	88.73797397
13bo181.D	4.501	0.3023	1702	1767	96.32144878
13bo12.D	4.92	0.3287	1834	1767	103.7917374
13bo311.D	2.097	0.2194	1280	1767	72.43916242
13bo295.D	4.33	0.301	1696	1767	95.98189021
13bo174.D	4.79	0.3022	1703	1767	96.37804188
13bo292.D	4.397	0.3079	1729	1767	97.84946237
13bo305.D	0.3386	0.02278	145.2	1767	8.217317487
13bo243.D	4.605	0.3137	1758	1767	99.49066214
13bo193.D	4.964	0.3386	1881	1768	106.3914027
13bo252.D	4.952	0.3812	2084	1768	117.8733032
13bo172.D	5.051	0.3173	1777	1768	100.5090498
13bo245.D	4.624	0.3131	1755	1768	99.26470588
13bo289.D	4.633	0.3245	1811	1768	102.4321267
13bo174.D	4.271	0.2865	1625	1768	91.91176471
13bo193.D	4.385	0.2962	1672	1768	94.57013575
13bo238.D	4.658	0.3146	1763	1768	99.71719457
13bo161.D	4.764	0.3248	1812	1769	102.4307518
13bo2-3.D	4.858	0.327	1825	1769	103.1656303
13bo165.D	5.151	0.3317	1846	1769	104.3527417
13bo308.D	1.08	0.078	465	1769	26.28603731
13bo260.D	4.254	0.3017	1699	1769	96.04296213

Maria Then
Origin of Proterozoic granites in Mt Boothby

13bo252.D	4.726	0.318	1782	1770	100.6779661
13bo172.D	4.431	0.2981	1682	1770	95.02824859
13bo302.D	4.567	0.3057	1719	1770	97.11864407
13bo9.D	4.74	0.3198	1790	1770	101.1299435
13bo214.D	4.313	0.2885	1633	1770	92.25988701
13bo167.D	4.669	0.2946	1667	1770	94.18079096
13bo217.D	4.539	0.3059	1720	1770	97.17514124
13bo18.D	4.626	0.3098	1739	1771	98.19311124
13bo40.D	4.808	0.3238	1808	1771	102.0892151
13bo4.D	4.883	0.3296	1836	1771	103.6702428
13bo28.D	4.402	0.2947	1664	1771	93.9582157
13bo165.D	4.569	0.3072	1726	1771	97.45906268
13bo161.D	4.62	0.3106	1743	1772	98.36343115
13bo17.D	4.713	0.3149	1764	1772	99.54853273
13bo31.D	4.743	0.3164	1772	1772	100
13bo42.D	5.107	0.3437	1903	1772	107.3927765
13bo222.D	3.36	0.2245	1301	1772	73.41986456
13bo293.D	4.259	0.2964	1673	1772	94.41309255
13bo307.D	4.269	0.3036	1708	1772	96.38826185
13bo16.D	4.644	0.3112	1747	1772	98.58916479
13bo281.D	0.261	0.0173	110.5	1773	6.232374506
13bo203.D	5.11	0.2628	1503	1773	84.7715736
13bo167.D	4.088	0.2723	1553	1773	87.59165257
13bo212.D	4.238	0.2843	1614	1773	91.0321489
13bo195.D	4.346	0.2983	1682	1773	94.86745629
13bo13.D	4.558	0.3052	1716	1773	96.78510998
13bo279.D	4.69	0.3055	1718	1773	96.89791314
13bo146.D	5.162	0.3504	1936	1774	109.1319053
13bo272.D	4.294	0.2974	1677	1774	94.53213078
13bo300.D	4.512	0.3044	1712	1774	96.50507328
13bo169.D	5.13	0.3216	1797	1774	101.2965051
13bo1.D	4.872	0.3274	1825	1774	102.8748591
13bo186.D	5.162	0.3307	1841	1774	103.7767756
13bo212.D	4.871	0.2176	1268	1774	71.47688839
13bo270.D	4.233	0.296	1670	1775	94.08450704
13bo220.D	4.665	0.3124	1752	1775	98.70422535
13bo190.D	5.123	0.3398	1886	1775	106.2535211
13bo195.D	3.917	0.2636	1509	1775	85.01408451
13bo283.D	4.576	0.3034	1707	1775	96.16901408
13bo203.D	4.535	0.3085	1733	1775	97.63380282
13bo38.D	4.787	0.3223	1802	1775	101.5211268
13bo288.D	4.727	0.328	1827	1775	102.9295775
13bo192.D	5.151	0.3424	1897	1775	106.8732394
13bo194.D	5.173	0.3497	1932	1776	108.7837838
13bo214.D	4.528	0.2381	1378	1776	77.59009009
13bo285.D	4.457	0.2958	1671	1776	94.08783784

Maria Then
Origin of Proterozoic granites in Mt Boothby

13bo186.D	4.427	0.2962	1671	1776	94.08783784
13bo266.D	4.21	0.2965	1673	1776	94.20045045
13bo259.D	4.465	0.3145	1762	1776	99.21171171
13bo306.D	4.725	0.316	1773	1777	99.77490152
13bo39.D	4.784	0.3215	1796	1777	101.0692178
13bo229.D	25.82	2.497	8059	1777	453.5171638
13bo229.D	4.449	0.2973	1676	1777	94.31626337
13bo190.D	4.437	0.2977	1680	1777	94.54136185
13bo169.D	4.454	0.2983	1682	1777	94.65391109
13bo36a.D	4.702	0.3145	1762	1777	99.1558807
13bo227.D	4.711	0.3173	1777	1777	100
13bo256.D	4.595	0.3192	1785	1777	100.450197
13bo11.D	4.793	0.32	1789	1778	100.6186727
13bo36b.D	4.811	0.3227	1802	1778	101.3498313
13bo146.D	5.201	0.3466	1917	1778	107.8177728
13bo312.D	0.1439	0.01696	108.4	1778	6.096737908
13bo194.D	4.603	0.3066	1723	1778	96.90663667
13bo178.D	4.831	0.3083	1731	1778	97.35658043
13bo34.D	4.693	0.3148	1765	1778	99.26884139
13bo173.D	5.065	0.3171	1777	1778	99.94375703
13bo10.D	4.93	0.333	1852	1778	104.1619798
13bo189.D	5.163	0.337	1871	1779	105.1714446
13bo233.D	6.074	0.3437	1904	1779	107.0264193
13bo207.D	5.707	0.2262	1314	1779	73.86172007
13bo210.D	5.811	0.2273	1321	1780	74.21348315
13bo192.D	4.501	0.2991	1686	1780	94.71910112
13bo294.D	4.534	0.3124	1751	1780	98.37078652
13bo152.D	4.918	0.3403	1887	1780	106.011236
13bo233.D	4.562	0.3061	1721	1780	96.68539326
13bo304.D	4.653	0.3065	1725	1780	96.91011236
13bo177.D	4.874	0.3103	1743	1780	97.92134831
13bo148.D	4.919	0.3353	1863	1780	104.6629213
13bo178.D	4.435	0.2937	1659	1781	93.14991578
13bo189.D	4.444	0.2969	1675	1781	94.04828748
13bo173.D	4.489	0.2997	1691	1781	94.94665918
13bo210.D	4.585	0.3077	1730	1781	97.1364402
13bo33.D	4.655	0.3105	1744	1781	97.92251544
13bo209.D	5.866	0.2268	1317	1781	73.94722066
13bo207.D	4.51	0.3018	1700	1782	95.39842873
13bo216.D	4.772	0.3175	1776	1782	99.66329966
13bo177.D	4.451	0.2958	1671	1782	93.77104377
13bo152.D	4.761	0.3162	1771	1782	99.38271605
13bo6.D	4.794	0.32	1789	1782	100.3928171
13bo237.D	4.9	0.3273	1822	1782	102.2446689
13bo159.D	4.899	0.3333	1853	1782	103.9842873
13bo150.D	4.904	0.3379	1877	1782	105.3310887

Maria Then
Origin of Proterozoic granites in Mt Boothby

13bo265.D	4.258	0.3019	1700	1783	95.34492428
13bo200.D	5.059	0.3075	1728	1783	96.91531127
13bo209.D	4.572	0.3075	1728	1783	96.91531127
13bo148.D	4.864	0.3216	1797	1783	100.7851935
13bo187.D	5.319	0.3446	1908	1783	107.0106562
13bo250.D	6.55	0.839	3922	1783	219.9663489
13bo264.D	4.198	0.2994	1688	1783	94.67190129
13bo225.D	4.71	0.3137	1758	1783	98.59786876
13bo160.D	4.711	0.32	1791	1784	100.3923767
13bo196.D	4.873	0.3314	1849	1784	103.6434978
13bo185.D	5.256	0.3339	1857	1785	104.0336134
13bo223.D	4.572	0.3054	1717	1785	96.19047619
13bo228.D	4.57	0.3068	1726	1786	96.64053751
13bo15.D	4.586	0.309	1735	1786	97.14445689
13bo8.D	4.664	0.3146	1764	1786	98.76819709
13bo200.D	4.826	0.3205	1791	1786	100.2799552
13bo154.D	4.914	0.3408	1890	1786	105.8230683
13bo147.D	5.098	0.3447	1908	1786	106.8309071
13bo274.D	4.534	0.3046	1713	1787	95.85898153
13bo299.D	4.548	0.3048	1714	1787	95.91494124
13bo187.D	4.563	0.3059	1720	1788	96.19686801
13bo159.D	4.736	0.314	1761	1788	98.48993289
13bo251.D	6.331	0.6076	3060	1788	171.1409396
13bo248.D	14.82	-1.407	-32000	1788	-1789.709172
13bo277.D	2.53	0.162	920	1789	51.42537731
13bo196.D	4.425	0.2951	1670	1789	93.34823924
13bo185.D	4.516	0.3004	1693	1789	94.63387367
13bo201.D	5.347	0.3121	1751	1790	97.82122905
13bo171.D	5.134	0.3184	1783	1790	99.60893855
13bo150.D	4.798	0.319	1786	1790	99.77653631
13bo257.D	4.59	0.3195	1786	1790	99.77653631
13bo5.D	4.87	0.3251	1814	1790	101.3407821
13bo32.D	4.646	0.3078	1730	1790	96.64804469
13bo179.D	4.838	0.3132	1757	1790	98.15642458
13bo248.D	4.711	0.3146	1764	1791	98.49246231
13bo244.D	4.845	0.3226	1802	1791	100.614182
13bo253.D	4.87	0.325	1813	1792	101.171875
13bo251.D	4.898	0.3256	1816	1793	101.2827663
13bo157.D	4.958	0.3398	1886	1793	105.1868377
13bo149.D	5	0.3404	1888	1795	105.1810585
13bo253.D	4.783	0.3414	1892	1795	105.4038997
13bo160.D	4.563	0.3036	1710	1799	95.05280712
13bo154.D	4.737	0.3147	1763	1799	97.99888827
13bo14.D	4.785	0.3181	1780	1800	98.88888889
13bo255.D	0.4199	0.02817	179.1	1801	9.944475292
13bo205.D	5.646	0.2468	1424	1802	79.02330744

Maria Then
Origin of Proterozoic granites in Mt Boothby

13bo201.D	5.032	0.3352	1863	1803	103.327787
13bo147.D	5.108	0.3371	1872	1803	103.8269551
13bo236.D	5.327	0.3548	1958	1804	108.5365854
13bo290.D	2.47	0.179	1010	1804	55.98669623
13bo280.D	4.529	0.2932	1657	1805	91.80055402
13bo179.D	4.475	0.2969	1677	1808	92.75442478
13bo171.D	4.485	0.298	1682	1808	93.03097345
13bo269.D	1.45	0.103	590	1809	32.61470426
13bo208.D	6.012	0.2315	1343	1813	74.07611693
13bo234.D	5.23	0.3036	1709	1814	94.21168688
13bo267.D	4.349	0.3036	1710	1815	94.21487603
13bo27.D	4.685	0.3109	1745	1815	96.14325069
13bo205.D	4.7	0.3126	1753	1815	96.58402204
13bo41.D	4.867	0.3227	1802	1816	99.22907489
13bo157.D	4.77	0.3157	1768	1817	97.30324711
13bo183.D	5.079	0.3195	1788	1817	98.40396258
13bo234.D	4.786	0.3211	1794	1818	98.67986799
13bo149.D	4.916	0.3238	1808	1818	99.44994499
13bo151.D	5.022	0.3453	1911	1819	105.057724
13bo145.D	5.342	0.358	1972	1819	108.411215
13bo273.D	0.4202	0.02844	180.9	1820	9.93956044
13bo208.D	4.701	0.3122	1751	1820	96.20879121
13bo183.D	4.4	0.291	1647	1821	90.44481054
13bo297.D	4.504	0.3006	1695	1821	93.08072488
13bo275.D	2.79	0.182	1020	1822	55.98243688
13bo218.D	4.689	0.3122	1752	1823	96.1053209
13bo262.D	4.334	0.3027	1704	1823	93.47229841
13bo151.D	4.876	0.3223	1800	1824	98.68421053
13bo145.D	5.44	0.3584	1974	1826	108.1051479
13bo23.D	6.565	0.4341	2322	1828	127.02407
13bo224.D	4.717	0.3132	1759	1829	96.17277201
13bo291.D	0.414	0.02827	179.7	1830	9.819672131
13bo211.D	5.92	0.2332	1352	1833	73.75886525
13bo263.D	4.366	0.3055	1719	1838	93.52557127
13bo184.D	5.088	0.3194	1789	1838	97.33405876
13bo43.D	5.126	0.337	1872	1843	101.5735214
13bo239.D	4.609	0.3074	1729	1844	93.76355748
13bo184.D	4.39	0.2898	1642	1852	88.66090713
13bo211.D	4.758	0.3128	1754	1855	94.55525606
13bo278.D	5.01	0.3202	1791	1856	96.49784483
13bo240.D	4.897	0.3239	1808	1856	97.4137931
13bo268.D	0.3956	0.02736	174	1858	9.364908504
13bo250.D	4.142	0.2757	1560	1859	83.91608392
13bo204.D	5.65	0.2526	1451	1861	77.96883396
13bo204.D	4.806	0.3126	1752	1865	93.94101877
13bo226.D	5.017	0.3204	1794	1889	94.97088407

Maria Then
Origin of Proterozoic granites in Mt Boothby

Source file OSM	Final207_235	Final206_238	FinalAge206_238	FinalAge207_206	Concordance
OSM1_12.D	3.908	0.2777	1808	1665	95
OSM2_4.D	4.483	0.3042	179.8	1710	100
OSM2_5.D	4.367	0.2957	1776	1719	97
OSM1_7.D	4.136	0.284	1579	1737	93
OSM2_9.D	5.017	0.3309	1788	1758	105
OSM1_22.D	5.056	0.3414	1834	1761	108
OSM1_37.D	5.059	0.3293	1887	1786	103
OSM2_1.D	5.118	0.3365	1802	1792	104
OSM1_31.D	4.773	0.3144	2343	1794	98
OSM2_13.D	5.111	0.3277	1849	1803	101
OSM2_15.D	5.581	0.3556	1688	1806	109
OSM1_30.D	5.137	0.3304	1769	1813	101
OSM1_20.D	0.4455	0.02908	184.8	1817	10
OSM1_2.D	4.783	0.3159	1754	1819	97
OSM2_14.D	5.111	0.3294	1895	1820	101
OSM1_36.D	5.181	0.3332	1925	1828	101
OSM1_13.D	4.905	0.3199	194.5	1833	98
OSM1_24.D	0.4746	0.03063	1894	1833	11
OSM1_6.D	4.921	0.3194	2164	1835	97
OSM1_27.D	5.031	0.3244	1810	1836	99
OSM2_2.D	5.381	0.3421	1879	1838	103
OSM1_1.D	5.031	0.3239	1957	1840	98
OSM1_19.D	4.648	0.2995	1974	1840	92
OSM1_11.D	4.894	0.317	1840	1841	96
OSM1_23.D	5.499	0.3481	1763	1855	104
OSM1_25.D	5.352	0.3417	1912	1858	102
OSM1_38.D	5.251	0.3338	1959	1859	100
OSM1_35.D	5.386	0.3413	206.3	1866	101
OSM1_21.D	4.93	0.3129	1892	1870	94
OSM1_8.D	4.69	0.3008	1853	1870	91
OSM1_9.D	4.95	0.3071	1834	1886	92
OSM1_4.D	5.189	0.3253	1856	1899	96
OSM1_10.D	0.4524	0.02829	1815	1901	9
OSM1_28.D	5.491	0.3382	1811	1901	99
OSM2_7.D	5.718	0.3496	1786	1901	102
OSM1_5.D	5.204	0.3241	1611	1908	95
OSM1_32.D	5.637	0.3455	1694	1916	100
OSM1_14.D	5.352	0.3292	1727	1921	95
OSM2_11.D	6.087	0.3679	1869	1928	105
OSM1_16.D	5.256	0.3226	2355	1934	93
OSM1_18.D	5.487	0.3319	2019	1957	94

Maria Then
Origin of Proterozoic granites in Mt Boothby

OSM1_33.D	5.94	0.355	2218	1964	100
OSM1_29.D	5.96	0.3549	1828	1975	99
OSM2_6.D	6.104	0.3594	1834	1978	100
OSM2_8.D	6.379	0.3727	1961	1991	103
OSM1_3.D	6.004	0.3583	1898	1993	99
OSM1_15.D	5.775	0.3403	1999	2001	94
OSM1_34.D	0.5601	0.03252	1715	2014.3	10
OSM2_3.D	6.562	0.364	1671	2070	97
OSM2_12.D	7.646	0.4109	1978	2147	103
OSM1_26.D	7.91	0.399	1932	2265	96
OSM2_10.D	9.41	0.4413	2041	2377	99
OSM1_17.D	9.77	0.4387	1842	2464	95
Source file	Final207_235	Final206_238	FinalAge206_238	FinalAge207_206	Concordance
12BO9.D	0.4588	0.02943	187	1844	10.14099783
12BO25.D	0.4489	0.02935	186.5	1806.7	10.32268777
12BO16.D	0.4487	0.0297	188.7	1802	10.47169811
12bo31.D	3.34	0.209	1170	1873	62.46663107
12BO18.D	7.2	0.3758	2056	2207	93.15813321
12BO20.D	4.463	0.2992	1687	1764	95.63492063
12BO15.D	4.351	0.2972	1677	1741	96.32395175
12BO6.D	4.877	0.3198	1788	1820	98.24175824
12BO21.D	4.901	0.3202	1791	1818	98.51485149
12BO23.D	6.002	0.3562	1963	1983	98.99142713
12BO24.D	5.026	0.3241	1809	1827	99.01477833
12BO5.D	4.603	0.3109	1745	1756	99.37357631
12BO26.D	6.377	0.3684	2021	2033	99.4097393
12BO27.D	5.264	0.3343	1860	1867	99.62506695
12BO13.D	5.666	0.3482	1925	1923	100.1040042
12BO14.D	5.936	0.3591	1977	1973	100.2027369
12BO3.D	5.054	0.3287	1832	1828	100.2188184
12BO11.D	5.169	0.332	1847	1835	100.653951
12BO30.D	3.97	0.2894	1638	1625	100.8
12BO17.D	13.04	0.5199	2698	2676	100.8221226
12BO4.D	4.526	0.3094	1738	1718	101.1641444
12BO8.D	5.246	0.3361	1867	1845	101.1924119
12BO22.D	4.451	0.3073	1728	1706	101.2895662
12BO19.D	7.496	0.4045	2189	2157	101.483542
12BO12.D	5.145	0.3332	1855	1822	101.8111965
12BO29.D	5.624	0.3497	1932	1897	101.8450185
12BO7.D	4.799	0.3221	1799	1764	101.984127
12BO1.D			1789	1741	102.7570362
12BO10.D	5.331	0.3435	1903	1839	103.4801523
12BO2.D	6.667	0.3853	2100	2029	103.4992607
12BO28.D	10.6	0.83	3390	1580	214.556962
Source file MB08-1B	Final207_235	Final206_238	Final206_238_Int2SE	FinalAge207_206	Concordance

Maria Then
Origin of Proterozoic granites in Mt Boothby

MB2-55	4.95	0.3593	0.0054	1579	125.3324889
MB1-40.D	4.849	0.3353	0.0057	1626	114.5756458
MB2-10	4.874	0.3328	0.005	1631	113.4273452
MB2-81	5.54	0.338	0.0058	1632	114.8284314
MB1-46.D	4.989	0.3371	0.0057	1635	114.6788991
MB2-13	4.762	0.3252	0.0045	1637	110.9346365
MB2-14	4.837	0.3285	0.004	1637	111.7898595
MB1-47.D	4.77	0.3247	0.0099	1638	110.5006105
MB2-57	4.318	0.3245	0.0044	1641	110.2985984
MB1-10.D	4.588	0.3189	0.0044	1675	106.4477612
MB2-15	4.764	0.3258	0.004	1682	108.0261593
MB1-65.D	4.209	0.3014	0.0043	1690	100.4142012
MB2-17	4.605	0.3174	0.0057	1690	105.147929
MB1-43.D	4.155	0.2998	0.0057	1694	99.64580874
MB2-42	4.824	0.3275	0.0053	1694	107.7922078
MB1-49.D	4.955	0.3299	0.0043	1697	108.3087802
MB1-64.D	4.654	0.3183	0.0046	1699	104.7675103
MB1-72.D	4.621	0.3192	0.0047	1700	104.9411765
MB2-12	4.82	0.3219	0.0049	1705	105.3958944
MB1-48.D	5.197	0.3364	0.0049	1705	109.5014663
MB1-12.D	4.719	0.3212	0.0057	1706	105.3927315
MB1-50.D	4.709	0.3182	0.0052	1707	104.2179262
MB1-35.D	4.588	0.3123	0.0046	1709	102.3990638
MB1-42.D	4.6	0.3148	0.005	1709	103.1012288
MB1-53.D	4.952	0.3257	0.0053	1711	106.0783168
MB2-11	4.674	0.3156	0.0045	1712	103.2126168
MB2-2	4.664	0.3158	0.0046	1712	103.3294393
MB1-69.D	4.483	0.3082	0.005	1713	101.0507881
MB1-41.D	4.52	0.3101	0.0047	1713	101.517805
MB2-16	4.747	0.318	0.0046	1714	103.7339557
MB2-8	4.445	0.3053	0.0042	1715	100.2915452
MB2-82	5.186	0.3119	0.0048	1716	101.9230769
MB2-85	5.38	0.315	0.01	1716	102.7972028
MB2-3	4.29	0.299	0.014	1718	97.96274738
MB2-24	5.61	0.3429	0.0073	1719	110.3548575
MB1-71.D	4.581	0.31	0.0043	1721	101.0459035
MB1-1.D	4.657	0.3138	0.0044	1721	102.1499128
MB1-61.D	4.465	0.3067	0.0046	1724	99.94199536
MB2-47	4.478	0.3079	0.0058	1724	100.2320186
MB1-3.D	4.892	0.3216	0.0046	1724	104.4083527
MB2-44	4.504	0.307	0.0043	1725	100.115942
MB1-76.D	4.576	0.3095	0.0042	1725	100.6956522
MB1-38.D	4.486	0.3052	0.0043	1727	99.36305732
MB1-2.D	4.713	0.3145	0.0055	1727	102.1424435
MB1-66.D	4.477	0.3058	0.0044	1728	99.47916667
MB1-80.D	4.759	0.3147	0.0042	1728	102.0833333

Maria Then
Origin of Proterozoic granites in Mt Boothby

MB1-22.D	4.494	0.3056	0.0053	1729	99.4794679
MB1-58.D	4.56	0.3073	0.0038	1729	99.8843262
MB1-9.D	6.689	0.3756	0.0055	1729	119.086177
MB1-75.D	5.107	0.3276	0.005	1730	105.4913295
MB1-51.D	4.654	0.3102	0.0036	1731	100.6354708
MB1-55.D	4.349	0.3	0.0051	1732	97.51732102
MB2-40	4.486	0.3014	0.0049	1733	97.86497403
MB1-29.D	4.473	0.3023	0.0041	1733	98.32660127
MB1-44.D	4.811	0.3152	0.0044	1733	102.1927294
MB2-1	6.88	0.3783	0.0058	1733	119.3883439
MB2-61	3.806	0.2967	0.005	1734	96.59746251
MB2-22	4.513	0.2984	0.0046	1734	97.0011534
MB2-21	4.813	0.3103	0.0052	1734	100.6343714
MB2-9	3.885	0.2777	0.0046	1735	91.06628242
MB1-39.D	4.264	0.2924	0.0048	1735	95.21613833
MB1-82.D	4.44	0.2989	0.0041	1735	97.11815562
MB1-52.D	4.66	0.3078	0.0043	1735	99.76945245
MB1-54.D	4.082	0.286	0.0041	1736	93.31797235
MB2-37	4.367	0.2942	0.0053	1736	95.62211982
MB2-50	4.423	0.2994	0.0048	1736	97.11981567
MB1-24.D	4.814	0.3122	0.0052	1736	100.8064516
MB1-4.D	4.71	0.3071	0.0052	1737	99.25158319
MB2-56	3.988	0.2939	0.0067	1738	95.51208285
MB2-45	4.311	0.2959	0.0053	1738	96.02991945
MB2-30	6.64	0.3621	0.0061	1738	114.7295742
MB2-41	4.38	0.2976	0.0041	1739	96.49223692
MB2-7	4.331	0.2923	0.0043	1740	94.88505747
MB1-6.D	6.437	0.3589	0.0055	1740	113.5057471
MB2-48	4.31	0.2924	0.0043	1741	95.11774842
MB2-19	4.606	0.3013	0.0042	1741	97.47271683
MB2-27	5.031	0.3113	0.0052	1743	100.2868617
MB2-62	4.682	0.3286	0.0062	1743	105.1635112
MB1-20.D	4.408	0.2936	0.0047	1744	95.06880734
MB2-35	4.479	0.295	0.0054	1744	95.41284404
MB2-18	4.737	0.3052	0.0052	1745	98.28080229
MB1-45.D	4.377	0.2924	0.0039	1746	94.61626575
MB1-37.D	4.448	0.2949	0.0046	1746	95.41809851
MB1-60.D	4.41	0.2933	0.0044	1748	94.73684211
MB1-15.D	4.21	0.2866	0.0039	1749	92.91023442
MB2-26	4.708	0.2976	0.0044	1749	96.05488851
MB2-34	9.7	0.4295	0.0074	1749	131.5037164
MB2-25	4.57	0.2945	0.005	1750	94.97142857
MB1-30.D	4.476	0.2956	0.0049	1750	95.31428571
MB2-28	4.887	0.3052	0.0049	1750	98.11428571
MB2-84	4.583	0.2773	0.0043	1751	90.00571102
MB2-4	4.257	0.2841	0.0041	1751	92.00456882

Maria Then
Origin of Proterozoic granites in Mt Boothby

MB1-77.D	4.175	0.2832	0.0047	1752	91.78082192
MB2-20	4.293	0.2868	0.0044	1752	92.69406393
MB1-31.D	4.401	0.2902	0.0046	1752	93.66438356
MB1-86.D	6.55	0.3556	0.0061	1752	111.8721461
MB2-58	3.28	0.2641	0.004	1753	86.13804906
MB1-18.D	4.122	0.2807	0.0048	1754	90.82098062
MB2-64	3.688	0.2853	0.0041	1754	92.36031927
MB1-62.D	6.19	0.3438	0.0068	1754	108.5518814
MB1-78.D	4.291	0.2881	0.0047	1755	92.87749288
MB1-14.D	4.566	0.2945	0.0044	1755	94.87179487
MB2-32	4.313	0.2822	0.0047	1757	91.23505976
MB1-70.D	9.52	0.419	0.017	1757	128.685259
MB1-33.D	4.086	0.2776	0.0047	1758	89.98862344
MB2-39	4.95	0.3053	0.0067	1758	97.72468714
MB2-36	4.018	0.2727	0.0046	1760	88.35227273
MB2-60	3.431	0.2707	0.0036	1761	87.73424191
MB1-17.D	4.142	0.2778	0.0039	1762	89.61407491
MB1-28.D	4.087	0.2786	0.0041	1762	89.84108967
MB1-13.D	3.32	0.2464	0.0035	1763	80.60124787
MB1-83.D	4.013	0.2725	0.0043	1763	88.14520703
MB1-7.D	4.219	0.2801	0.0042	1763	90.30062394
MB1-68.D	9.94	0.425	0.02	1763	129.4951787
MB1-21.D	3.896	0.2671	0.0072	1764	86.33786848
MB2-43	4.34	0.2864	0.0046	1764	91.95011338
MB2-53	4.526	0.29	0.0049	1764	93.08390023
MB1-73.D	10.55	0.4336	0.0081	1764	131.9727891
MB2-63	3.538	0.2732	0.0039	1765	88.15864023
MB1-63.D	5.022	0.3046	0.0042	1766	96.9988675
MB2-29	4.729	0.2888	0.0048	1767	92.58630447
MB1-5.D	5.575	0.3198	0.0047	1768	101.0746606
MB1-8.D	4.11	0.2727	0.0044	1769	87.90276993
MB2-46	3.928	0.2659	0.0055	1770	85.93220339
MB1-32.D	4.168	0.2734	0.0046	1772	87.86681716
MB1-16.D	3.935	0.2657	0.004	1774	85.56933484
MB2-65	3.23	0.2574	0.0046	1775	83.21126761
MB2-38	7.74	0.3689	0.0062	1775	113.915493
MB1-27.D	3.338	0.244	0.0042	1779	79.0331647
MB1-25.D	3.878	0.2618	0.0036	1781	84.11005053
MB2-68	2.927	0.2407	0.0034	1782	78.05836139
MB2-31	3.693	0.2506	0.0037	1782	80.80808081
MB2-77	3.578	0.2568	0.0042	1782	82.60381594
MB1-81.D	3.782	0.2573	0.0049	1782	82.996633
MB2-80	4.261	0.2614	0.0049	1782	83.89450056
MB2-51	4.259	0.2717	0.0042	1782	86.98092031
MB1-19.D	3.828	0.26	0.0068	1784	83.40807175
MB2-69	3.24	0.2521	0.0038	1785	81.12044818

Maria Then
Origin of Proterozoic granites in Mt Boothby

MB2-54	3.994	0.2622	0.0042	1785	84.03361345
MB1-84.D	7.24	0.3531	0.0056	1785	109.2436975
MB2-89	4.523	0.2616	0.0043	1790	83.57541899
MB1-74.D	8.76	0.3824	0.0065	1790	116.7597765
MB1-34.D	3.747	0.2531	0.0043	1791	81.23953099
MB2-92	4.373	0.2586	0.0043	1791	82.69123395
MB2-87	4.171	0.246	0.0045	1795	79.1643454
MB2-78	3.556	0.2527	0.0042	1795	80.94707521
MB2-104	3.721	0.249	0.0041	1801	79.62243198
MB2-5	3.86	0.2574	0.0046	1804	81.76274945
MB2-49	3.784	0.2555	0.0043	1810	80.93922652
MB1-56.D	3.93	0.2547	0.0077	1813	80.5846663
MB2-6	3.85	0.2542	0.0035	1820	80.16483516
MB1-67.D	3.309	0.2323	0.0055	1822	73.81997805
MB1-36.D	5.02	0.2917	0.0049	1822	90.45005488
MB2-67	2.783	0.2288	0.0044	1824	72.75219298
MB2-74	3.243	0.2422	0.004	1824	76.75438596
MB2-94	3.832	0.2378	0.0044	1826	75.24644031
MB2-66	2.925	0.2351	0.0038	1840	73.91304348
MB2-103	3.609	0.2405	0.0044	1842	75.46145494
MB2-86	4.136	0.242	0.004	1843	75.85458492
MB1-57.D	3.812	0.2473	0.0053	1849	77.23093564
MB2-93	3.889	0.2375	0.004	1850	74.37837838
MB2-71	3.25	0.243	0.0037	1851	75.68881686
MB2-52	4.065	0.2555	0.0051	1865	78.55227882
MB2-72	3.145	0.2354	0.0039	1866	73.09753483
MB2-91	3.876	0.2344	0.0036	1880	72.18085106
MB2-79	3.366	0.2348	0.0042	1886	72.00424178
MB1-59.D	3.509	0.2351	0.0046	1893	71.94928685
MB2-75	3.003	0.2249	0.003	1940	67.4742268
MB2-102	3.826	0.2422	0.0041	1950	71.64102564
MB1-85.D	5.969	0.3044	0.0043	1975	86.78481013
MB2-70	3.005	0.2296	0.0036	2010	66.21890547
MB2-59	3.095	0.2317	0.004	2045	65.62347188
MB2-83	3.88	0.2309	0.0074	2065	64.74576271
MB2-73	3.033	0.2267	0.0032	2083	63.1781085
MB2-76	3.113	0.2249	0.0038	2088	62.7394636
MB2-100	3.37	0.2185	0.0037	2091	61.07125777
MB2-88	4.91	0.2537	0.005	2111	69.06679299
MB2-101	3.764	0.2313	0.0038	2116	63.51606805
MB2-95	3.459	0.2146	0.004	2122	59.00094251
MB2-90	4.083	0.2266	0.0041	2130	61.83098592
MB2-98	3.247	0.2088	0.0035	2237	54.62673223
MB2-97	3.32	0.2046	0.0032	2318	51.72562554
MB2-99	3.104	0.1992	0.0034	2342	50.04269855
MB2-33	2.928	0.1948	0.0038	2457	46.64224664

Maria Then
Origin of Proterozoic granites in Mt Boothby

MB2-23	3.783	0.205	0.0048	2472	48.54368932
MB2-96	2.479	0.1588	0.0051	2512	37.77866242
MB1-23.D	2.704	0.15	0.002	2540	35.47244094
MB1-26.D	1.691	0.1045	0.0024	2606	24.59708365
Spot name OG1	$^{206}\text{Pb}/^{238}\text{U}$	$^{207}\text{Pb}/^{235}\text{U}$	Conc. (%)²	$^{207}\text{Pb}/^{206}\text{Pb}$	$^{206}\text{Pb}/^{238}\text{U}$
Z67_1	0.31294	4.71152	98	1786.2	1755.1
Z68_2	0.30853	4.70882	96	1811.3	1733.5
Z71_2	0.30913	4.70879	96	1807.8	1736.4
Z72_1	0.32012	4.86309	99	1802.8	1790.3
Z72_2	0.30504	4.66147	95	1813.5	1716.3
Z73_1	0.32051	4.86655	99	1801.8	1792.2
Z28_2	0.30925	4.66269	97	1789.2	1737
Z44_1	0.33003	5.17584	99	1860.2	1838.5
Z42_3	0.30454	4.59798	96	1791.3	1713.8
Z44_2	0.32172	4.90099	99	1807.6	1798.1
Z45_1	0.32181	4.90754	99	1809.4	1798.6
Z51_2	0.31726	4.79506	99	1793.3	1776.3
Z52_1	0.31664	4.80425	98	1800.6	1773.3
Z52_2	0.33314	5.07546	103	1807.9	1853.6
Z56_2	0.3463	5.38145	104	1843.8	1916.9
Z57_2	0.31265	4.81089	96	1826.1	1753.7
Z58_1	0.32601	4.89662	102	1781.9	1819
Z58_2	0.31796	4.80551	99	1793.2	1779.8
Z59_2	0.32911	5.15122	99	1856.7	1834.1
Z59_1	0.32126	4.84485	100	1789.3	1795.9
Z61_2	0.30342	4.57473	95	1789.1	1708.2
Z65_1	0.32364	4.91847	100	1803.2	1807.5
Z70_2	0.30371	4.66771	94	1823.8	1709.7
Z27_2	0.29566	4.43143	94	1778.8	1669.8
Z45_1	0.29331	4.46834	92	1807.7	1658.1
Z48_1	0.29008	4.46023	90	1824.5	1641.9
Z56_3	0.28505	4.50417	86	1873.9	1616.7
Z57_1	0.29632	4.52696	92	1813.1	1673
Z61_1	0.27625	4.19493	87	1802.1	1572.4
Z28_1	0.31563	4.96316	95	1865.6	1768.4
Z29_1	0.35081	6.9305	85	2268.4	1938.5
Z29_2	0.31136	4.55596	101	1735.3	1747.4
Z29_3	0.30166	4.45757	97	1752.5	1699.5
Z30_1	0.313	4.55685	102	1725.8	1755.5
Z30_2	0.31449	4.66349	100	1759.1	1762.7
Z31_1	0.30935	4.66103	97	1788.2	1737.5
Z32_1	0.30811	4.51973	100	1739.5	1731.4
Z33_1	0.23836	3.55214	78	1767.9	1378.1
Z34_1	0.27668	4.04823	91	1734	1574.6
Z35_1	0.31408	4.59953	101	1736.1	1760.8
Z35_2	0.32412	4.87945	101	1786	1809.8

Maria Then
Origin of Proterozoic granites in Mt Boothby

Z36_21	0.4057	7.53428	102	2160.4	2195.2
Z36_2	0.3165	4.68201	101	1754.3	1772.6
Z37_1	0.33626	5.22606	101	1844.1	1868.6
Z37_2	0.33905	5.09362	106	1782.7	1882.1
Z38_1	0.33103	5.00857	103	1795.5	1843.4
Z39_1	0.31435	4.67382	100	1763.7	1762.1
Z39_3	0.31607	4.79332	98	1799.3	1770.5
Z40_2	0.32073	4.83592	100	1788.8	1793.3
Z40_3	0.31939	4.77729	101	1774.1	1786.8
Z41_2	0.31193	4.76781	97	1813.6	1750.2
Z43_1	0.21271	3.31783	67	1850.2	1243.2
Z43_2	0.31585	4.66388	101	1750.7	1769.5
Z45_3	0.27321	3.74282	97	1612.4	1557.1
Z46_1	0.31594	4.79313	98	1800.1	1769.9
Z47_1	0.31308	4.72606	98	1791	1755.8
Z48_2	0.18227	2.85382	58	1857.3	1079.4
Z48_3	0.32831	4.95537	102	1790.8	1830.2
Z49_1	0.3086	4.54468	99	1745.9	1733.8
Z50_1	0.28692	4.35287	90	1800.1	1626.1
Z51_1	0.31167	4.72656	97	1799.4	1748.9
Z53_1	0.07856	1.40918	23	2099.4	487.5
Z54_1	0.33464	5.0426	104	1787.9	1860.8
Z55_1	0.31889	4.78065	100	1778.5	1784.3
Z55_2	0.31949	4.79947	100	1782.2	1787.2
Z56_1	0.34775	6.83772	85	2259.5	1923.9
Z56_4	0.29364	4.23324	97	1706.9	1659.7
Z60_1	0.30101	4.53186	95	1786.2	1696.3
Z60_2	0.30778	4.61415	97	1778.6	1729.8
Z62_1	0.31787	4.83085	99	1803.2	1779.3
Z63_1	0.28776	4.4388	89	1830.1	1630.3
Z63_2	0.06069	1.38908	15	2517.7	379.8
Z64_1	0.30295	4.52544	96	1771.7	1705.9
Z66_1	0.29818	4.6867	90	1864.2	1682.3
Z67_2	0.30874	4.5827	99	1760.2	1734.5
Z68_1	0.4979	12.49224	98	2670.5	2604.8
Z69_1	0.32079	4.81595	101	1781.4	1793.6
Z69_2	0.33339	5.24699	99	1866.5	1854.8
Z70_1	0.30807	4.62903	97	1782.9	1731.2
Z71_1	0.32242	5.04394	97	1855.7	1801.6
Spot name OG2	$^{206}\text{Pb}/^{238}\text{U}$	$^{207}\text{Pb}/^{235}\text{U}$	Conc. (%)²	$^{207}\text{Pb}/^{206}\text{Pb}$	$^{206}\text{Pb}/^{238}\text{U}$
1	0.32342	4.80364	102	1764	1806.4
2	0.31339	4.70289	99	1780.6	1757.4
4	0.31227	4.70665	98	1788.7	1751.8
5	0.31156	4.60373	100	1752.3	1748.4
6	0.33562	5.1114	103	1807.6	1865.6
7	0.31186	4.67151	98	1777.4	1749.8

Maria Then
Origin of Proterozoic granites in Mt Boothby

8	0.3141	4.67274	100	1764.8	1760.8
9	0.31459	4.74485	99	1789.6	1763.2
11	0.31471	4.70855	99	1774.6	1763.9
12	0.31195	4.61156	100	1752.9	1750.3
13	0.31489	4.76406	98	1795.5	1764.7
15	0.3154	4.72281	99	1776.6	1767.2
16	0.33061	5.02181	102	1802.2	1841.3
17	0.33957	5.13871	105	1795.1	1884.6
19	0.31976	4.7983	100	1780	1788.6
20	0.3227	4.77057	103	1752.7	1802.9
21	0.31237	4.68653	98	1779.6	1752.4
22	0.31415	4.77013	98	1801.8	1761.1
23	0.32146	4.78718	102	1766.2	1796.9
25	0.32025	4.82808	100	1788.7	1791
26	0.31808	4.78319	100	1784	1780.4
27	0.33563	5.0249	105	1775.8	1865.6
28	0.31809	4.757	100	1774.1	1780.4
30	0.27839	3.73609	101	1573.7	1583.3
3	0.27888	4.0932	91	1739.4	1585.7
10	0.3397	5.10206	106	1781.7	1885.2
14	0.1949	2.91866	65	1776.3	1147.9
18	0.27707	4.11555	90	1761.5	1576.6
24	0.29297	4.43159	92	1794.9	1656.3
29	0.3662	5.78251	107	1872.5	2011.5
Spot name OG3	$^{206}\text{Pb}/^{238}\text{U}$	$^{207}\text{Pb}/^{235}\text{U}$	Conc. (%)²	$^{207}\text{Pb}/^{206}\text{Pb}$	$^{206}\text{Pb}/^{238}\text{U}$
Z08	0.30747	4.70844	95	1817.1	1728.2
Z09	0.30914	4.74363	95	1820.7	1736.5
Z10	0.31811	4.91554	97	1833.5	1780.5
Z14	0.30256	4.58047	95	1796.2	1704
Z15	0.30465	4.56681	96	1778.2	1714.3
Z16	0.30366	4.56759	96	1784.4	1709.4
Z17	0.30261	4.58804	95	1799	1704.2
Z18	0.31694	4.71651	101	1764.8	1774.7
Z20	0.30529	4.56702	97	1774.4	1717.5
3	0.31557	4.7433	99	1783.7	1768.1
9	0.32443	4.94861	100	1809.9	1811.3
11	0.31767	4.8482	98	1810.7	1778.3
15	0.31646	4.78344	99	1794.2	1772.4
20	0.3119	4.71124	98	1793.3	1750.1
21	0.31856	4.80505	100	1789.6	1782.7
22	0.3043	4.58276	96	1786.7	1712.6
23	0.32632	4.91374	102	1786.7	1820.5
25	0.29994	4.46568	96	1765.9	1691
28	0.32274	4.89743	100	1800.4	1803.1
29	0.30574	4.66714	95	1811.5	1719.7
31	0.32904	5.07776	100	1831.3	1833.7

Maria Then
Origin of Proterozoic granites in Mt Boothby

33	0.30074	4.52126	95	1784	1695
34	0.32022	4.87506	99	1806.6	1790.8
37	0.31525	4.81905	97	1814.4	1766.5
Z02	0.29285	4.51919	90	1831.1	1655.7
Z04	0.27382	3.84262	94	1657.2	1560.2
Z05	0.27783	4.26022	87	1819.7	1580.4
Z06	0.22287	3.48895	70	1857.4	1297
Z12	0.29017	4.44788	90	1818.7	1642.4
Z13	0.27421	4.27284	84	1848.7	1562.1
Z19	0.27837	4.10764	90	1749.5	1583.2
1	0.2479	3.58784	83	1713.9	1427.6
2	0.29754	4.5928	92	1831.5	1679.1
4	0.29242	4.48071	91	1818.4	1653.6
7	0.27667	4.19069	88	1798	1574.6
8	0.24753	4.19252	71	1998.4	1425.7
10	0.30163	4.58691	94	1804.4	1699.4
12	0.31592	5.08281	93	1907	1769.8
13	0.28218	4.27462	89	1797.3	1602.3
14	0.25904	3.83887	85	1756.8	1484.9
17	0.29192	4.33751	94	1763	1651.1
18	0.27719	4.22356	87	1809	1577.2
26	0.31023	5.10302	90	1946.1	1741.8
27	0.28992	4.25019	94	1737.7	1641.1
32	0.23267	4.61371	59	2274.1	1348.5
35	0.38009	7.35882	93	2232.8	2076.7
38	0.28265	4.56127	84	1912.4	1604.7
39	0.25731	4.71598	69	2137.3	1476.1
40	0.29841	4.53344	93	1803.3	1683.4
Z03	0.3033	4.45646	98	1741.9	1707.6
36	0.30683	4.49514	99	1736.6	1725.1
Z01	0.3272	5.1216	98	1856.9	1824.8
6	0.42538	8.26071	102	2238.1	2284.8
16	0.33183	5.25299	98	1877.9	1847.2
19	0.32069	5.10368	95	1888.2	1793.1
24	0.31978	5.06382	95	1877.8	1788.7
5	0.48643	11.87013	97	2625.2	2555.2
Z11	0.26485	3.52452	97	1558	1514.6
Z07	0.32672	5.08044	99	1844.8	1822.5
Spot name MS1	$^{206}\text{Pb}/^{238}\text{U}$	$^{207}\text{Pb}/^{235}\text{U}$	Conc. (%)²	$^{207}\text{Pb}/^{206}\text{Pb}$	$^{206}\text{Pb}/^{238}\text{U}$
001-2	0.52216	14.21758	97	2805.3	2708.3
001-3	0.43341	9.08718	98	2369.3	2321.1
001-5	0.33946	5.6325	96	1962.2	1884.1
001-6	0.29772	4.48326	94	1787.3	1680
001-8	0.33503	5.55589	95	1960.9	1862.7
001-9	0.26605	3.61572	95	1597.8	1520.7
001-11	0.4281	8.95632	97	2365.8	2297.2

Maria Then
Origin of Proterozoic granites in Mt Boothby

001-12	0.43249	8.86039	99	2329.5	2316.9
001-15	0.4133	8.24848	98	2284.7	2230
001-16	0.35929	5.74467	104	1895.2	1978.8
001-17	0.30928	4.74197	95	1819.3	1737.2
001-18	0.36908	6.26893	101	2002.7	2025.1
001-19	0.46227	9.94635	101	2413.7	2449.6
001-20	0.33842	5.4465	99	1906.6	1879.1
001-21	0.53274	13.8969	101	2735.6	2753
001-22	0.53165	13.86094	101	2734	2748.4
001-25	0.4405	8.82343	103	2291.1	2352.9
001-28	0.42902	8.80163	99	2332.5	2301.3
001-29	0.30558	4.63547	95	1800.2	1718.9
001-30	0.34875	5.6817	100	1928.7	1928.6
001-31	0.44348	9.82594	96	2463.4	2366.2
001-32	0.33624	5.24824	101	1851.5	1868.6
001-34	0.41554	8.44473	97	2316.1	2240.2
001-35	0.34832	5.42174	104	1847.3	1926.6
001-36	0.43902	9.19308	99	2368.7	2346.2
001-37	0.428	8.8863	98	2353.1	2296.7
001-38	0.44956	10.26213	95	2514	2393.3
001-40	0.33825	5.21383	103	1828.9	1878.3
001-41	0.51761	12.88622	101	2658.5	2689
001-42	0.37257	6.18491	104	1963.2	2041.5
001-44	0.33328	5.29222	98	1883	1854.3
001-45	0.54826	15.06449	100	2820.9	2817.9
001-47	0.40317	7.40457	102	2141.2	2183.6
001-48	0.44223	8.88084	103	2296.1	2360.6
001-49	0.44057	8.60437	105	2248	2353.2
001-50	0.41874	8.09129	101	2229.5	2254.8
001-51	0.3294	5.33122	96	1917.4	1835.5
001-52	0.33142	4.97732	104	1781.6	1845.3
001-54	0.39225	7.6209	95	2239.2	2133.2
001-55	0.42126	8.22699	101	2247.4	2266.2
001-57	0.4974	12.47358	97	2670.8	2602.6
001-58	0.35144	5.39381	107	1821.3	1941.5
001-59	0.45376	10.0394	98	2461.1	2411.9
001-61	0.34202	5.35834	102	1858.7	1896.4
001-63	0.41521	8.0955	100	2244.8	2238.7
001-65	0.29673	4.38481	96	1752.6	1675.1
001-66	0.29116	4.27113	95	1738.8	1647.3
001-67	0.44191	8.95205	102	2311.5	2359.2
001-68	0.40992	8.34163	96	2318.9	2214.6
001-69	0.33536	5.15624	102	1825.7	1864.3
001-70	0.37522	6.55993	100	2054.3	2053.9
001-71	0.31436	4.74552	98	1792.2	1762.1
001-72	0.34784	5.92949	96	2009.4	1924.3

Maria Then
Origin of Proterozoic granites in Mt Boothby

001-73	0.33334	5.08395	102	1810.3	1854.5
001-74	0.31294	4.74767	97	1800.6	1755.2
001-76	0.31653	4.52908	105	1693.7	1772.8
001-77	0.41836	7.74846	104	2156	2253
001-78	0.35065	5.8363	98	1967.4	1937.7
001-79	0.47207	10.32001	102	2441	2492.6
001-80	0.3266	5.0706	99	1842.4	1821.9
001-82	0.40017	7.38882	101	2150.8	2169.8
001-83	0.4701	10.27434	102	2440.7	2484
001-84	0.51045	12.92118	99	2686.3	2658.5
001-85	0.46232	10.75128	96	2545	2449.8
001-86	0.44075	9.7391	96	2459.2	2354
001-87	0.5013	12.38164	99	2646	2619.4
001-88	0.43787	8.78698	102	2294.9	2341.1
001-89	0.37463	6.50309	100	2042.1	2051.1
001-90	0.33678	5.3667	99	1889.6	1871.2
001-92	0.41392	8.12811	99	2257.8	2232.8
001-93	0.34824	5.54228	102	1887.5	1926.2
001-94	0.33577	5.22966	101	1848.6	1866.3
001-95	0.33708	5.15458	103	1815.4	1872.6
001-97	0.46308	10.68646	97	2532.5	2453.1
001-98	0.46512	10.4932	99	2495	2462.1
001-99	0.33706	5.22678	102	1840.6	1872.5
001-100	0.3585	5.95535	101	1964.2	1975.1
001-103	0.40318	7.30537	103	2117.6	2183.7
001-104	0.4143	7.81653	102	2189	2234.6
001-107	0.33164	5.03161	103	1801.2	1846.3
001-108	0.34926	5.40293	105	1836	1931
001-109	0.35241	5.70981	101	1919.9	1946.1
001-110	0.4701	10.37187	101	2457	2484
001-111	0.37717	6.36634	104	1993.1	2063.1
001-112	0.36283	5.89634	104	1925.1	1995.6
001-113	0.51204	13.05033	99	2698	2665.3
001-114	0.45526	9.8471	100	2423	2418.6
001-115	0.39347	7.30264	99	2161.2	2138.9
001-116	0.50095	12.08999	100	2606.9	2617.9
001-117	0.50351	12.25309	100	2622	2628.8
001-118	0.49478	11.87227	100	2597.9	2591.3
001-119	0.3405	5.26995	103	1837.7	1889.1
001-120	0.33364	5.15905	101	1835.6	1856
001-7	0.36082	5.59328	108	1839.6	1986.1
001-13	0.2938	4.43712	93	1791.4	1660.5
001-14	0.35333	6.46426	91	2133.7	1950.5
001-23	0.36447	6.96387	91	2210.2	2003.3
001-24	0.35941	6.69249	91	2164.7	1979.4
001-27	0.47308	11.97921	93	2686.6	2497

Maria Then
Origin of Proterozoic granites in Mt Boothby

001-33	0.35106	5.30967	108	1794.2	1939.6
001-39	0.36577	6.9836	91	2209	2009.5
001-46	0.42009	9.15138	93	2434.7	2260.9
001-60	0.39897	8.39398	91	2375.9	2164.3
001-62	0.35506	5.48202	107	1832.2	1958.7
001-64	0.29007	4.35387	92	1781	1641.9
001-75	0.37859	7.46704	91	2265.3	2069.7
001-91	0.35225	6.38193	92	2117.7	1945.3
001-102	0.36832	6.93712	92	2186.2	2021.5
001-106	0.33783	5.03916	106	1769.6	1876.2
001-1	0.43585	16.12867	71	3297.3	2332
001-4	0.31985	5.81373	84	2122.4	1789
001-10	0.34328	6.29885	89	2139.6	1902.4
001-26	0.31268	5.38396	86	2027.9	1753.9
001-43	0.26551	3.89743	87	1740.4	1518
001-53	0.35691	7.05391	87	2268.7	1967.5
001-56	0.34326	7.04931	81	2334.5	1902.3
001-81	0.31775	5.4228	88	2012.1	1778.7
001-96	0.33468	6.35249	85	2198.6	1861
001-105	0.24911	3.40934	89	1611.3	1433.9
Spot name MS2	$^{206}\text{Pb}/^{238}\text{U}$	$^{207}\text{Pb}/^{235}\text{U}$	Conc. (%)²	$^{207}\text{Pb}/^{206}\text{Pb}$	$^{206}\text{Pb}/^{238}\text{U}$
1	0.65639	26.10237	95	3409.7	3253.1
2	0.30192	4.51758	96	1775.3	1700.8
3	0.33262	5.29536	98	1887.8	1851.1
4	0.3104	4.65954	98	1781	1742.7
5	0.30338	4.56162	96	1783.9	1708
6	0.33382	5.31413	98	1887.5	1856.9
8	0.3201	4.83995	100	1794.4	1790.2
10	0.34113	5.53414	98	1921.7	1892.1
16	0.36963	6.35309	100	2024.1	2027.7
17	0.36862	6.36384	100	2031.6	2022.9
20	0.31724	4.93683	96	1846.2	1776.2
22	0.33025	5.15043	99	1850.3	1839.6
23	0.33983	5.46048	99	1904	1885.8
25	0.44824	9.67735	99	2419.4	2387.4
1b	0.32963	5.10302	100	1836.2	1836.6
3b	0.35097	6.12734	95	2051.1	1939.2
5b	0.33582	5.27803	100	1863.7	1866.5
6b	0.31796	4.87704	98	1819.5	1779.8
8b	0.32171	5.00677	97	1846.1	1798.1
9b	0.31368	4.79711	97	1814.1	1758.8
10b	0.32516	5.0534	98	1843.7	1814.9
14b	0.32501	5.03674	99	1838.5	1814.1
16b	0.31581	4.93279	95	1852.8	1769.2
17b	0.33161	5.24716	98	1876.3	1846.2
18b	0.34305	5.70874	97	1966.7	1901.3

Maria Then
Origin of Proterozoic granites in Mt Boothby

20b	0.3306	5.1071	100	1833	1841.3
21b	0.3223	5.00633	98	1843.2	1800.9
22b	0.38848	7.29549	97	2179.9	2115.8
24b	0.32149	4.99549	97	1843.7	1797
26b	0.30217	4.58084	95	1799.7	1702.1
27b	0.33302	5.13637	101	1831.2	1853
28b	0.32548	5.04846	99	1841	1816.4
31b	0.33989	5.4717	99	1908.1	1886.1
32b	0.33018	5.00529	102	1799.3	1839.2
34b	0.33817	5.2006	103	1825.4	1877.8
36b	0.31279	4.61304	100	1748.8	1754.4
37b	0.3183	4.9345	97	1840	1781.4
38b	0.3133	4.70478	99	1781.9	1756.9
39b	0.32413	4.94055	100	1809.5	1809.9
41b	0.33304	5.01259	104	1786	1853.1
42b	0.47347	11.20608	97	2574.5	2498.7
44b	0.388	7.42553	96	2212.7	2113.5
45b	0.33216	5.11089	101	1826.1	1848.8
46b	0.37408	6.85777	96	2137.9	2048.6
47b	0.32644	5.06311	99	1840.4	1821.1
48b	0.31642	4.85782	97	1822.3	1772.2
49b	0.3678	5.90302	106	1901.8	2019
51b	0.34353	5.37716	103	1856.7	1903.6
52b	0.31673	4.81534	98	1803.6	1773.7
53b	0.40939	7.74299	101	2192.1	2212.1
54b	0.32888	4.98439	102	1798.5	1832.9
11b	0.29732	4.53316	93	1809.1	1678
13b	0.2941	4.45438	92	1797.2	1662
25b	0.37661	7.07542	94	2180.7	2060.4
4b	0.35467	5.41409	108	1811	1956.9
30b	0.41421	8.85432	93	2403.3	2234.1
7	0.27117	3.56677	101	1536.4	1546.7
9	0.27929	3.76881	100	1584.2	1587.8
11	0.28312	3.80501	102	1576.5	1607.1
12	0.28188	3.76593	102	1565.4	1600.8
13	0.27877	3.74732	101	1576.8	1585.2
14	0.27054	3.59031	99	1552.8	1543.5
24	0.26762	3.54698	99	1550.5	1528.7
26	0.27598	3.62217	103	1532	1571.1
27	0.26195	3.50879	96	1570.3	1499.8
28	0.26895	3.59073	98	1564.1	1535.5
33	0.26859	3.61788	97	1580.6	1533.6
2b	0.26489	3.59897	95	1596.3	1514.8
15b	0.26523	3.57467	96	1581.8	1516.5
19b	0.27321	3.74842	96	1615.1	1557.1
23b	0.27708	3.76248	99	1596.4	1576.6

Maria Then
Origin of Proterozoic granites in Mt Boothby

29b	0.27323	3.63982	100	1561.1	1557.2
33b	0.27002	3.67361	96	1600	1540.9
35b	0.26842	3.5666	99	1555.7	1532.8
40b	0.25776	3.42816	95	1557.6	1478.4
50b	0.2769	3.71115	100	1571.4	1575.7
29	0.33452	5.17151	84	1834.2	1860.2
30	0.3266	5.03399	82	1828.8	1821.9
31	0.33327	5.16878	83	1840.2	1854.2
32	0.33774	5.20423	82	1828.2	1875.8
7b	0.29224	4.62593	88	1877	1652.7
15	0.30581	4.50261	98	1746.6	1720.1
18	0.31939	4.72473	102	1754	1786.8
19	0.31752	4.70334	101	1756.3	1777.6
21	0.31751	4.88905	97	1827.1	1777.6
12b	0.30458	4.51845	97	1759.1	1714
43b	0.30869	4.5624	99	1752.7	1734.3
Spot name MF1	$^{206}\text{Pb}/^{238}\text{U}$	$^{207}\text{Pb}/^{235}\text{U}$	Conc. (%)²	$^{207}\text{Pb}/^{206}\text{Pb}$	$^{206}\text{Pb}/^{238}\text{U}$
Z01	4.82905	0.31829	99	1799.6	1781.4
Z02	4.38837	0.29537	95	1761.5	1668.3
Z03	4.65367	0.31152	99	1771.4	1748.2
Z04	4.68336	0.30872	96	1799.7	1734.4
Z05	4.61159	0.31283	100	1746.9	1754.6
Z06	4.68638	0.30995	97	1793.4	1740.4
Z07	4.70832	0.31378	99	1779.4	1759.3
Z09	4.75347	0.31407	98	1795.6	1760.7
Z10	5.02256	0.32773	100	1819.5	1827.4
Z11	4.67529	0.3127	99	1773.4	1754
Z12	4.76779	0.31672	99	1785.8	1773.7
Z13	4.60063	0.30812	98	1770.9	1731.4
Z14	4.76694	0.31362	97	1803.9	1758.5
Z15	4.8162	0.31632	98	1807	1771.7
Z16	4.51105	0.30561	98	1750.4	1719.1
Z17	4.55027	0.30784	99	1752.6	1730.1
Z19	4.72876	0.32117	103	1745.7	1795.5
Z18	4.60461	0.3061	96	1784.9	1721.5
Z20	4.67458	0.31474	100	1761.4	1764
Z21	4.64436	0.31013	98	1776.5	1741.4
Z22	4.55649	0.3052	97	1770.9	1717
Z23	4.94651	0.32576	101	1802.9	1817.8
Z25	4.59171	0.30414	#REF!	1733.4	1703.1
Z26	4.42239	0.30237	98	1773.8	1774.7
Z27	4.73852	0.31694	100	1771.9	1810.5
Z28	4.84353	0.32425	102	1772.6	1733.4
Z29	4.6116	0.30851	98	1776.4	1700.4
Z30	4.52004	0.30183	96	1735.4	1600.9
1	4.45736	0.29872	95	1770.1	1685

Maria Then
Origin of Proterozoic granites in Mt Boothby

2	4.61105	0.30846	98	1773.2	1733.1
4	4.46132	0.30022	96	1761.9	1692.4
5	4.75568	0.31992	101	1763	1789.3
6	4.75189	0.31788	100	1772.7	1779.4
7	4.76262	0.31223	97	1810	1751.7
9	4.56486	0.30575	97	1770.9	1719.7
11	4.75477	0.31511	99	1790.5	1765.8
12	4.57776	0.30755	98	1765.5	1728.6
15	4.71844	0.31287	98	1789.3	1754.8
16	4.92316	0.33186	105	1759.5	1847.4
17	4.67091	0.31425	100	1763.1	1761.6
18	4.73355	0.31784	101	1766.9	1779.2
21	4.58187	0.30578	97	1777.4	1719.9
23	4.63222	0.30967	98	1774.2	1739.1
24	4.38235	0.30036	98	1728.6	1693.1
27	4.60464	0.30782	98	1774.2	1730
28	4.60808	0.30796	98	1774.8	1730.7
29	4.61671	0.3091	98	1771.6	1736.3
32	4.52304	0.30199	96	1776.6	1701.2
33	4.4987	0.30037	95	1776.5	1693.2
35	4.55163	0.30374	96	1777.5	1709.8
36	4.54677	0.30144	95	1789.5	1698.5
42	4.61226	0.31319	101	1745.8	1756.4
43	4.47523	0.3023	97	1755.2	1702.7
44	4.86922	0.32713	103	1765.5	1824.5
45	4.64251	0.3134	100	1756.4	1757.4
46	4.75115	0.32007	102	1760.2	1790.1
48	4.64989	0.30748	96	1794.3	1728.3
49	4.84234	0.32382	102	1773.6	1808.4
50	4.82168	0.32386	102	1765.5	1808.6
51	4.86573	0.32325	101	1785.6	1805.6
54	4.78791	0.32133	102	1767.1	1796.2
55	4.62603	0.30694	97	1787.9	1725.7
56	4.65718	0.30952	97	1784.9	1738.3
57	4.80796	0.31739	99	1797.3	1777
58	4.74302	0.31753	100	1771.7	1777.7
59	4.83641	0.31896	99	1799.3	1784.7
60	4.60705	0.30231	95	1808.3	1702.8
61	4.75697	0.31447	98	1794.8	1762.7
62	4.52164	0.30258	96	1772.2	1704.1
63	4.72439	0.31903	102	1755.7	1785
65	4.61317	0.31064	99	1761.2	1743.8
66	4.65987	0.31452	100	1756.7	1762.9
67	4.54493	0.30121	95	1790.1	1697.3
68	4.48215	0.30074	96	1767.5	1695
Z08	4.46167	0.28998	90	1825.7	1641.4

Maria Then
Origin of Proterozoic granites in Mt Boothby

Z24	4.12752	0.28189	92	1791.3	1711.8
3	5.15155	0.34408	107	1776.1	1906.3
10	5.02552	0.33821	107	1762.2	1878
19	5.20977	0.34905	109	1770.6	1930
20	4.9373	0.33359	106	1755.2	1855.7
25	4.21667	0.28715	94	1740.4	1627.3
26	4.42149	0.29618	94	1770.5	1672.3
30	4.54625	0.29988	94	1798.6	1690.7
37	4.41191	0.2947	94	1775.6	1665
38	4.4695	0.29686	94	1786.1	1675.7
39	4.37877	0.28997	92	1791.6	1641.4
47	4.9404	0.33091	105	1770.6	1842.8
53	4.45206	0.29193	91	1809.6	1651.2
13	4.62679	0.31499	89	1617.3	1442.8
14	4.94369	0.33384	101	1741.4	1765.2
22	3.44587	0.25083	99	1788.8	1769.7
31	4.76315	0.31591	91	1779.7	1619.1
34	4.28368	0.28552	100	1735.9	1741
41	4.54165	0.31006	101	1757	1779.8
52	4.7116	0.31796	106	1730.5	1837.3
64	4.81668	0.32978	106	1756.2	1857
Z03_1	0.31708	4.77395	99	1786.5	1775.5
Z05_1	0.30889	4.61307	98	1771.6	1735.2
Z06_2	0.29601	4.38385	95	1756.5	1671.5
Z08_1	0.31506	4.75292	99	1790	1765.5
Z12_1	0.32433	4.86198	102	1778.2	1810.8
Z14_1	0.29899	4.41494	96	1750.6	1686.3
Z14_2	0.2929	4.31366	95	1745.8	1656
Z16_1	0.30404	4.58549	96	1789.5	1711.3
Z17_1	0.30434	4.64617	95	1811.8	1712.8
Z18_1	0.31421	4.75643	98	1796.2	1761.4
Spot name MF2	$^{206}\text{Pb}/^{238}\text{U}$	$^{207}\text{Pb}/^{235}\text{U}$	Conc. (%)²	$^{207}\text{Pb}/^{206}\text{Pb}$	$^{206}\text{Pb}/^{238}\text{U}$
Z21_1	0.32591	4.95003	101	1802.2	1818.5
Z22_1	0.31778	4.82115	99	1800.1	1778.9
Z24_1	0.29359	4.34347	95	1754.5	1659.5
Z25_2	0.30385	4.5209	97	1764.2	1710.4
Z29_1	0.30997	4.61713	99	1766.1	1740.6
Z30_1	0.30981	4.72614	96	1809.9	1739.8
Z31_2	0.30549	4.64839	95	1805.3	1718.5
1	0.3173	4.83712	98	1809.3	1776.5
2	0.32299	4.89952	100	1800.5	1804.3
4	0.33118	4.99978	103	1791.5	1844.1
6	0.31982	4.91807	98	1824.2	1788.9
7	0.31399	4.54347	103	1713.7	1760.3
10	0.31408	4.81218	97	1818.1	1760.8
11	0.30257	4.41593	99	1729.3	1704

Maria Then
Origin of Proterozoic granites in Mt Boothby

12	0.30185	4.55567	95	1790.3	1700.5
13	0.32435	4.94197	100	1808.5	1810.9
15	0.33683	5.12673	104	1806.1	1871.4
16	0.31495	4.79311	98	1805.7	1765
17	0.31819	4.90991	97	1831.1	1780.9
18	0.33752	5.0863	105	1787.8	1874.7
19	0.31561	4.72059	100	1774.3	1768.2
22	0.30789	4.6022	98	1773.3	1730.3
24	0.31936	4.69543	102	1743.3	1786.6
26	0.31803	4.85049	98	1810.1	1780.1
27	0.30808	4.60767	98	1774.7	1731.2
30	0.31301	4.71438	98	1787.2	1755.5
31	0.31325	4.67322	99	1770.7	1756.7
32	0.31441	4.70225	99	1775	1762.4
Z01_1	0.22948	3.40007	76	1757.3	1331.8
Z02_1	0.26055	3.99892	82	1821.3	1492.7
Z04_1	0.22416	3.35652	73	1776.6	1303.8
Z05_2	0.26127	3.65938	90	1653.6	1496.4
Z06_1	0.27454	4.0234	90	1737.1	1563.8
Z07_1	0.26938	3.76908	93	1651.8	1537.6
Z07_2	0.23413	3.09382	88	1545	1356.1
Z09_1	0.29317	4.37239	94	1768.8	1657.3
Z11_1	0.26312	3.92909	85	1771.1	1505.8
Z11_2	0.28289	4.18702	92	1755	1605.9
Z13_1	0.29355	4.41056	93	1782.2	1659.3
Z15_1	0.28482	4.20534	92	1751	1615.6
Z19_1	0.27492	4.04512	90	1744.1	1565.7
Z20_1	0.26858	3.94459	88	1741.1	1533.6
Z20_2	0.29758	4.51074	93	1798.7	1679.3
Z23_1	0.27822	4.22361	88	1801.2	1582.4
Z24_2	0.23433	3.61591	74	1830.7	1357.2
Z25_1	0.21626	3.26925	70	1793.2	1262.1
Z26_1	0.26369	3.94037	85	1771.9	1508.7
Z27_1	0.27292	4.07698	88	1771.2	1555.6
Z27_2	0.29351	4.42487	93	1788	1659.1
Z28_1	0.27802	4.10782	90	1751.1	1581.4
Z31_1	0.28436	4.23478	91	1765.8	1613.3
3	0.23512	3.64251	74	1838	1361.3
5	0.28262	4.13829	92	1735.8	1604.6
8	0.27536	3.9014	94	1675	1568
9	0.26158	3.67239	90	1658	1497.9
14	0.29697	4.61714	91	1844.5	1676.3
21	0.32195	5.29882	92	1947.1	1799.2
23	0.25139	3.79896	81	1793.5	1445.6

Maria Then
Origin of Proterozoic granites in Mt Boothby

Maria Then
Origin of Proterozoic granites in Mt Boothby